Dry bands on polluted insulation

Löberg, Johan Ove

DRY BANDS ON

POLLUTED INSULATION

by

Johan Ove Löberg

Thesis submitted for the Degree of Master of Science in the Faculty of Engineering Science, University of Durham.

April, 1970.

DRY BANDS ON POLLUTED INSULATION

by

Johan Ove Löberg

SUMMARY OF THESIS

The present literature concerning surface resistivity and voltage distribution on a polluted insulator has been reviewed.

A theoretical system of temperature distribution across a polluted surface has been developed considering the various ways of heat loss from the surface.

Research has been carried out to determine the voltage, resistivity and temperature distribution across a surface at a range of humidities at a constant ambient temperature for increasing applied voltage. The iniation and the collapse of the dry band has been discussed, and the conditions leading to the phenomenon have been considered.

The effect on the width of the dry band due to varying convection rates has been studied and discussed.

The temperature of the dry band has been measured remotely by an infrared thermometer developed for this purpose. The results obtained have been analysed and compared with results obtained previously by a known relationship between surface resistivity and temperature.

Some points have been made with regard to reducing the failure of insulators due to dry bands forming and leading to tracking and flashover.

ACKNOWLEDGMENTS

The author is indebted to the following:-

Dr. E. C. Salthouse for his continued help and encouragement.

The technicians at the Engineering Science laboratory for their help in building the necessary equipment.

Mrs. G. Binah for typing and layout of the Thesis.

I N D E X

LIST OF SYMBOLS

This list gives the most common symbols used throughout the Thesis.

A	-	cross sectional area.
E	-	voltage gradient.
I_s	-	surface leakage current.
J_s	-	surface current density.
K_s	-	surface thermal conductivity.
L	-	length of surface.
P	-	power dissipation.
R_s	-	dry band resistance.
R_{so}	-	initial surface resistance.
$R_{s\infty}$	-	final surface resistance.
T_a	-	ambient temperature.
T_s	-	surface temperature.
V	-	applied voltage.
V_c	-	critical voltage.
W	-	dry band width.
X	-	width of film.
d	-	distance between probe and probe casing.
h	-	heat transfer coefficient.
q_s	-	electrical power dissipated per unit area.
s	-	distance between probe casing and sample.
δ	-	thickness of film.
θ	-	temperature above ambient.
ρ_{so}	-	initial surface resistivity.
$\rho_{s\infty}$	-	final surface resistivity.
ρ_v	-	volume resistivity.
σ_s	-	surface electrical conductivity.

1.0. INTRODUCTION

Failure in Power Transmission owing to pollution on insulators is a major problem and has been for many years. In fact, as far back as 1878, Johnson and Phillips[1] took out a patent on an anti-deposit insulator and since then various ideas have been put forward and tried in service, particularly in the period 1920-1940. The improvement in insulators is of course welcome, but it does by no means solve the problem of breakdown owing to pollution; not even the most recent developments can cope with this, nor is there much hope in the near future that anyone will be able to produce a perfect insulator.

To give an idea of the magnitude of the problem one may compare the number of faults caused by pollution with those caused by lightning. In the period 1950-1955 the number of faults caused by pollution were 0.6 faults per 100 route-miles of 132kv line per year, compared with lightning which were 1.1 faults over the same period on the same type of line. More recently a similar period of time shows that the faults caused by pollution have increased to 1.02 per 100 route-miles per year. This is a very large increase and gives cause for concern as to what can be done to reduce the number of faults.

A lot of research has been carried out in order to explain the behaviour of a polluted insulator, particularly in connection with flashover and tracking. It has been shown in various papers, e.g. Hampton[2], Alston[3] and James[1] that moisture plays a vital part in the breakdown

of insulators.

When an insulator, after having been covered with a layer of pollution, is subjected to a humid atmosphere a surface leakage current will flow. This is explained by the formation of an electrolytic layer caused by parts of the pollution being dissolved in the moisture absorbed by the surface. Depending on the composition of the pollution and the degree of absorbtion of moisture, the leakage current flowing can be sufficiently large to cause a considerable power dissipation to take place, as shown later in this work. The result of this power dissipation is a non-uniform drying up of the electrolytic film; Forrest[4], Hampton[2], McIlhagger[5] et al and Salthouse[6]. The non-uniform drying of the electrolyte results in what is known as a dry band, first reported by Forrest[4]. It is quite clear that once a dry band has formed, giving a region of high resistance on the insulator, a larger proportion of voltage will be distributed across this section. Thus locally the power dissipation may increase, although there is a marked decrease in the current.

There are several types of pollution which contribute to breakdown, some being less severe and more prolonged than others. The more severe types of pollution may be listed as pollution from various kinds of industry such as cement factories, chemical plants, coal-fired plants, etc. Perhaps the most severe of all is salt spray on stations and transmission lines situated along the coast. This causes a very rapid build-up of a conducting layer and

almost inevitably results in outages during stormy weather.

Generally the chemical composition of pollution is quite complex. A typical example is fly ash which in a dry state has a very high resistivity, but when dissolved conducts current quite readily. Its composition may be found as 57% SiO_2, 12% Fe_2O_3, 19% Al_2O_3, 7% CaO, 3.5% MgO, 1.5% SO_3.(1)

According to British Standards 137(7) an area of high pollution is one in which the rate of deposition ranges from 240 to 600 tons per square mile per year. This equals 3 to 7 ounces per square yard per year, a somewhat frightening quantity. A moderate rate of pollution is set at 90 tons per square mile per year; still a high rate compared with less industrialised countries.

A more innocent, but still troublesome form of pollution was bird droppings along insulator strings. This was effectively dealt with by erection of bird guards when the cause of the trouble was eventually found. In the meantime many theories were put forward explaining this phenomenon which occurred at random all over the country, particularly at dawn; thus it was reasonable to believe that dew formation was the cause of the trouble. This phenomenon became so well known and caused so much speculation that it eventually earned the name of "Morning Effect".

Several points may be taken into consideration in order to prevent flashover and breakdown of insulators such as:-

1. Providing a long leakage path and thus reducing the electric stress on the insulator surface.

2. Shaping the insulator so that rain helps to wash the deposit off.
3. Shaping the insulator so as to prevent a continuous layer of pollution being formed.
4. To keep the insulator dry by means of a semi-conducting layer built into the insulator thus allowing a permanent flow of current and heat to be dissipated. The main drawback of this is that the surface is vulnerable to corrosion and easily damaged by discharges.
5. Greasing of insulators to prevent a continuous film of moisture forming. This method has been well tried out, but was found to be completely unsatisfactory as the greasing had to be repeated at intervals depending on the rate of pollution and weather conditions. It was also necessary to wash off the old grease before new could be applied. This was a lengthy and elaborate operation and not particularly economical.
6. Live washing is at present very popular. This obviously involves some safety precautions, but these can be overcome by various methods:-
   (a) By ensuring that the water used has a very low conductivity.
   (b) By interrupting the flow of water either by chopping or by applying it as a fine spray.

Breakdown of insulation may also be due to tracking.

This is generally caused by small discharges along the surface of the insulator. In organic insulation these small sparks can cause carbonization and the carbon tracks formed, can bridge points of different potentials. Hence an increase in the surface leakage current is inevitable. These small carbon tracks may eventually link up with each other and form a continuous conducting path along the surface and result in flashover[10].

Some organic insulator materials are more resistant to tracking than others, and it is reasonable to believe that this is closely connected to its chemical structure. However, it has been shown by Parkman[10] that the carbon content alone is not a measure of how readily tracking may occur. Take for instance, Polystyrene, with a carbon content of 92% and compare with Polycarbonate with a carbon content of 77%. The former is far more resistant to tracking than the latter; the difference appears in the chemical reaction caused by the sparks. The carbon may be removed as a gas, as is the case with Polystyrene, or from a carbon track leading to further tracking. Consequently one avoids using materials with a high tendency for tracking, but this does not eliminate the problem altogether.

Then what can be done to stop discharges and tracking? There is no easy and straight forward answer, but it is of importance to analyse the pre-discharge behaviour of the insulator to give a better understanding of the initiation of tracking and flashover.

The aim of this work is to examine one aspect of the pre-discharge behaviour of insulation and to discuss the

effects of the various factors involved. Discharges only occur where a dry band is present, thus it is necessary to look into the formation of dry bands.

The questions which require answers include:- When is a dry band initiated? What are the factors which control its growth? To answer such questions it will be necessary to examine the electrical and thermal characteristics of a polluted surface. This thesis describes some measurements carried out on a model system to find out how the dry band develops and specifically how the dry band width and temperature vary with power dissipation. No attempt has been made to examine the discharge initiation.

2.0. A REVIEW OF PREVIOUS WORK ON DRY BAND FORMATION.

Not a great deal of work has been done on dry bands on polluted insulation. The first to report dry bands was Forrest[4], and later Hampton[2] studied the formation of dry bands by measuring the voltage distribution along a polluted surface. He showed that the evaporation of moisture from the surface was non-uniform.

Loss of moisture from a contaminated moist surface owing to power dissipation has also been reported by Johnson[11],[12] McIlhagger, McCausland and Girvan[5]. This work was based on a uniform loss of moisture from a dielectric surface. However, in a more recent work McIlhagger[13] has extended his theory to cover non-uniform evaporation and has developed a criterion for dry band formation.

Because of leakage current in a contaminated surface, the power dissipated initiates a non-uniform evaporation. This has been studied by Salthouse[6] and he has developed a criterion for initiation of water loss from a contaminated moist surface.

To measure the voltage distribution across a conventional insulator is very difficult because of the complexity of its shape. The problem can be much simplified by using a flat strip of insulation coated with artificial pollution, and thus establishing the dry band formation for this geometry.

A thin glass plate was used by Hampton[2] coated with a layer of artificial pollution consisting of a mixture of

kieselguhr, dextrin and salt. His electrodes were connected across the output of a 0-20kV, 20kVA regulated transformer, and the voltage distribution was measured at ten points by probes attached to the underside of the glass sheet. Each probe was connected to earth through a large capacitor, thus a capacitance divider circuit was obtained. The capacitance between the probes on one side of the glass plate and the polluted side completed the divider circuit. The spacing of the probes was such that one probe was located under each electrode and the remaining eight were evenly spaced out between them. The capacitance between each of the probes and the polluted layer was less than 1pF and would not effect the voltage being measured. The output from each of the ten probes was connected to the Y plates of an oscilloscope through a switch, and by synchronizing the oscilloscope with the position of the switch, a complete scan was made in 1ms. With a 50 $^{c}/s$ supply, the voltage was scanned 10 times for each half cycle.

The test sample was surrounded by an atmosphere of very high humidity in a cabinet, and by using a high speed camera coupled with a semi-silvered mirror he was able to photograph the formation of dry bands and discharges together with the corresponding trace on the oscilloscope.

Fig. 2.1 shows a typical sequence of voltage distribution obtained on an initially dry specimen and then subjected to a dense fog.

From Fig. 2.1 it can be seen that the voltage distri-

FIG. 2·1.

TYPICAL VOLTAGE DISTRIBUTIONS ON A POLLUTED STRIP

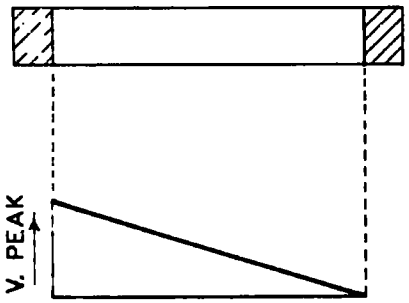

a. WETTING BEGINS
$i \simeq$ 10 MA

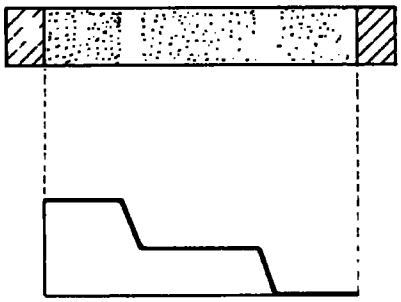

b. DRY BANDS FORM
$i <$ 1 MA

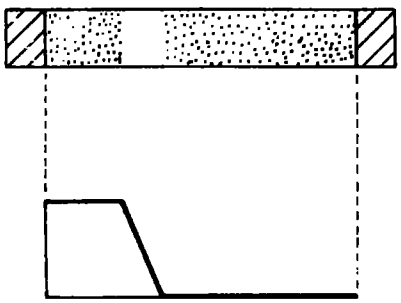

c. ONE DRY BAND PREDOMINATES.
$i <$ 1 MA.

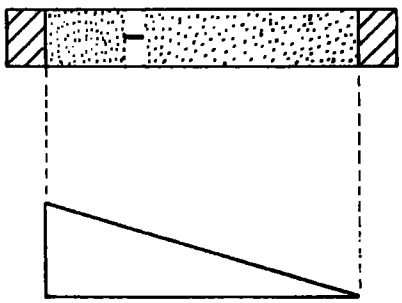

d. DRY BAND FLASHES OVER.
$i \simeq$ 100 MA

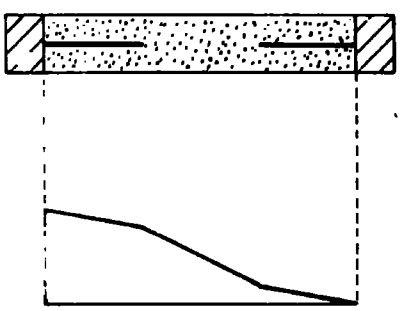

e. ARCS EXTEND
$i \simeq$ 200 MA

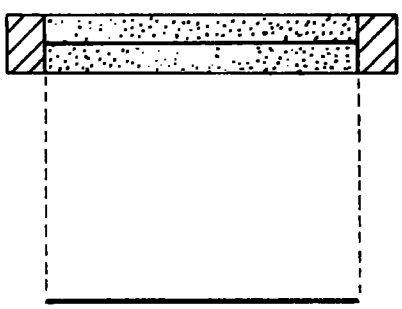

f. FLASHOVER COMPLETE.
$i \simeq$ 5A.

bution was linear; this according to Hampton[2] was because of an initial uniform resistivity. However, this condition is unstable as there must be areas with slightly higher resistance than the rest of the surface. These areas dissipate more heat and consequently dry out faster and this process leads to high resistance dry bands. Hampton[2] found it impossible to produce a polluted layer so uniform that when a leakage current was flowing it did not produce one or more dry bands within a short time. He also found that invariably when several dry bands formed, one would predominate after a short time and hence very nearly all the voltage was distributed across this one dry band. Hampton[2] found that the width of the dry band altered until the voltage stress across it was just less than that required to initiate a discharge in the air. Thus when any small water particle fell on the dry band this distorted the electric field and the breakdown value of air was exceeded. Consequently a discharge was initiated and a surge of current increased the heat dissipation until the dry band was re-established. The frequency of the surges was such that the mean power dissipated in the dry band was just sufficient to keep it dry. A small but gradual increase in the voltage applied, merely caused the dry band to widen whereas a small but sudden increase could cause a complete flashover. It was found that most discharges extinguished, but occasionally they could extend to span the whole dry band and hence lead to flashover. Hampton[2]

found that when this happened the arc extinguished at zero current, but would restrike on the next half cycle and rapidly extend to span the whole surface. The diagrams d. e. and f. show the voltage distribution on successive cycles under this condition. On the first of these cycles (shown in d.) the voltage distribution is relatively linear, but on the subsequent cycle the arc has extended and a greater proportion of the voltage is dropped across the remaining part of the polluted surface. This in turn leads to another dry band forming and flashing over immediately, and finally the discharges combine to span the whole surface.

The work on uniform loss of moisture has been carried out by McIlhagger and others[5] and a relationship between final resistivity $\rho_{s\infty}$ and the voltage gradient derived. This work was carried out in humidities ranging from 40% to 95% relative humidity. The surface resistivity was determined by current voltage measurements with a certain amount of care, using in-phase component of current to avoid errors, and also shielding to avoid stray capacitance. In the examination of this phenomenon they used miscroscope slides taken directly from the manufacturer's pack. These slides already fairly uniformly contaminated, proved to be consistent throughout the whole box.

A typical curve of $\rho_{s\infty}$ versus voltage gradient E for a particular humidity is reproduced on Fig. 2.2 and the curve conforming to the suggested relationship is shown in broken lines.

FIG. 2.2

SPECIMEN 'H'
RELATIVE HUMIDITY, 65 %.
TEST Nº 10.

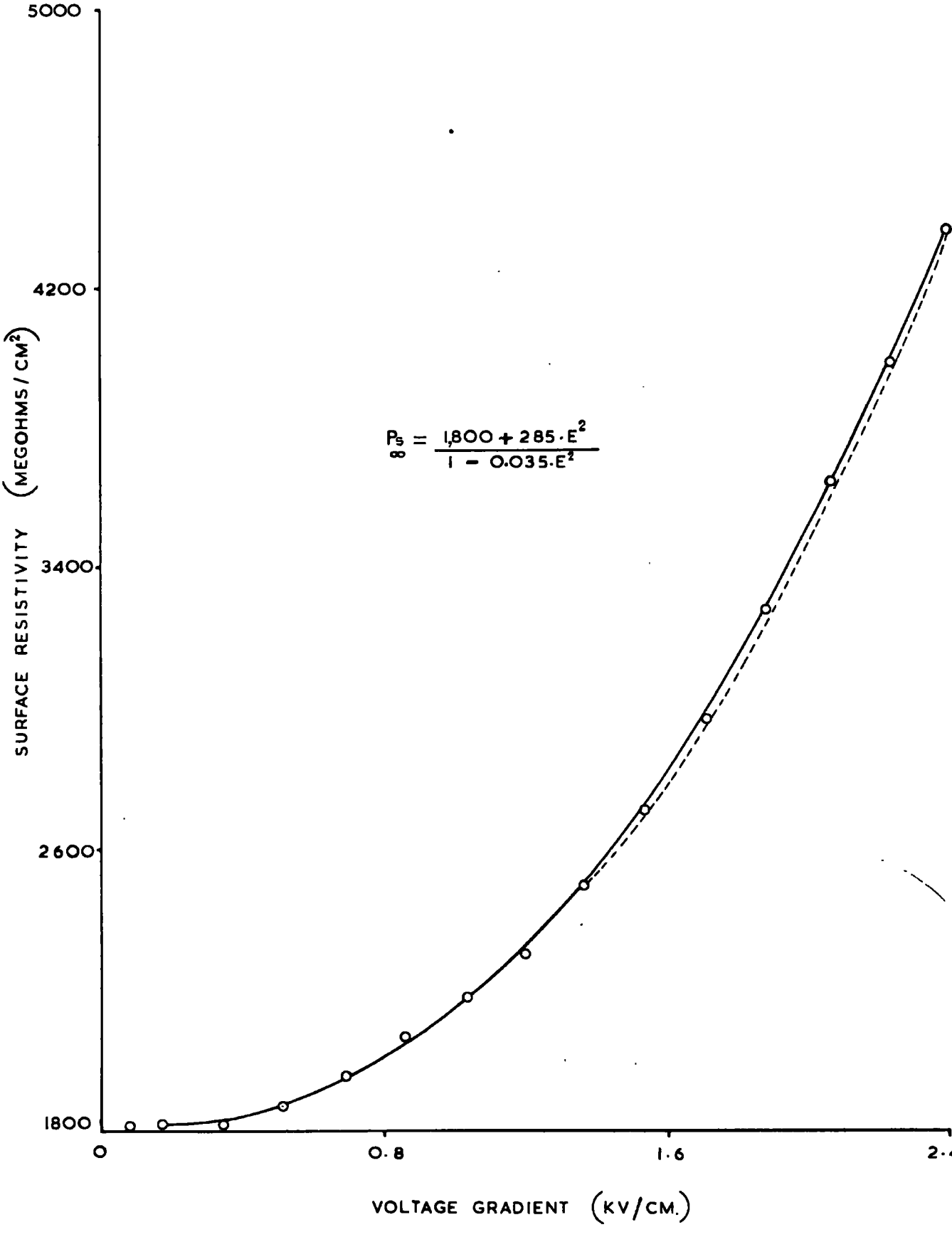

There are only small deviations between the experimental and theoretical curves.

The theoretical relationship arrived at by McIlhagger (5) et al. originates from three factors concerning the loss and deposition of moisture on the contaminated surface:-

1. Joulean evaporation, owing to heat generated in the surface.
2. Electrostatic attraction of moisture to the surface.
3. Van der Vaal's forces transferring moisture to or from the surface.

The rate of evaporation of moisture must be a function of the power applied to the specimen.

Let power dissipated per unit area $= \frac{E^2}{\rho_{s\infty}}$

hence rate of evaporation of moisture $= K_1 \frac{E^2}{\rho_{s\infty}}$

The rate of deposition (or depletion) of moisture owing to electrostatic forces $= K_2 E^2$

The rate of deposition owing to Van Der Vaal's forces $= K(t_o - t_\infty)$ or $K_3\left(\frac{1}{\rho_{so}} - \frac{1}{\rho_{s\infty}}\right)$

In a state of equilibrium, the rate of loss of moisture must equal the rate of deposition of moisture.

Therefore $K_1 \frac{E^2}{\varsigma_{s\infty}} = K_2 E^2 + K_3\left(\frac{1}{\varsigma_{so}} - \frac{1}{\varsigma_{s\infty}}\right)$

this gives $$\varsigma_{s\infty} = \frac{\varsigma_{so} + AE^2}{1 + BE^2}$$

where $A = \varsigma_{so} \frac{K_1}{K_3}$ and $B = \varsigma_{so} \frac{K_2}{K_3}$

McIlhagger[5] found that in most cases of his work the index B, in the above expression for $\varsigma_{s\infty}$ was so small as to suggest that the effect of electrostatic forces was negligible. This reduces the above expression to the form

$$\varsigma_{s\infty} = \varsigma_{so} + AE^2$$

$$= \varsigma_{so}(1 + aE^2)$$

The above equation may be expressed in terms of resistance rather than resistivity.

Thus $$R_{s(v)} = R_{s(o)} + AV^2$$

where $R_{s(o)}$ is initial resistance and $R_{s(v)}$ is final resistance. This equation was used by Salthouse[6] in his work on initiation of dry bands on polluted insulation.

This can be rewritten as follows:-

let $a = \frac{R_{s(v)}}{R_{s(o)}}$ and $K = \frac{A}{R_{s(o)}}$

then $$a = 1 + KV^2$$

which can be written as:-

$$\text{LOG}_{10}(\alpha - 1) = \text{LOG}_{10} K + 2\,\text{LOG}_{10} V$$

Fig. 2.3 is reproduced from Salthouse[6] showing $\text{LOG}_{10}(\alpha - 1)$ plotted as a function of $\text{LOG}_{10} V$ for increasing contamination levels.

The contaminant used here was lithium chloride.

It can be seen that the slope is close to 2, except for greater contamination levels than 0.6mg per square cm. At higher concentrations of contamination the slope increases and a visible wet film is formed on the surface.

The maximum difference of final resistance to initial resistance from these results is of the order of a thousand times greater.

Thus $$\alpha = \frac{R_{s(v)}}{R_{s(o)}} = 1000$$

These results cover a much larger range of resistance than those of McIlhagger where α is of the order of:-

$$\alpha \approx \frac{5000}{2000} = 2{\cdot}5$$

McIlhagger has in a later work[13] studied the non-uniform evaporation of moisture and developed a criterion for the onset of dry band formation.

Using the same type of slides as before, and deliberately introducing a band cleaner than the rest of the slide perpendicular to the direction of current flow, a simple

FIG. 2.3

VARIATION IN DRY BAND RESISTANCE WITH APPLIED VOLTAGE.

WEIGHT OF LITHIUM CHLORIDE PER SQUARE CENTIMETRE :-

o - 0.096 MG.

X - 0.3 MG.

△ - 0.6 MG.

● - 1.2 MG.

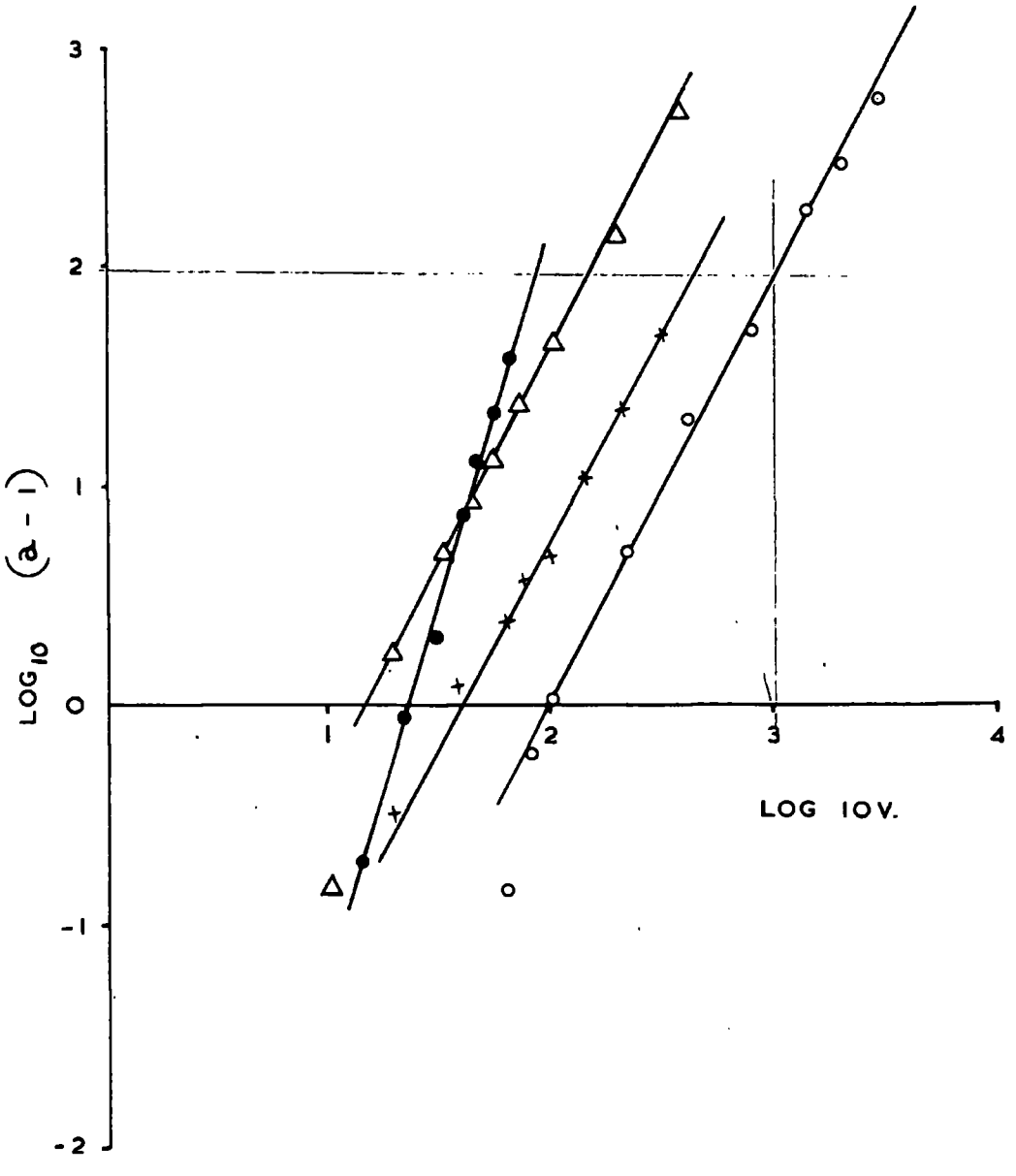

non-uniform contamination was achieved.

Considering this type of sample with a band length of W per unit with a voltage gradient of E_1 per unit, and the remaining part of the sample (1 - W) per unit with a voltage gradient of E_2 per unit, at a supply voltage of V per unit and a leakage current of I per unit, then:-

$$V = WE_1 + (1 - W)E_2$$

The relationship between E_1, E_2 and I according to McIlhagger[13] are reproduced in Fig. 2.4 and the E/I curves, being identical but transposed, conform to the law:-

$$\rho_{s\infty} = \rho_{so}(1 + E^2)$$

For any value of E_1 chosen, the corresponding value of I can be found by reference to Fig. 2.4. Then having found I, E_2 can be found by cross reference to the curve E/I concerning the remaining part of the sample (I - W). Now considering ascending values of E_1, it can be seen that for a certain value of E_1, I is at its maximum and the corresponding value of E_2 is given by the curves in Fig. 2.4, say E_2'. It is quite clear that if E_1 is increased beyond this value, the current will decrease and so will the corresponding value of E_2. Thus for any value of E_1, $E_2' < E_{2\text{maximum}}$ must hold, hence the voltage gradient in the portion (I - W) never reaches a value where the power dissipated can cause a dry band to form. Whereas the power dissipated in the section W will cause moisture to be lost from the surface and hence alter its resistivity

FIG. 2.4

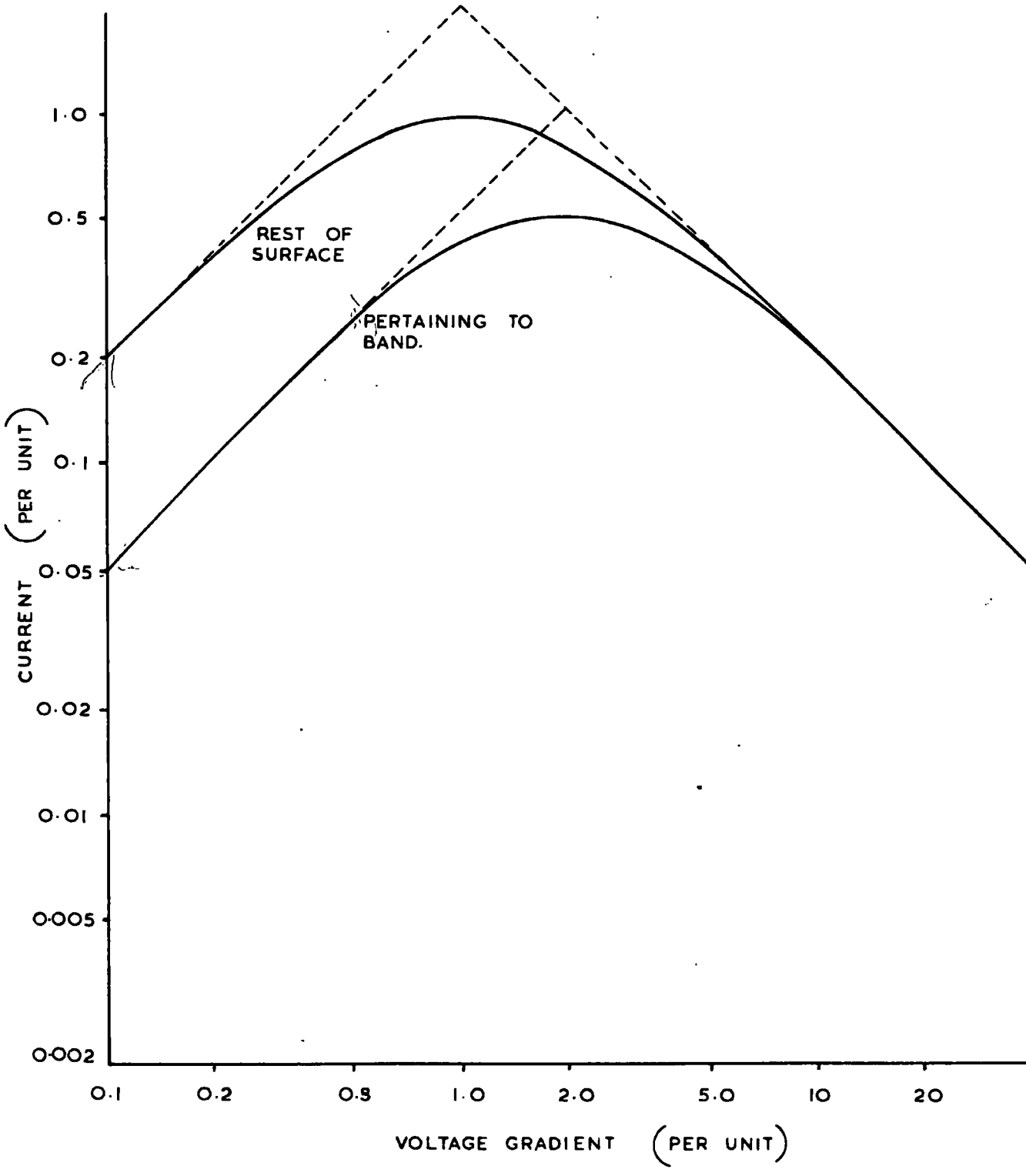
1·0
0·5
0·2
0·1
0·05
0·02
0·01
0·005
0·002
CURRENT (PER UNIT)
REST OF SURFACE
PERTAINING TO BAND.
0·1
0·2
0·5
1·0
2·0
5·0
10
20
VOLTAGE GRADIENT (PER UNIT)

for values of E_l beyond the I maximum point.

Having repeated the experiment for various values of W, McIlhagger[13] found that for band lengths smaller than or equal to 0.025 per unit the voltage gradient E_l rose instantaneously to a dangerous value when the applied voltage was increased. However, for band lengths greater than 0.025 per unit the system was stable, hence no sudden increase in voltage gradient occurred.

McIlhagger[13] does, however, find it probable that such a surface, having a critical applied voltage at a low humidity would have a lower critical voltage at a higher humidity. Alternatively for a surface with a given applied voltage there may well be a critical humidity above which an instaneous increase in voltage gradient may take place.

Salthouse[6] has studied the initiation of dry bands and derived a criterion for the initiation of water loss from the surface of an insulator. He has defined the current density in amps per unit width, surface current density rather than volume current density, and relates the field strength by the surface resistivity.

$$\bar{E}_s = \varsigma_s \bar{J}_s$$

Thus the power dissipated per unit area is:-

$$P_s = E_s J_s = \frac{E_s^2}{\varsigma_s}$$

From his work he found that most of this heat was lost by convection.

According to Newton's law of cooling, the heat trans-

ferred per unit area of surface per second by convection is:-

$$P_c = h_s \Delta T$$

where h_s = heat transfer coefficient

and ΔT = temperature difference between surface and ambient.

At equilibrium the heat loss must be equal to heat generated in the surface by the leakage current:-

Thus $$P_c = P_s$$

hence $$h_s \Delta T = \frac{E_s^2}{\rho_s}$$

If the temperature rise necessary to cause a change in the resistivity is known then the minimum field strength necessary to initiate evaporation can be found:-

$$E_{s\,min} = \sqrt{h_s \Delta T_{min} \rho_s}$$

3.1. HEAT TRANSFER FROM A POLLUTED SURFACE

The flow of current through a resistive surface film causes power dissipation in the film. In the case of a polluted surface on an insulator, the resistivity of the polluted layer is some function of the moisture absorbed by it. Invariably the resistance of this layer is much less than the actual surface resistance of the insulator; thus in comparison, the surface resistance may be ignored. Because of the power dissipation in the surface film the temperature will rise. The temperature rise will cause moisture loss from the surface film and this will, in turn, increase the resistivity of the film. The resistivity will continue to increase until a state of equilibrium is reached at which the moisture loss from the surface equals the moisture absorbed by the surface. By further increasing the current through the surface film, the process described above is repeated up to a point where non-uniform evaporation takes place.

The non-uniform evaporation may be caused by non-uniformity in the surface film which may be in the form of differences in thickness or uneven film density. A small difference in thickness will affect the bulk resistance per unit length of the film and hence cause a slight non-uniform field distribution.

An unevenness in the film density will affect the film's ability to absorb moisture and this will result in irregularities in the surface resistivity of the film and hence cause a non-uniform field distribution.

If a non-uniform field distribution exists in a surface this means that certain sections of the surface have a higher voltage drop per unit length than others. Consequently the power dissipation in such a section is higher than anywhere else along the specimen. The temperature is higher and the rate of loss of moisture is higher and therefore the ~~per unit~~ resistivity is higher.

Considering the heat losses from the film, there are three ways in which heat can be dissipated from the point where it is generated. The least significant is radiation. The temperature difference between the specimen and ambient is only of the order of 10 °C and therefore radiation can safely be ignored when considering the heat loss from the film.

Convection is of a far greater importance and must be considered more carefully. For convection to take place there must be a transfer of heat energy from the specimen to the air molecules adjacent to the surface of the specimen. This transfer of heat is dependent on the velocity of the air above the surface as well as the temperature difference. Hence a forced cooling where the velocity is kept constant will simplify matters as this leaves only the temperature difference as a variable along the surface.

Conduction plays a large part in carrying the heat away from the point where it is generated. Although a large amount of the heat is conducted away, most of it will eventually be transferred to the air molecules along the surface film and thus be carried away be convection. The

immediate effect of conduction is thus to distribute the heat more evenly along the surface, flowing from the point of highest temperature to points of lower temperature. Because of conduction there cannot be a sharply defined area of higher temperature, thus the temperature of an adjacent small area will be higher than the temperature caused by its own heat dissipation. Consequently the heat conduction in the surface film will affect the width and shape of any dry band formed.

For the purpose of the following discussion it is useful to think in terms of a simple system as shown in Fig.3.1. This consists of a strip of insulation contaminated on one side and suspended between two electrodes. Owing to the current flow, heat will be generated in the surface, and the temperature will rise. Considering a point P along the surface where the surface resistivity is ς_s , then the electric field strength at P, ignoring the resistivity of the insulator strip, is given by:-

$$\bar{E}_s = \varsigma_s \bar{J}_s$$

where $\bar{J}_s$ is the surface current density.
Just as ς_s is not a true resistivity $\bar{J}_s$ is not a true current density, but is defined as the current flow per unit width of surface perpendicular to the direction of current flow.

The power dissipated per unit area is given by:-

$$P_s = E_s J_s = \varsigma_s J_s^2 = \frac{E_s^2}{\varsigma_s}$$

FIG. 3·1

SCHEMATIC DIAGRAM OF THE SAMPLE AND ELECTRODES.

I_S - SURFACE LEAKAGE CURRENT.
L - TOTAL LENGTH OF SPECIMEN.

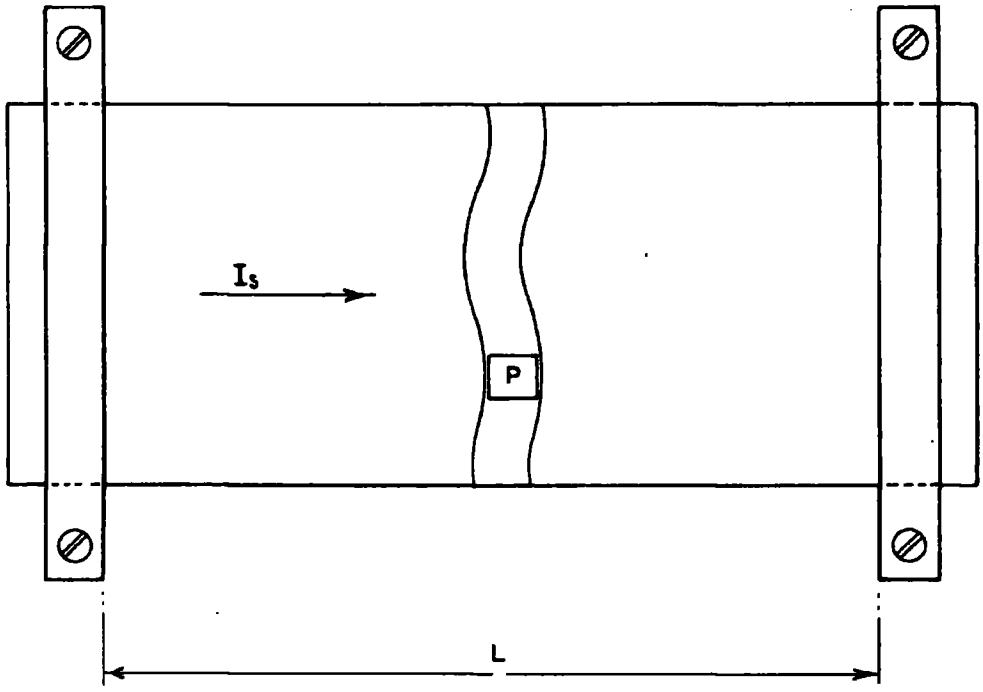

The behaviour of the surface film due to current flow can be studied as a function of the voltage applied to it, in which case it can be split into two parts:-

Part 1 - is considering the case in which the voltage applied to the film is less than the critical level, V_c . In this region the film behaves essentially in a linear manner, so that when voltage is increased, current flow increases correspondingly. This part is termed as uniform evaporation.

Part 2 - is considering the behaviour of the film for applied voltages above the critical level. For applied voltage above this level the evaporation of moisture becomes significant, and as mentioned previously, the resistivity will alter and the relationship between current and applied voltage is no longer linear; in fact, the current decreases with increasing voltage.

Salthouse[6] has shown that the critical voltage corresponds to the power dissipation necessary to raise the surface temperature to the minimum required to initiate evaporation. Assuming that the heat generated is transferred from the film by convection then:-

$$V_c = \text{constant} \times \sqrt{R_{s(o)}}$$

where $R_{s(o)}$ is the initial resistance of the surface assuming a uniform ς_s .

The constant is derived from a given system and depends on the geometry of the system as well as the heat transfer coefficient.

3.2. TEMPERATURE DISTRIBUTION FOR UNIFORM SURFACE RESISTIVITY.

In the previous discussion the heat lost by conduction in the film has been ignored as it was found to be small in comparison with heat lost by convection. It is, however, possible to work out a theoretical temperature distribution along a wet contaminated surface allowing for heat conduction as well as convection. This work is based on an equation given by Jacob[17] of the temperature Θ at a distance X from the centre of a rod.

$$(\Theta - \Theta_o) = 2\left(\Theta_o - \frac{q'''}{Km^2}\right)\left(\sinh \frac{mX}{2}\right)^2 \qquad 3.1$$

where Θ_o is maximum temperature at $X = O$

If the length of the rod is $2L$ and $\Theta = O$ at $X = L$ then the equation becomes:-

$$\Theta_o = \frac{2\left(\frac{q'''}{Km^2}\right)\left(\sinh \frac{mL}{2}\right)^2}{1 + 2\left(\sinh \frac{mL}{2}\right)^2} \qquad 3.2$$

where q''' = electrical power dissipated per unit volume of the rod.

K = thermal conductivity of the rod.

$$m^2 = \frac{hc}{KA}$$

where h = heat transfer coefficient (surface)

c = circumference of the rod.

A = cross sectional area.

By drawing an analogy between the parameters used by Jacob[17] in his equation and those related to a wet surface film, it is possible to work out the theoretical temperature distribution along the surface.

Let q_s = electrical power dissipated per unit area of film, and this will be analogous to q''' in Jacob's equation[17].

Therefore:- $$q_s = q''' = \frac{J_s^2}{\sigma_s}$$

where J_s = surface current density

and σ_s = surface electrical conductivity

Now A = cross sectional area, which in case of the film is:-

$$A = C \cdot \delta$$

where C = width of the film

and δ = thickness of the film

In Jacob's equation[17]: $$m^2 = \frac{hc}{KA}$$

In the case of the film substituting for A gives:-

$$m^2 = \frac{h}{K\delta} = \frac{h}{K_s}$$

where K_s is the surface thermal conductivity,

$$K_s = \delta K$$

and signifies the heat transferred across a unit square of the surface when the temperature difference between opposing sides is $1^{\circ}C$.

The paramer K_s has units of watts per $^{\circ}C$.

Now h has units, watts $^{\circ}C^{-1}\ cm^{-2}$ and therefore m has dimensions of cm^{-1} .

Substituting the parameters related to the film in Jacob's equation[17] gives:-

$$\frac{q'''}{Km^2} = \frac{q_s}{K_s m^2} = \frac{J_s^2}{\delta_s K_s m^2} = \frac{J_s^2}{\delta_s h}$$

Hence the total equation 3.1 can be rewritten as follows:-

$$(\theta - \theta_o) = 2\left(\theta_o - \frac{J_s^2}{\delta_s K_s m^2}\right)\left(\sinh \frac{mX}{2}\right)^2 \qquad 3.3$$

Similarly equation 3.2 can be rewritten:-

$$\theta_o = \frac{2\left(\frac{J^2}{\delta_s K_s m^2}\right)\left(\sinh \frac{mL}{2}\right)^2}{1 + 2\left(\sinh \frac{mL}{2}\right)^2} \qquad 3.4$$

Now if $mL >> 10$, equation 3.4 simplifies to:-

$$\theta_o \doteq \left(\frac{J_s^2}{\delta_s K_s m^2}\right) \doteq \left(\frac{J_s^2}{\delta_s h}\right) \qquad 3.5$$

It is quite evident that the form of the solution of equation 3.3 depends largely on the magnitude of mL and if $mL >> 10$ there is no significant change in temperature over the surface except at the electrodes. However, if mL is less than 10, a considerable change in temperature occurs across the surface.

By using the following values, graphs were drawn

for $\theta \sim X$ for different values of mL.

$$q_s = 10^{-3} \text{ watts /cm}^2$$

$$h = 10^{-3} \text{ watts cm}^{-2} {}^{\circ}\text{C}^{-1}$$

Therefore $\theta_{o(max)} = 1^{\circ}\text{C}$.

The graph in Fig.3.2 shows that for values of K_s less than 10^{-4} watts ${}^{\circ}\text{C}^{-1}$, the surface temperature is virtually constant across the surface up to the electrodes.

If m is large, then equation 3.3 can be written:-

$$(\theta - \theta_o) = \left(\theta_o - \frac{J_s^2}{\sigma_s h}\right) e^{\frac{mX}{2}} \qquad 3.6$$

Then relaxation distance is $\frac{2}{m}$ which is an indication of the order of the distance over which the temperature change occurs.

Valuation of K_s :-

For water: $K = 5{\cdot}6 \times 10^{-3}$ watts cm^{-1} ${}^{\circ}\text{C}^{-1}$

Assuming a film thickness: $\delta = 40 \times 10^{-3}$ cm

Therefore:- $K_s = 2{\cdot}24 \times 10^{-4}$ watts C^{-1}

This gives a relaxation distance of the order of 1 cm .

FIG. 3.2

TEMPERATURE DISTRIBUTION FOR K_S
INDEPENDENT OF TEMPERATURE

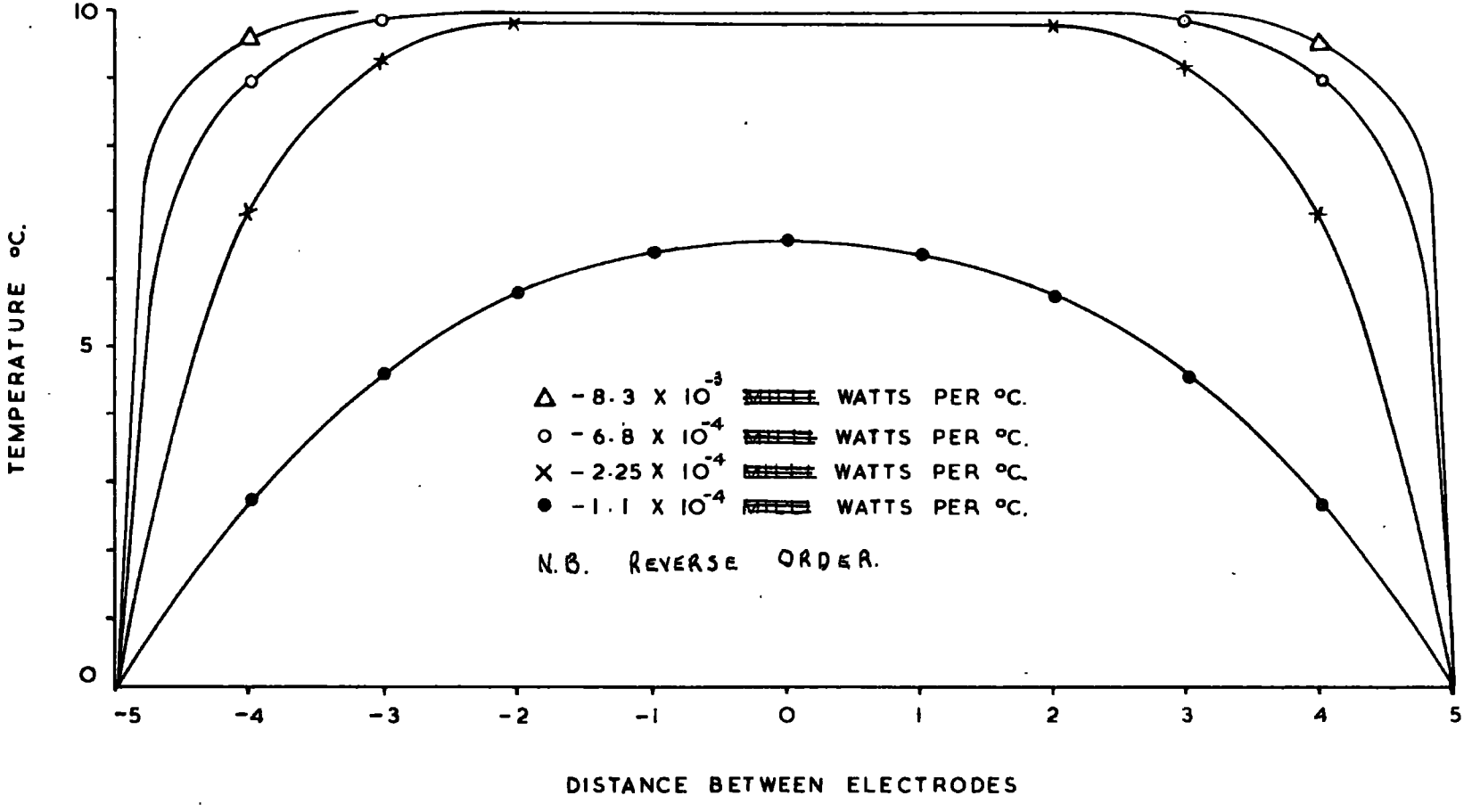

3.3. TEMPERATURE DEPENDENCE OF SURFACE RESISTIVITY

At temperatures above the critical temperature evaporation of moisture from the surface can no longer be neglected. Consequently the resistivity of the polluted surface can no longer be treated as being independent of temperature. The polluted layer on an insulator is electrolytic, thus the resistivity of this layer is dependent on the amount of moisture content of the layer, hence at temperatures higher than the critical temperature for evaporation, moisture will be lost from the surface and one would expect a change in surface resistivity.

Smail, Brooksbank and Thornton[14] showed by experiments that the surface resistance of clean glass increased logarithmically with an increase in surface temperature above ambient.

It is quite clear that no simple relationship exists between the amount of water absorbed by a polluted surface and the relative humidity of its surrounding atmosphere. Nor is there any simple relationship between the surface resistivity and the relative humidity. However, from experimental results the surface resistivity varies with temperature in a manner shown in Fig. 4.17.

An increase in surface temperature with respect to the ambient temperature increases the saturated vapour pressure adjacent to the surface and therefore the relative humidity at the surface is decreased. Because of the decrease in the relative humidity the equilibrium between evaporation and absorption is disturbed and more moisture

will evaporate from the surface until a new equilibrium is reached. Because of this loss of moisture there is an increase in surface resistivity and the experimental work shows that this increase in resistivity related to temperature is governed by the following equation:-

$$\rho_s = \rho_{so}\, e^{\alpha\theta}$$

where $\theta = T_s - T_a$

and $\alpha = 0{\cdot}77 / ^{\circ}C$

and $T_s =$ surface temperature

and $T_a =$ ambient temperature

and $\rho_{so} =$ initial surface resistivity

The temperature constant of the equation:-

$$\theta_c = 1/\alpha = 1{\cdot}3\ ^{\circ}C$$

is related to the minimum temperature rise above ambient required to cause an appreciable change in surface resistivity and consequently evaporation owing to power being dissipated. Thus by definition θ_c is the critical temperature.

The constant α is depending on the initial electrical and thermal properties of the pollution and it is thus impossible to determine its value in any other way than by experimental results.

3.4. DRY BAND FORMATION

The forming of dry bands on the surface of polluted insulation may be compared with a simple model consisting of several thermistors connected in series; all having a positive temperature coefficient and identical characteristics and being connected in close proximity to each other. The voltage current characteristic of the thermistor is very close to that of a polluted surface, in as much as the peak current corresponds to the power dissipation required to raise the temperature to such a level that a change in resistance becomes effective. Furthermore, once this critical dissipation occurs, only a slight increase in temperature has a drastic effect on the increase in resistance. Because of the increase in resistance a much larger proportion of the applied voltage appears across one particular element compared with the others. Consequently, once this condition is established the power dissipated in this element is greater than in any of the others, and as the current is limited by this element and decreasing with increasing voltage, an increase in voltage cannot initiate such a condition in any of the other elements.

This has been shown by Löberg and Salthouse[15] by plotting the experimental characteristics of two identical p.t.c. thermistors back to back on the same graph, as shown in Fig. 3.3.

This clearly indicates that there are two positions of equilibrium, one at point (a) and one at point (b).

FIG. 3.3

VOLTAGE DIVISION BETWEEN TWO IDENTICAL P.T.C. THERMISTORS WITH 25 VOLTS APPLIED.

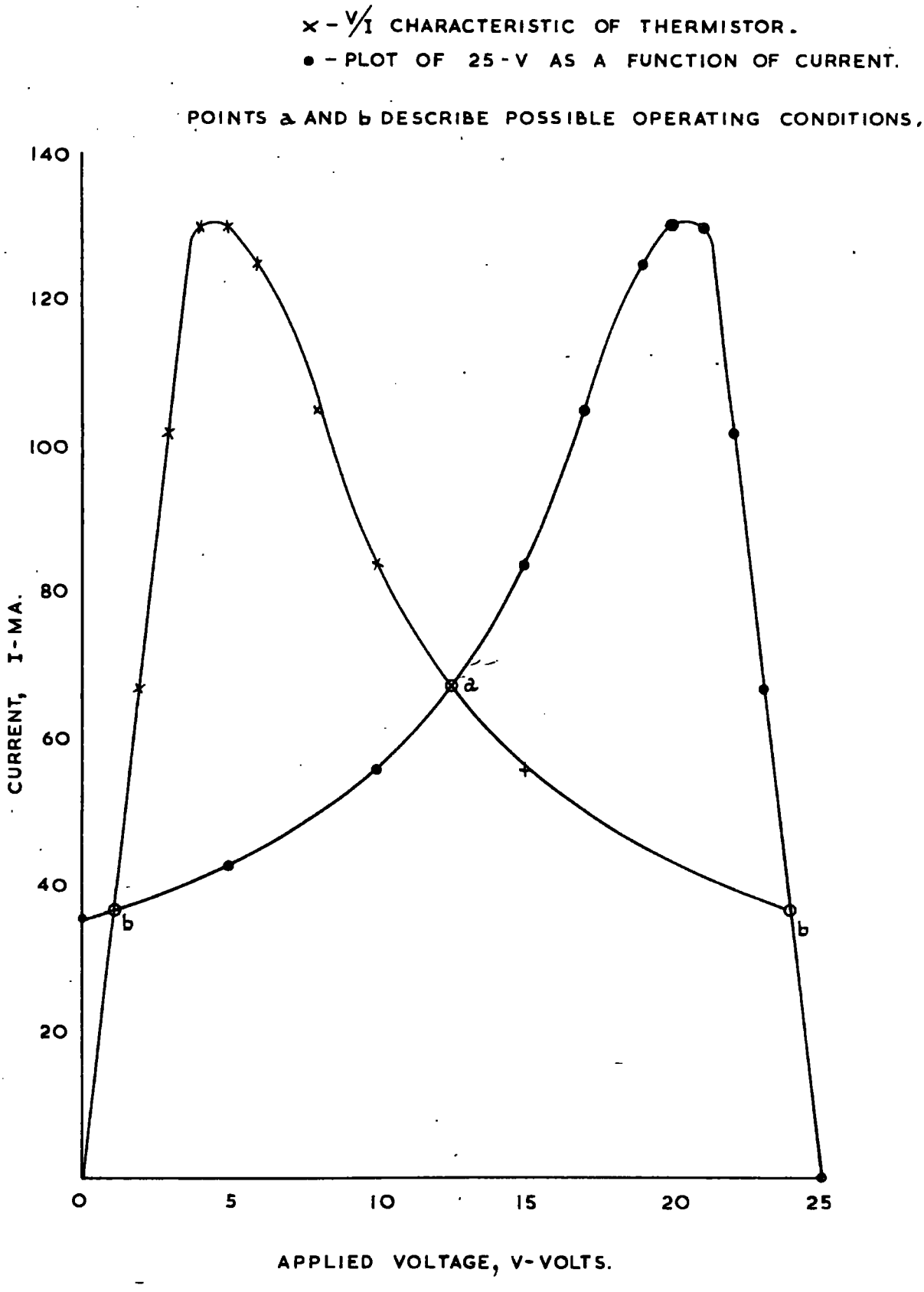

Point (a) corresponds to equal voltage division and point (b) to unequal division and from experimental results the former is unstable and the latter is stable.

Considering point (a) at which the resistance of the two elements are equal, R_1 and R_2 respectively. Let R_1 be increased by a small amount and R_2 will therefore decrease by an equally small amount thus:-

$$\frac{dR_1}{dV} \simeq \frac{dR_2}{dV}$$

The power dissipated in R_1 is:-

$$P_1 = \frac{V^2}{(R_1 + R_2)^2} R \simeq \text{constant} \times R_1$$

Therefore $$\frac{dP_1}{dR_1} \simeq \text{constant, and positive.}$$

This shows that a small increase in R_1 will cause runaway and consequently point (a) is unstable.

At point (b), $$R_1 >> R_2$$

and $$P_1 \simeq \left(\frac{V}{R_1}\right)^2 R_1$$

Therefore $$\frac{dP_1}{dR_1} = - \frac{V^2}{R_1^2}$$

This is negative and corresponds to a stable state.

The main difference between the behaviour of a series of p.t.c's to that of a polluted surface is the abrupt change from a uniform voltage distribution to the state

of a distinctly non-uniform distribution using p.t.c's. compared with the slower and less distinct transition in the case of a polluted surface.

The main reasons for this difference may be accounted for by the fact that the thermal conductivity in the case of the p.t.c's was very much less than that of the polluted surface, and also the different temperature levels at which the transition took place.

The thermal coupling between the thermistors was rather poor, thus sideways conduction was small compared with the continuous surface film on an insulator. Because of this the heat generated in one element had very little effect on the neighbouring element. Once the transition point was reached in one element, less heat would be generated in the neighbouring elements and these would therefore cool down corresponding to their own heat dissipation, and thus individually follow their own resistance temperature characteristic.

The transition from uniform to non-uniform state took place at a much higher temperature than was the case with the polluted surface. The difference in temperature between the two systems at the point of uniform to non-uniform voltage distribution was of the order of $100^{o}C$. Because of this high temperature the elements, having a decreasing power dissipation, would cool much faster and thus exhibit a more rapid decrease in resistance compared with the polluted surface adjacent to a dry band.

However, it was noted that by increasing the fan

speed in the case of polluted insulation the transition period was greatly reduced and more marked. This was owing to a higher rate of cooling of the surface and consequently a higher rate of power dissipation was required to raise the temperature sufficiently to initiate the transition. As soon as the dry band was formed, the sections of the surface adjacent to the dry band would cool down to a comparatively lower temperature and have a more marked decrease in their resistivity than at a lower fan speed. Consequently, the dry band would be narrower and more sharply defined.

A polluted surface film, having a temperature above its critical temperature for dry band formation behaves as a distributed net-work of p.t.c. resistors with a low critical temperature and appreciable limitation in heat conduction along the surface. This means that although a polluted surface tends to form a dry band at any voltage above its critical voltage, an immediate collapse to a narrow width depends on its sideways conduction which tends to determine the temperature distribution. Thus if the lateral conduction is reduced or the critical temperature increased, then the transmission from uniform voltage distribution to non-uniform distribution will be more sharply defined.

The condition required to enable a polluted surface to give a fast collapse of the dry band is a higher critical temperature. This is achieved in a thick and very wet film, say $\frac{1}{8}$" thick where the temperature necessary to

cause considerable evaporation would be of the order of $100^{o}C$. This increase in thickness would give rise to a higher lateral conductivity of the heat generated which would tend to widen the dry band. However, the effect of the critical temperature appears to be more important. Therefore it can be concluded that the wetter the surface film, the more drastic is the transition from a uniform state to a non-uniform state.

3.5. DRY BAND WIDTH

As no simple relationship exists between the surface resistivity, temperature and the moisture evaporated from the surface, it is impossible to deduce a relationship for the actual width of the dry band in terms of the electrical and thermal properties of the surface. If, however, the heat conduction can be ignored and just the heat lost by convection considered, a very simple expression can be found. For a well established dry band this is substantially correct as the heat lost by conduction is much smaller than the heat lost by convection.

Then heat lost from the dry band is:-

$$h_s L X \Theta \quad \text{watts}$$

where Θ is the temperature of the dry band above ambient. Assuming all the applied voltage appears across the dry band, then the power dissipated is:-

$$P = \frac{V^2}{R_s}$$

where R_s is the total dry band resistance.
In a state of equilibrium, the heat lost must equal the heat generated, therefore:-

$$\frac{V^2}{R_s} = h_s L X \Theta$$

but $$R_s = R_{so} e^{\alpha\Theta}$$

and $$R_{so} = \rho_{so} \frac{X}{L}$$

where X = the width of the dry band

and L = the distance across the dry band (i.e. width of the specimen)

Therefore by substituting for R_s and R_{so} in the foregoing equation, one gets a relationship between dry band width and temperature;

$$\frac{V^2 L}{\rho_{so} X} = h_s L X \Theta \, e^{\alpha\Theta}$$

$$\frac{V^2}{h_s \rho_{so} X^2} = \Theta \, e^{\alpha\Theta}$$

But $\frac{1}{h_s \rho_{so}}$ is a constant

Therefore, $\text{Constant} \times \frac{V^2}{X^2} = \Theta \, e^{\alpha\Theta}$

Although an analysis of the dry band behaviour in terms of resistivity and current density is useful it does not, strictly speaking, give an accurate account of the physical properties of the dry band, as the film thickness is unknown. In the foregoing analysis the film has been treated as having no volume, thus only a surface current density has been used whereas the true current density is a function of the film thickness.

Although the film thickness is unknown, one must bear in mind that the true current density will increase in the dry band as this contains less moisture and hence

represents a thinner electrolytic film than the rest of the sample. As the current density is increased, the power dissipated per unit volume of pollution will be higher as this relates to current density in the manner shown.

$$P = J^2 \varrho_v$$

where ϱ_v is volume resistivity.

Thus the foregoing analysis of the behaviour of a surface film is valid for a film having an unknown thickness as far as the criterion for instability is concerned.

4.0. EXPERIMENTAL RESULTS

The full experimental details of the specimen, humidity chamber and measurement techniques are given in the appendix. The following notes are intended to serve as an introduction to the results.

The specimens used in the experiments as shown in Fig.4.1. were cut from Eastman Chromagram Sheets which had previously been doped with a solution of Cobalt Chloride in Methanol.

The specimen and electrodes were kept in a constant humidity chamber which was submerged in a water bath at constant temperature. The humidity was kept constant by a saturated salt solution in the bottom of the humidity chamber.

The voltage distribution across the specimen was measured by a capacitance probe scanned across the surface, for increasing values of applied voltage up to 5kV. The surface leakage current was recorded simultaneously.

Measurements of surface resistivity against temperature were also made and were used to determine the temperature distribution along the specimen. An infrared thermometer was developed to scan the specimen and thus it was possible to verify the temperature distribution obtained by using the relationship between surface resistivity and temperature.

Measurements were also made of leakage current and dry band width at a range of convection rates.

FIG. 4·1

DIAGRAM SHOWING THE DIMENSIONS OF
PERSPEX BLOCK, ELECTRODES AND SPECIMEN.

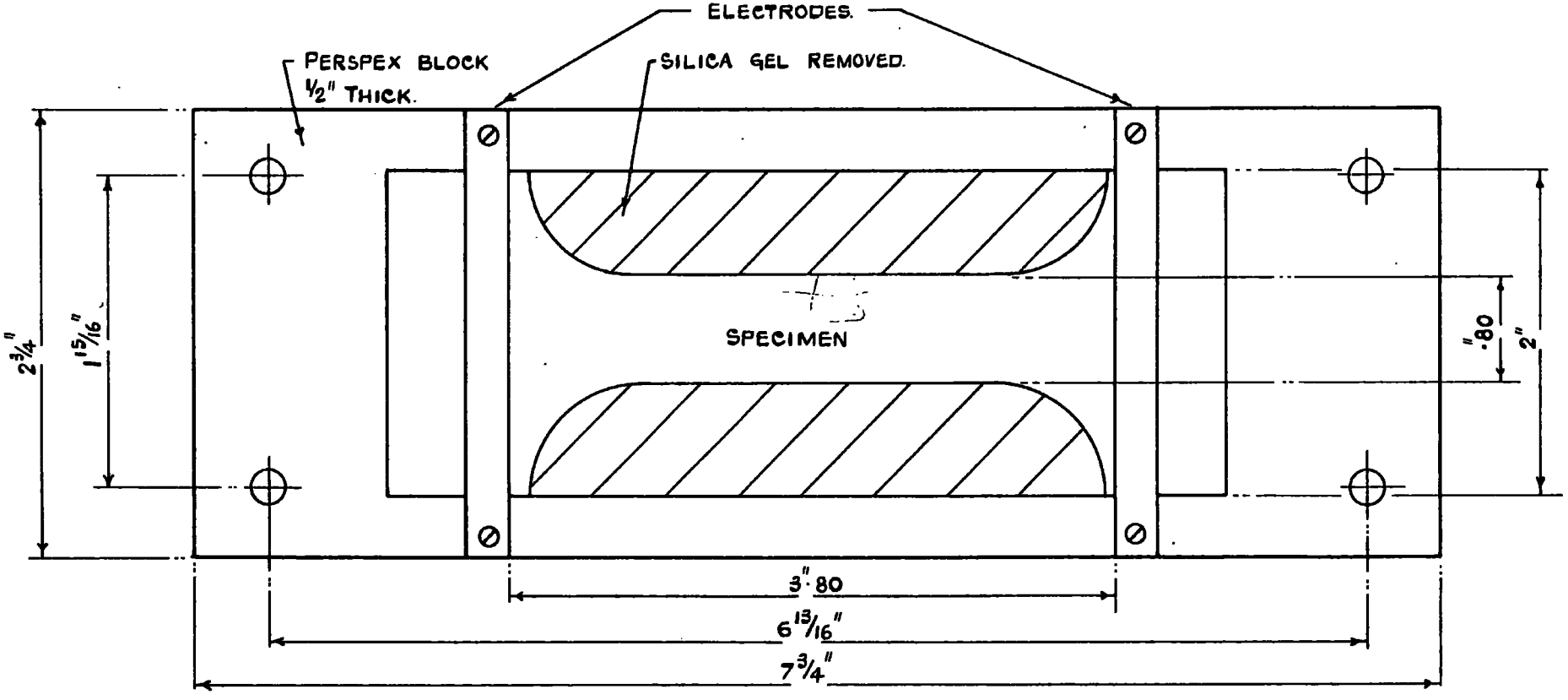

4.1. DRY BAND WIDTH AND CRITICAL VOLTAGE

For voltages less than the minimum voltage required to initiate evaporation, the relationship between leakage current and applied voltage is completely linear. This is true as the resistivity of the surface is a function of the moisture absorbed by it and will thus stay constant until moisture is lost from the surface. This is in agreement with the experimental results as can be seen in Fig.4.3.where the curve is a straight line at low voltages. When the applied voltage has exceeded the minimum required to cause loss of moisture, the resistance begins to alter and the relationship between current and voltage is no longer linear. For increasing voltages up to the value of applied voltage, which corresponds to the peak value of current, the evaporation of moisture is uniform and is increasing with increasing voltages. Uniform evaporation is maintained until the voltage reaches a point where the current reaches its peak value. This voltage is referred to as the critical voltage, Vc, because the dry band is initiated at this point. When the voltage is increased beyond this point a dry band is formed and the voltage distributed across the specimen collapses and nearly the whole supply voltage appears across the dry band. This is illustrated in Fig.4.3. where the dry band width and leakage current are plotted as functions of applied voltage.

The experimental results plotted in Fig. 4.4. show that once a dry band is initiated and the voltage is collapsing the band is reduced to a narrow band very

FIG. 4. 3

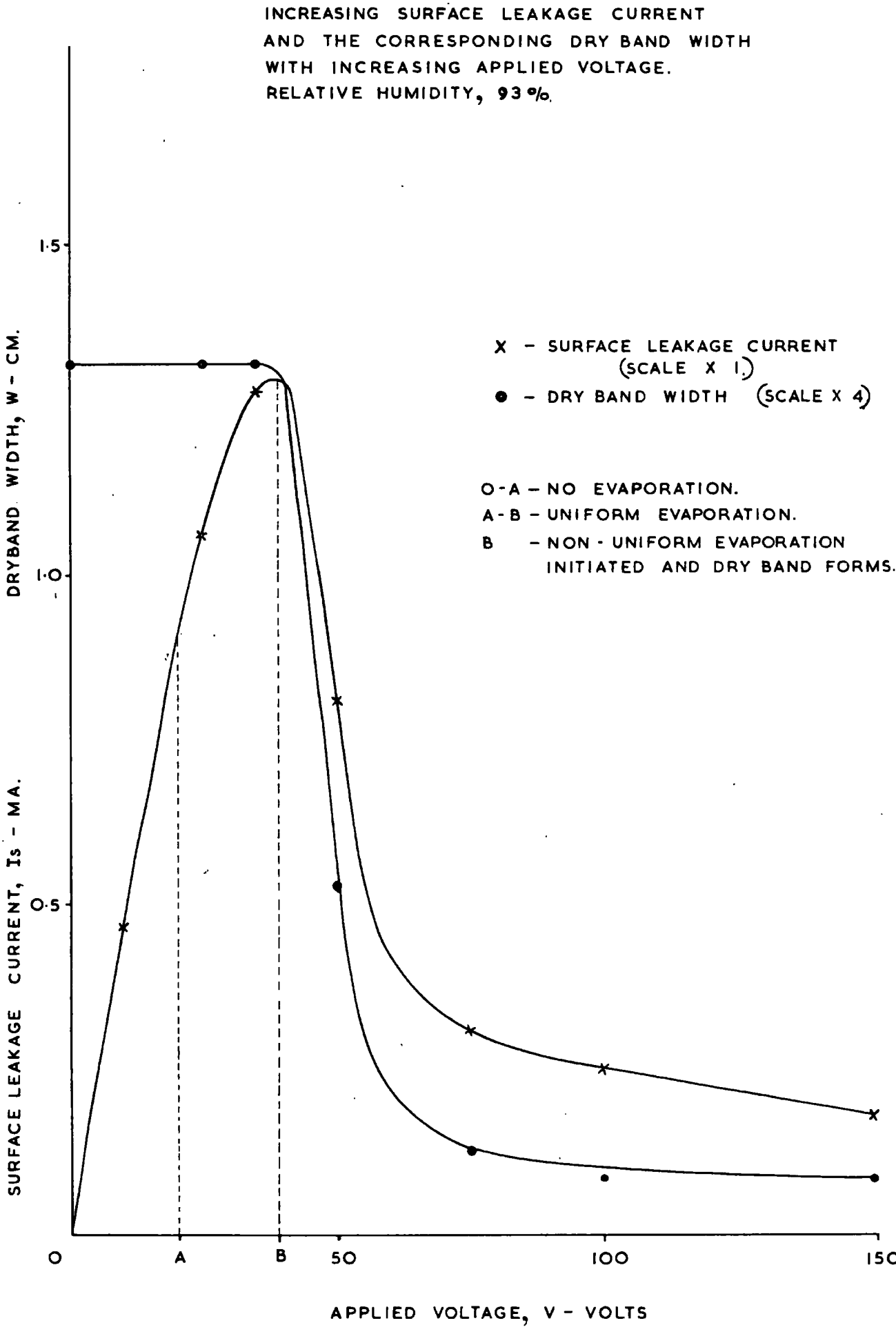
INCREASING SURFACE LEAKAGE CURRENT
AND THE CORRESPONDING DRY BAND WIDTH
WITH INCREASING APPLIED VOLTAGE.
RELATIVE HUMIDITY, 93%
X - SURFACE LEAKAGE CURRENT (SCALE X 1)
● - DRY BAND WIDTH (SCALE X 4)
O-A - NO EVAPORATION.
A-B - UNIFORM EVAPORATION.
B - NON-UNIFORM EVAPORATION INITIATED AND DRY BAND FORMS.
DRYBAND WIDTH, W - CM.
SURFACE LEAKAGE CURRENT, Is - MA.
1·5
1·0
0·5
O
A
B
50
100
150
APPLIED VOLTAGE, V - VOLTS

FIG. 4.4

VARIATION IN DRY BAND WIDTH WITH APPLIED VOLTAGE FOR INCREASING RELATIVE HUMIDITY.

□ - 52 % RELATIVE HUMIDITY.
△ - 65 % RELATIVE HUMIDITY.
○ - 75.67 % RELATIVE HUMIDITY.
■ - 86.50 % RELATIVE HUMIDITY.
▲ - 93 % RELATIVE HUMIDITY.

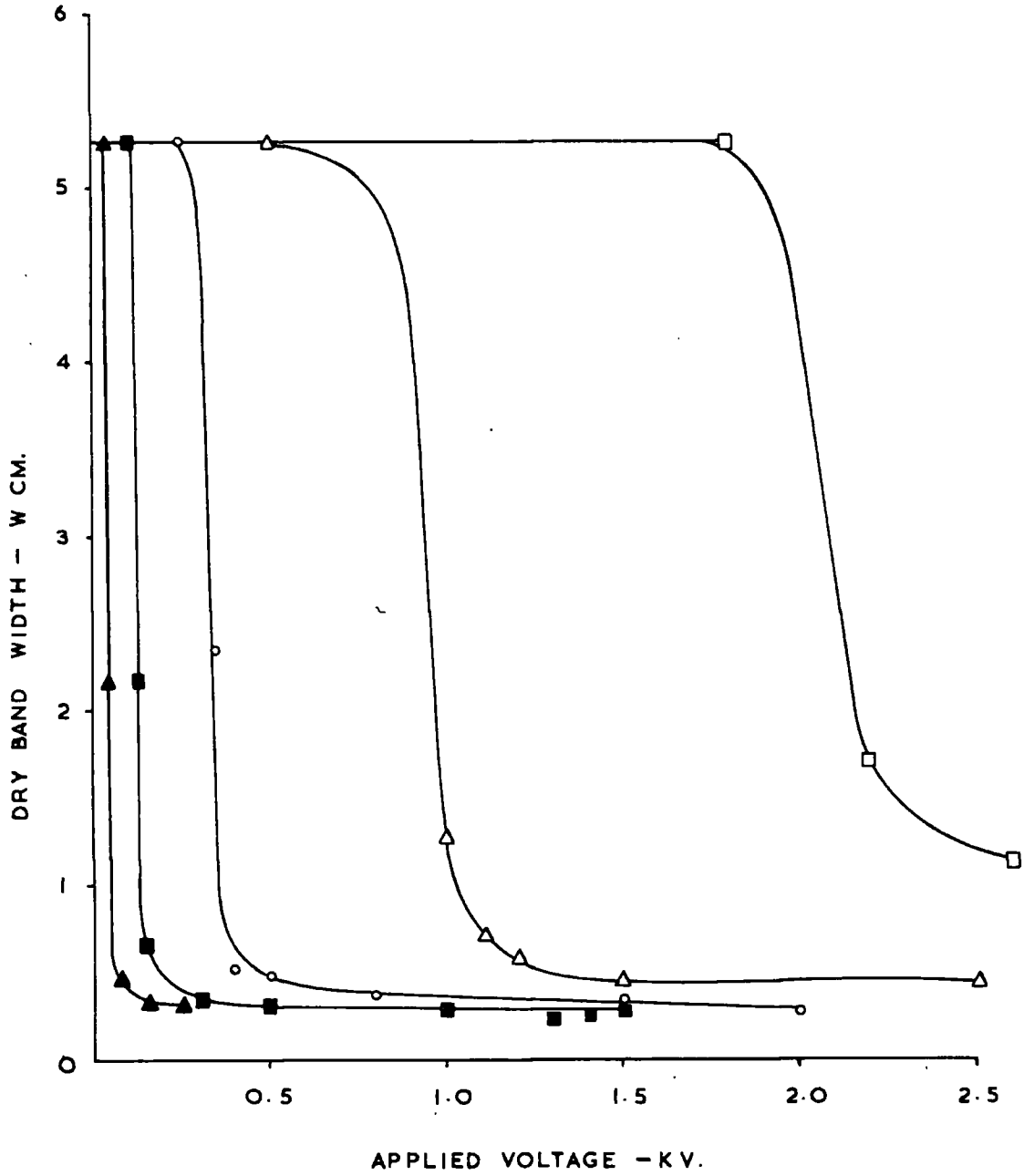

rapidly. This is due to the accelerating effect of the collapsing voltage which increases the power dissipated per unit area. The dry band width decreases until a state of equilibrium occurs, where the heat dissipated is equal to the heat generated. It is rather difficult to obtain measurements in the region of the critical voltage as the system is in an unstable condition, where the slightest change in any of the parameters involved causes a large change in the current voltage characteristics. The results also show quite clearly that once a dry band is established, its width is decreasing with increasing voltages. This is limited only by discharges and breakdown due to flashover across the band.

It was noted that as the humidity was increased the critical voltage was lower and the peak current, higher. It has already been established that the initial resistivity ρ_{so} is a function of moisture content of the film, thus for a higher humidity the resistivity would be reduced, hence a higher initial slope of the voltage current curve. It is also obvious that evaporation of moisture from the surface is initiated at a lower applied voltage as this is a function of the initial surface resistance. The surface resistance is related to the applied voltage by:-

$$R_{s\infty} = R_{so} + A V^2$$

where R_{so} is the initial surface resistance

and $R_{s\infty}$ is the final surface resistance

If

$$\alpha = \frac{R_{s\infty}}{R_{so}}$$

then the foregoing equation can be written:-

$$\text{LOG}\,(\alpha - 1) = \text{LOG}\,K + 2\,\text{LOG}\,V$$

where $$K = \frac{A}{R_{so}}$$

In Fig. 4.24 $\text{LOG}(\alpha - 1)$ has been plotted as a function of $\text{LOG}\,V$ for increasing relative humidities, where the slope of the graph is close to 2. This is in agreement with work done by Salthouse[6].

Fig. 4.25. shows the dry band width versus power per unit area of the dry band for increasing relative humidities. Once the dry band is initiated, only a small increase in voltage, and thus power per unit area, will cause the band to collapse. Once the band has collapsed its width is independent of humidity. The power per unit area required to increase the temperature to a value where non-uniform evaporation would take place is reached at a lower voltage because of the lower value of surface resistance.

Fig. 4.5. shows the relationship between the critical voltage and the initial surface resistance, and this is in agreement with the equation used by Salthouse[6]:-

$$V_c = \text{Constant} \times \sqrt{R_{so}}$$

Not only does the dry band form at a lower voltage, but the critical voltage at which it is initiated is more sharply defined, at higher relative humidities, as shown in Fig. 4.2. where surface leakage current is plotted against applied voltage for a range of humidities.

FIG. 4.24

$LOG_{10}(a-1)$ AGAINST $LOG_{10} V$ FOR INCREASING RELATIVE HUMIDITY, USING THE OVERALL RESISTANCE.
SLOPE = 1·93.

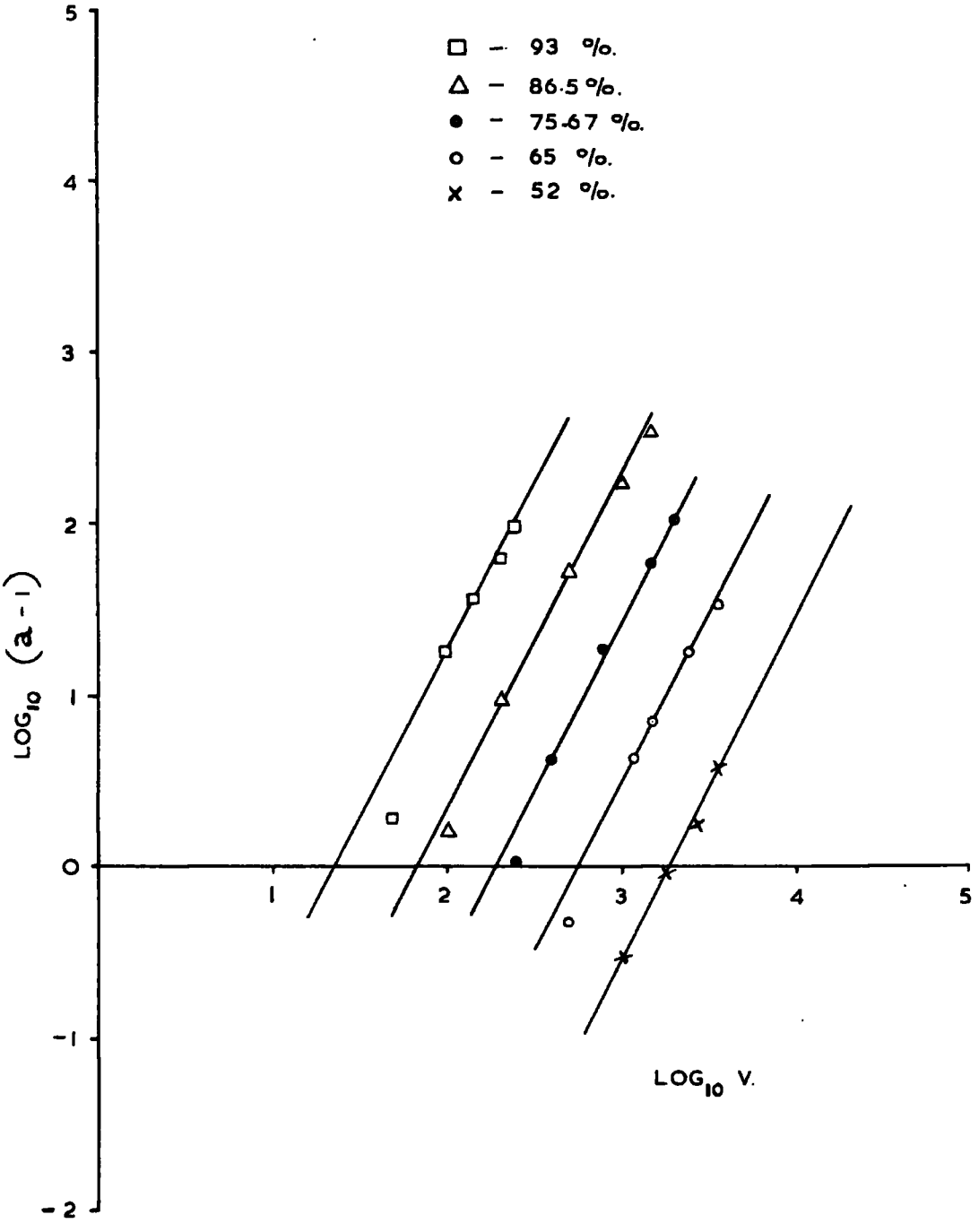

FIG. 4.25

DRY BAND WIDTH VERSUS POWER DISSIPATION PER UNIT AREA IN THE DRY BAND.

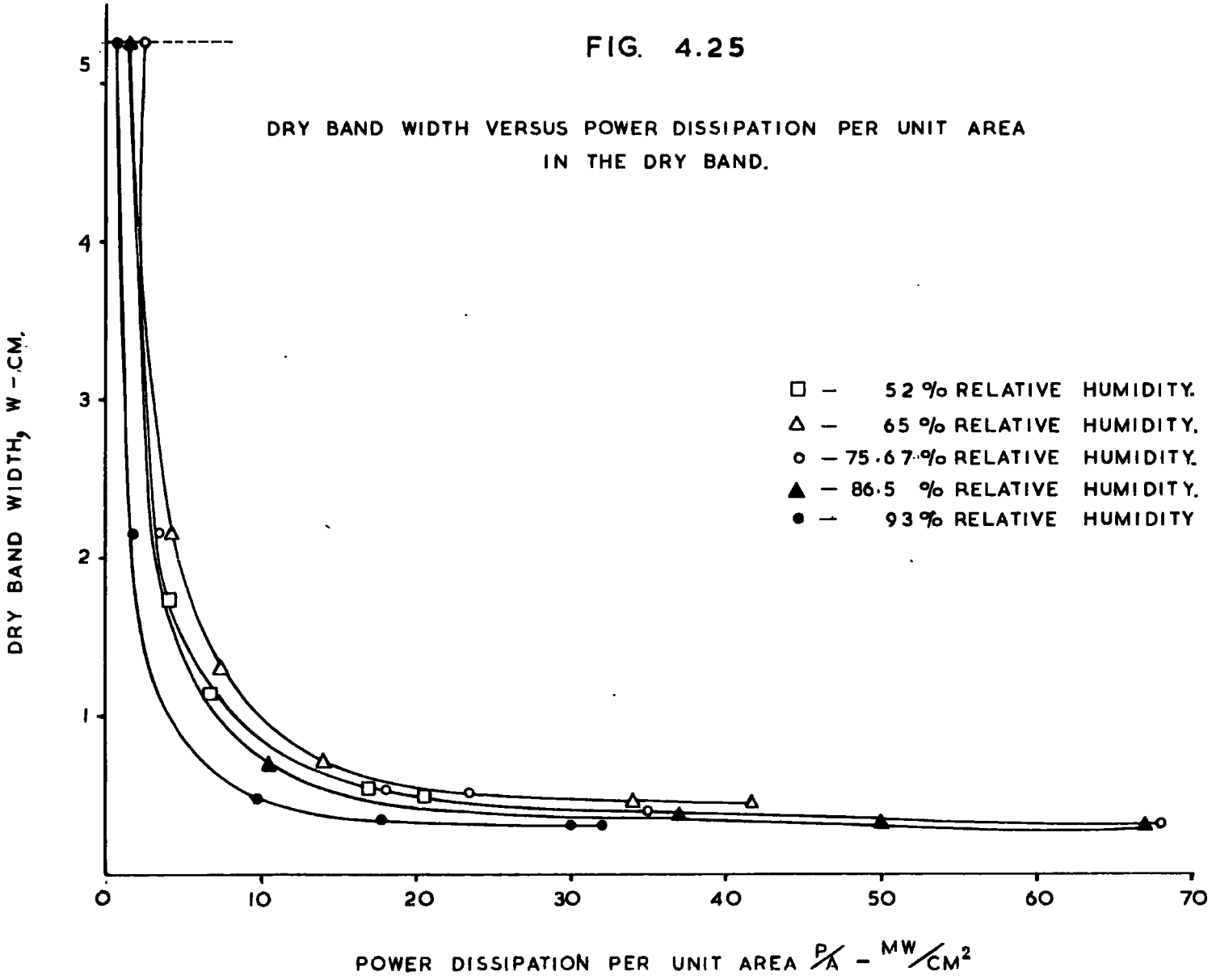

FIG. 4.5

VARIATION IN CRITICAL VOLTAGE WITH INCREASING INITIAL SURFACE RESISTANCE.

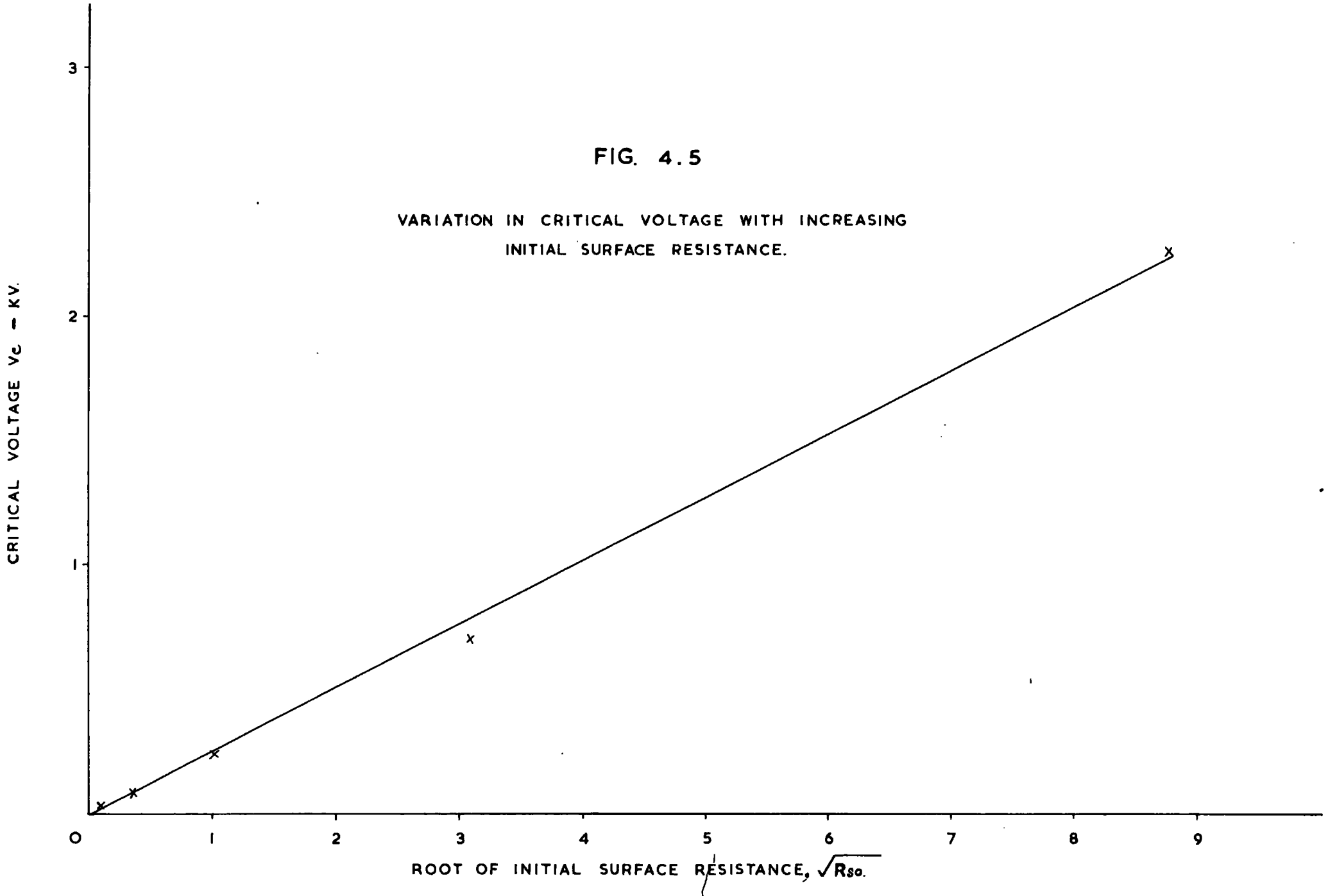

FIG. 4.2

VARIATION IN SURFACE LEAKAGE CURRENT WITH APPLIED VOLTAGE FOR INCREASING RELATIVE HUMIDITIES.

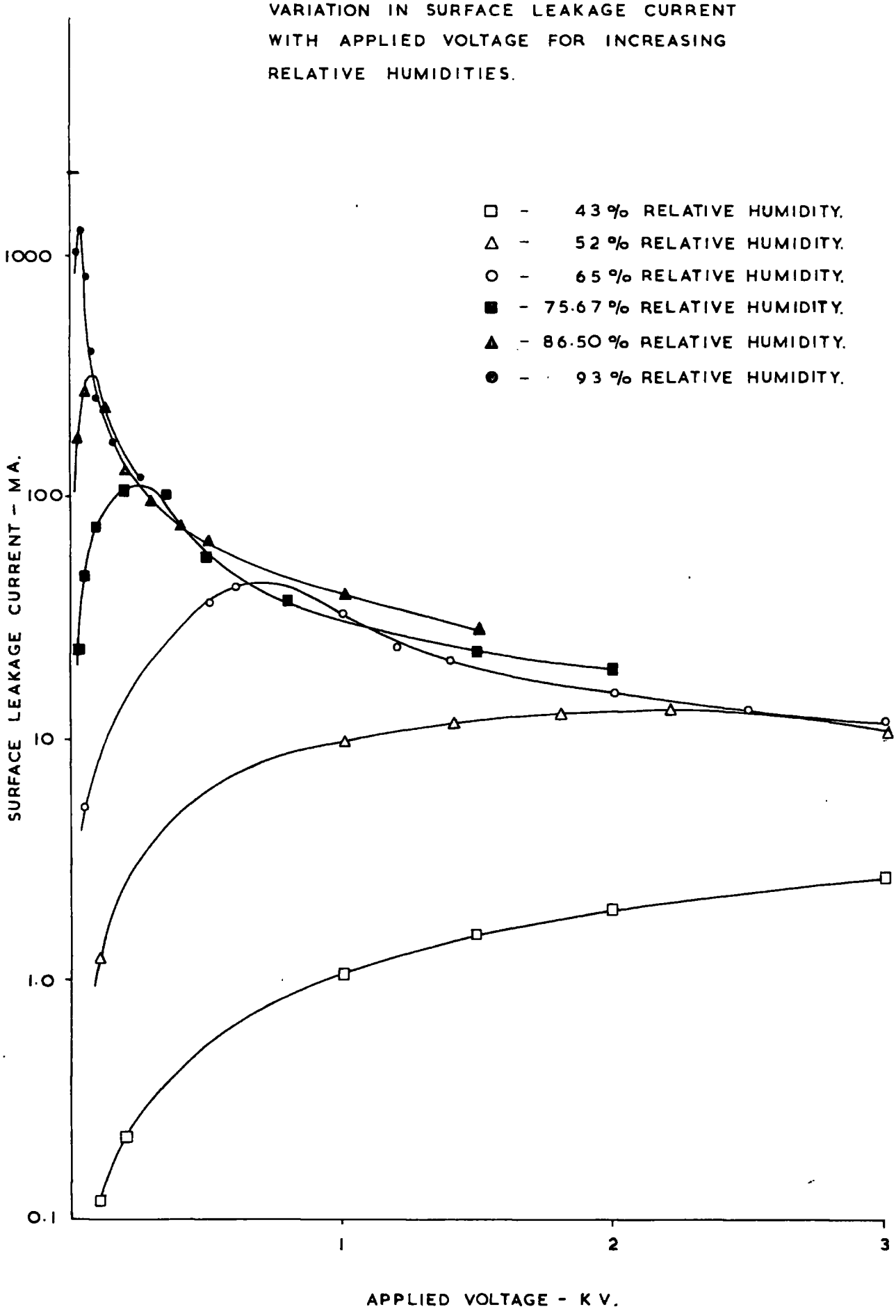

4.2. DRY BAND STRUCTURE

The voltage distribution across the dry band was measured by a capacitive probe scanned across the surface. The signal from the probe was fed to a chart recorder and a typical set of curves is shown in Fig.4.6. A set of field distribution curves for each humidity was derived from these chart recordings and this is shown in Figs. 4.7 - 4.11. Care was taken to get an accurate calibration of the recordings as these were used in determining not only the voltage, field and resistivity distribution, but also gave the basic information concerning the width of the dry band and the temperature distribution across it.

The field distribution curves give a fairly good account of the build up of the dry band in as much as they show that a large proportion of the applied voltage actually occurs across the dry band. It also shows that this voltage increases with increasing applied voltage, whereas the voltage for the rest of the sample stays fairly constant.

It was noted that the transition between the actual dry band and the remaining part of the surface was not particularly sharp. This was as expected as some of the heat generated in the dry band would be dissipated by conduction and thus affect the polluted surface on either side of the dry band. Because of this rounding off of the dry band, it was necessary to establish a point on the curve which could be referred to when measuring the width

FIG. 4·6 ILLUSTRATED VOLTAGE DISTRIBUTION CURVES

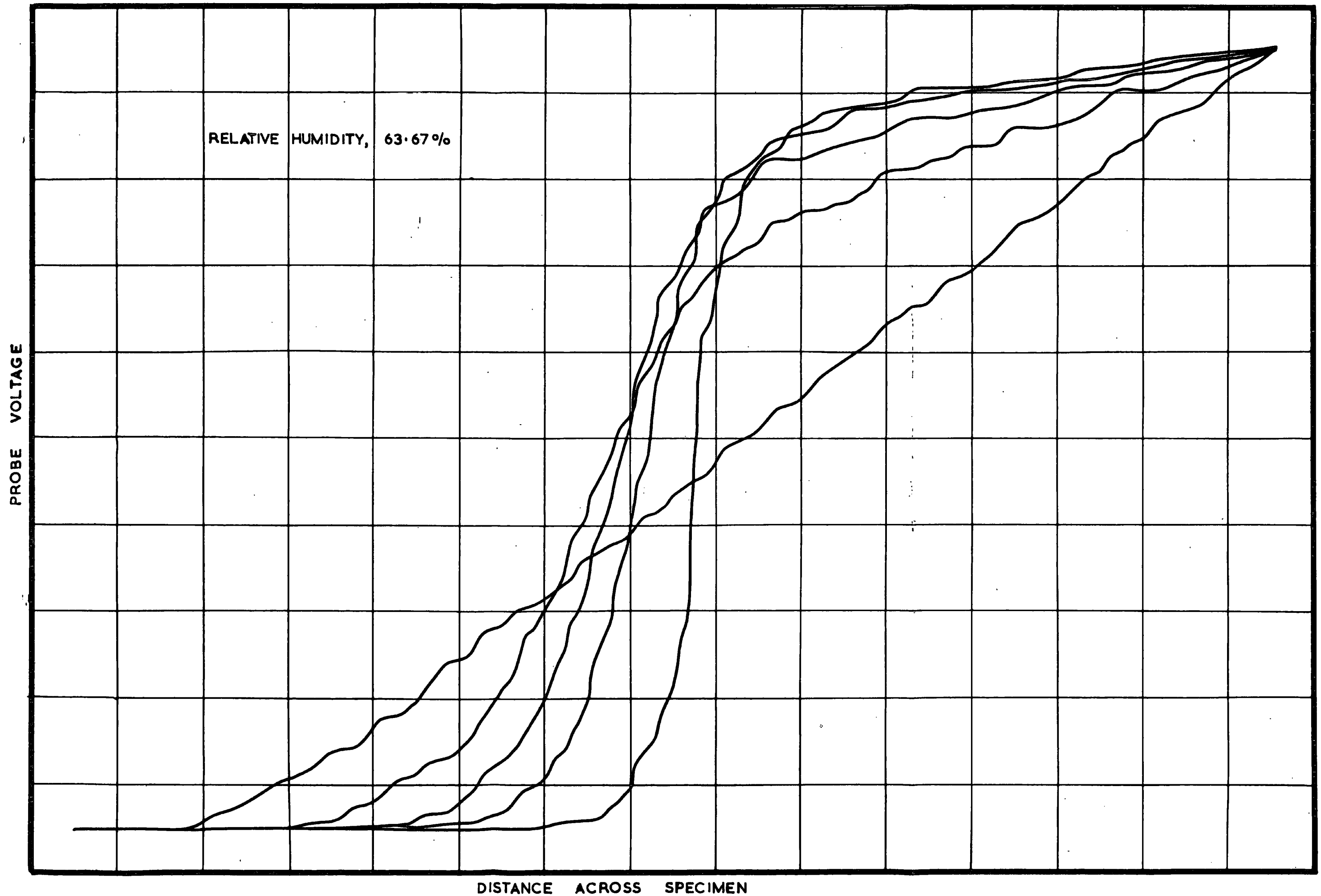

FIG. 4.7

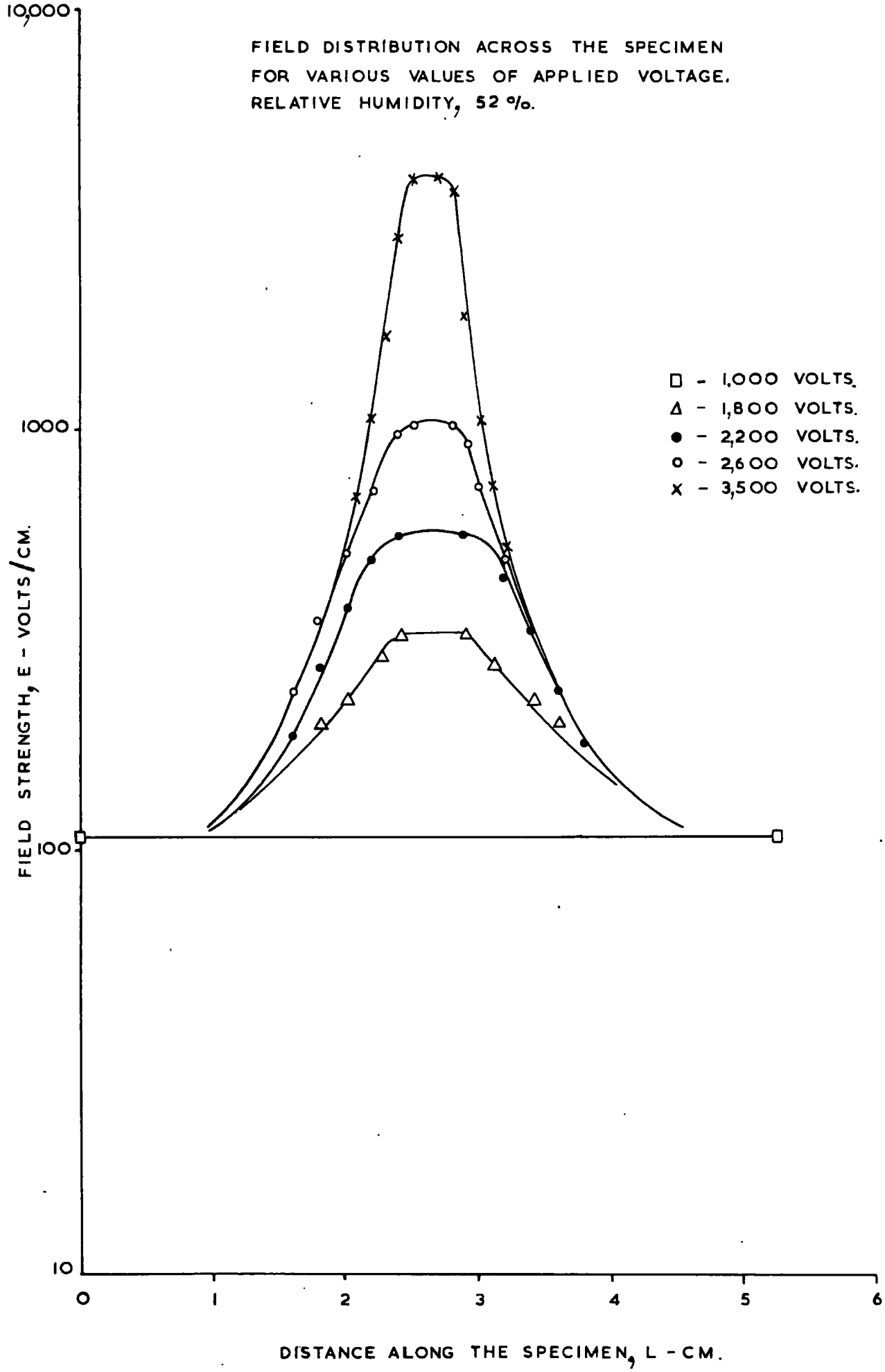
FIELD DISTRIBUTION ACROSS THE SPECIMEN
FOR VARIOUS VALUES OF APPLIED VOLTAGE.
RELATIVE HUMIDITY, 52 %.
□ - 1,000 VOLTS.
Δ - 1,800 VOLTS.
● - 2,200 VOLTS.
o - 2,600 VOLTS.
X - 3,500 VOLTS.
10,000
1000
100
10
FIELD STRENGTH, E - VOLTS/CM.
0
1
2
3
4
5
6
DISTANCE ALONG THE SPECIMEN, L - CM.

FIG. 4.8

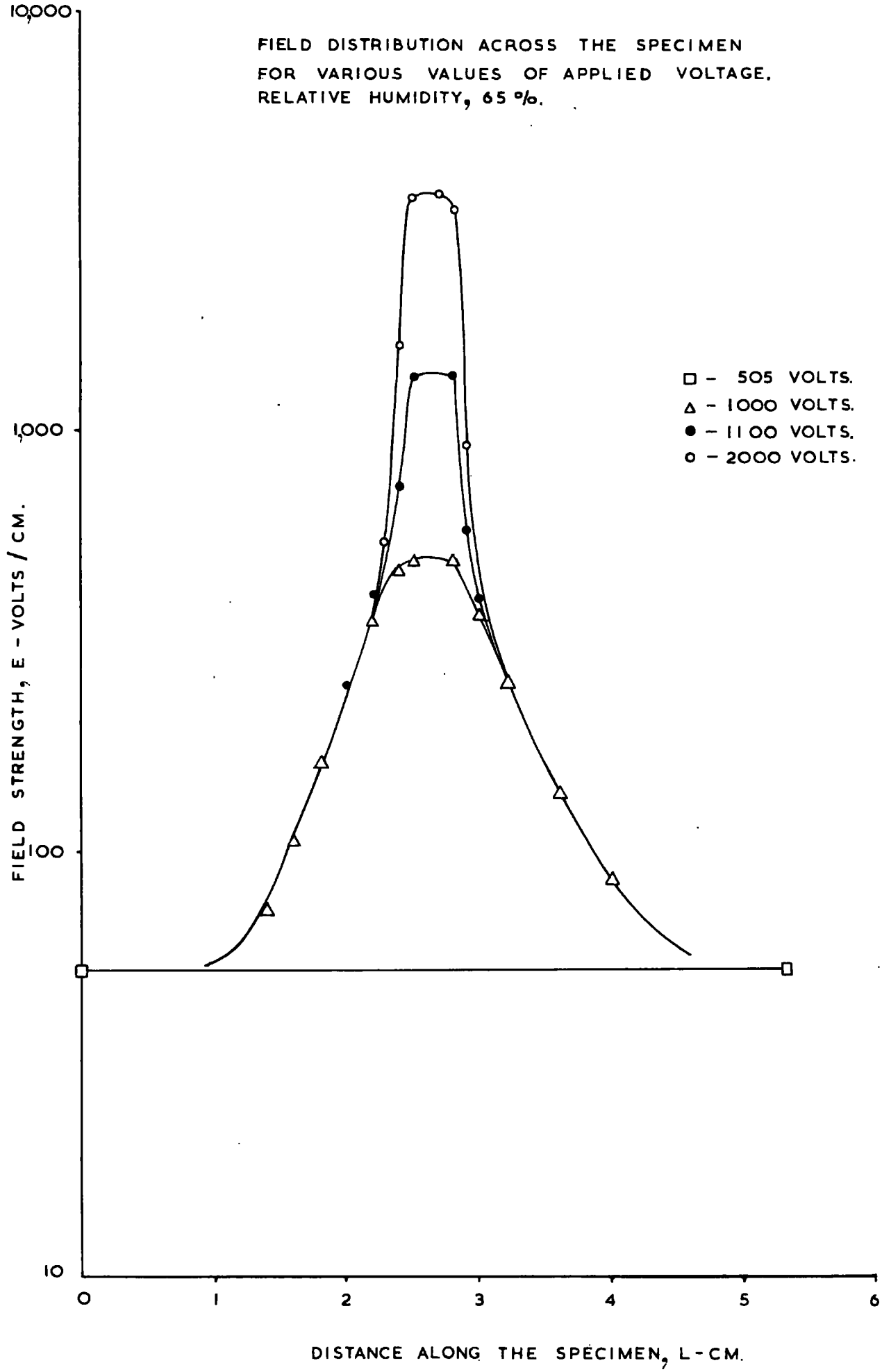
FIELD DISTRIBUTION ACROSS THE SPECIMEN
FOR VARIOUS VALUES OF APPLIED VOLTAGE.
RELATIVE HUMIDITY, 65 %.
□ - 505 VOLTS.
△ - 1000 VOLTS.
● - 1100 VOLTS.
o - 2000 VOLTS.
10,000
1,000
100
10
FIELD STRENGTH, E - VOLTS / CM.
0
1
2
3
4
5
6
DISTANCE ALONG THE SPECIMEN, L - CM.

FIG. 4.9

FIELD DISTRIBUTION ACROSS THE SPECIMEN FOR VARIOUS VALUES OF APPLIED VOLTAGE. RELATIVE HUMIDITY, 75·67 %.

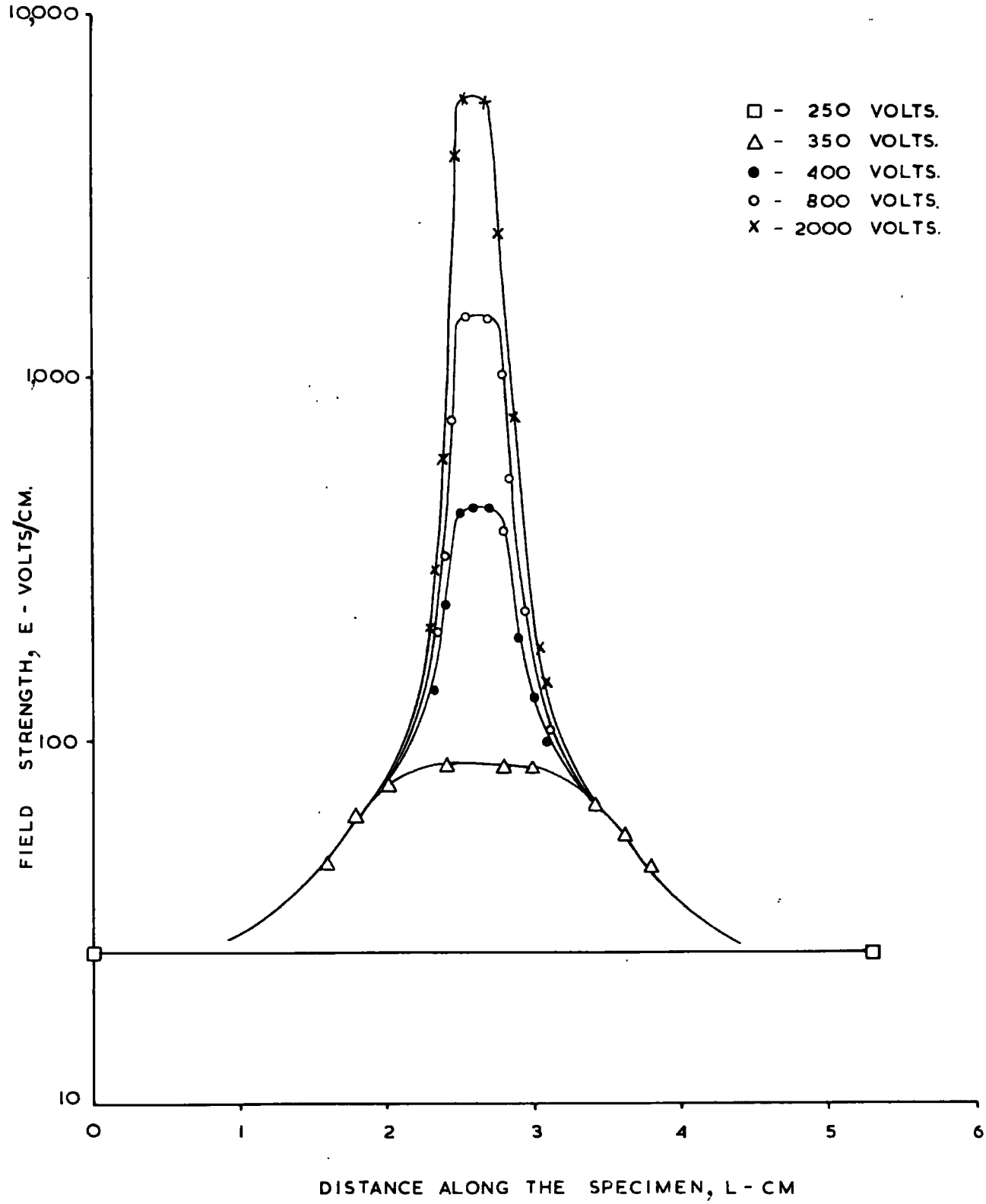

FIG. 4.10

FIELD DISTRIBUTION ACROSS THE SPECIMEN FOR VARIOUS VALUES OF APPLIED VOLTAGE. RELATIVE HUMIDITY, 86.5 %.

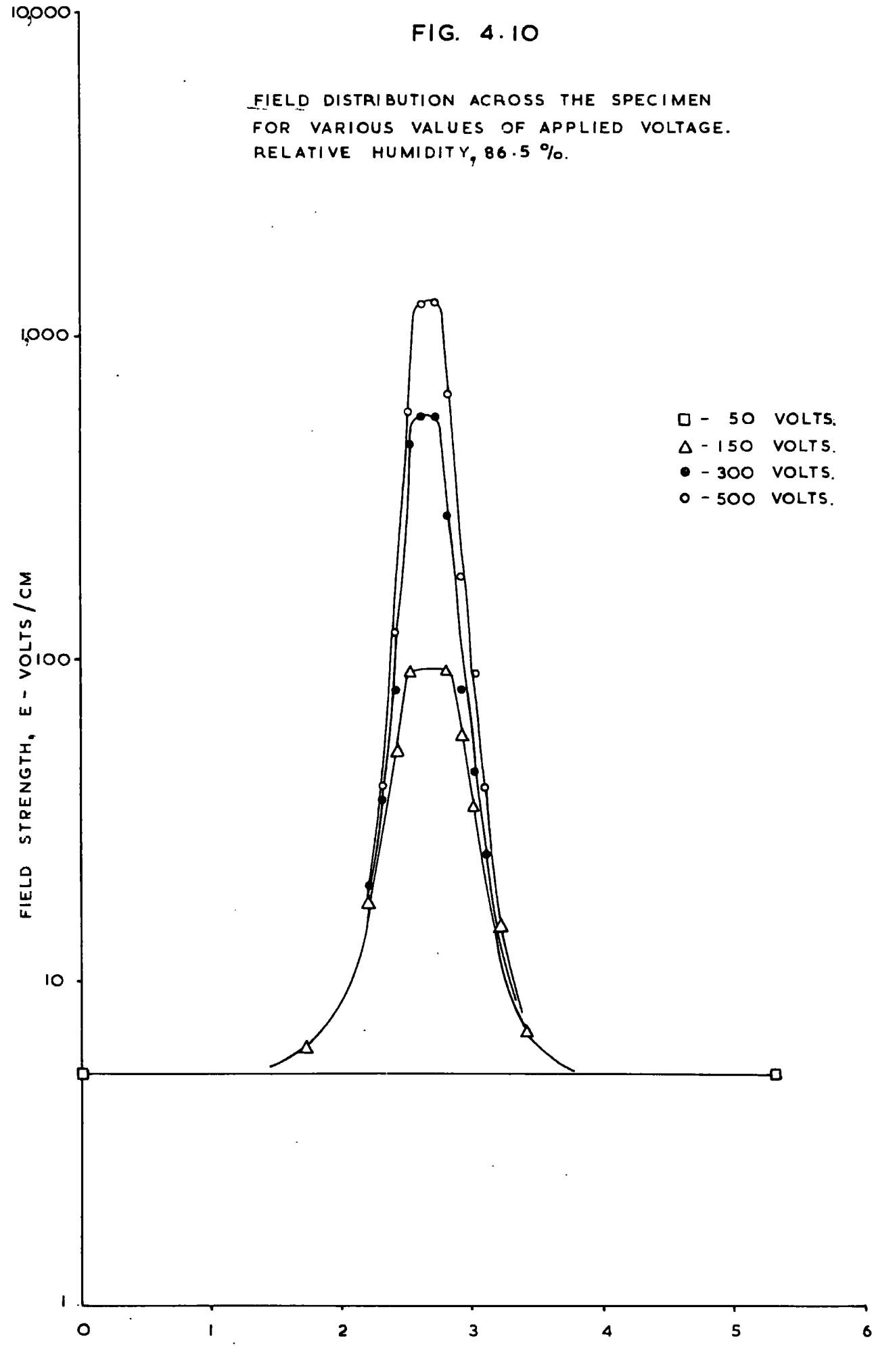

FIG. 4.11

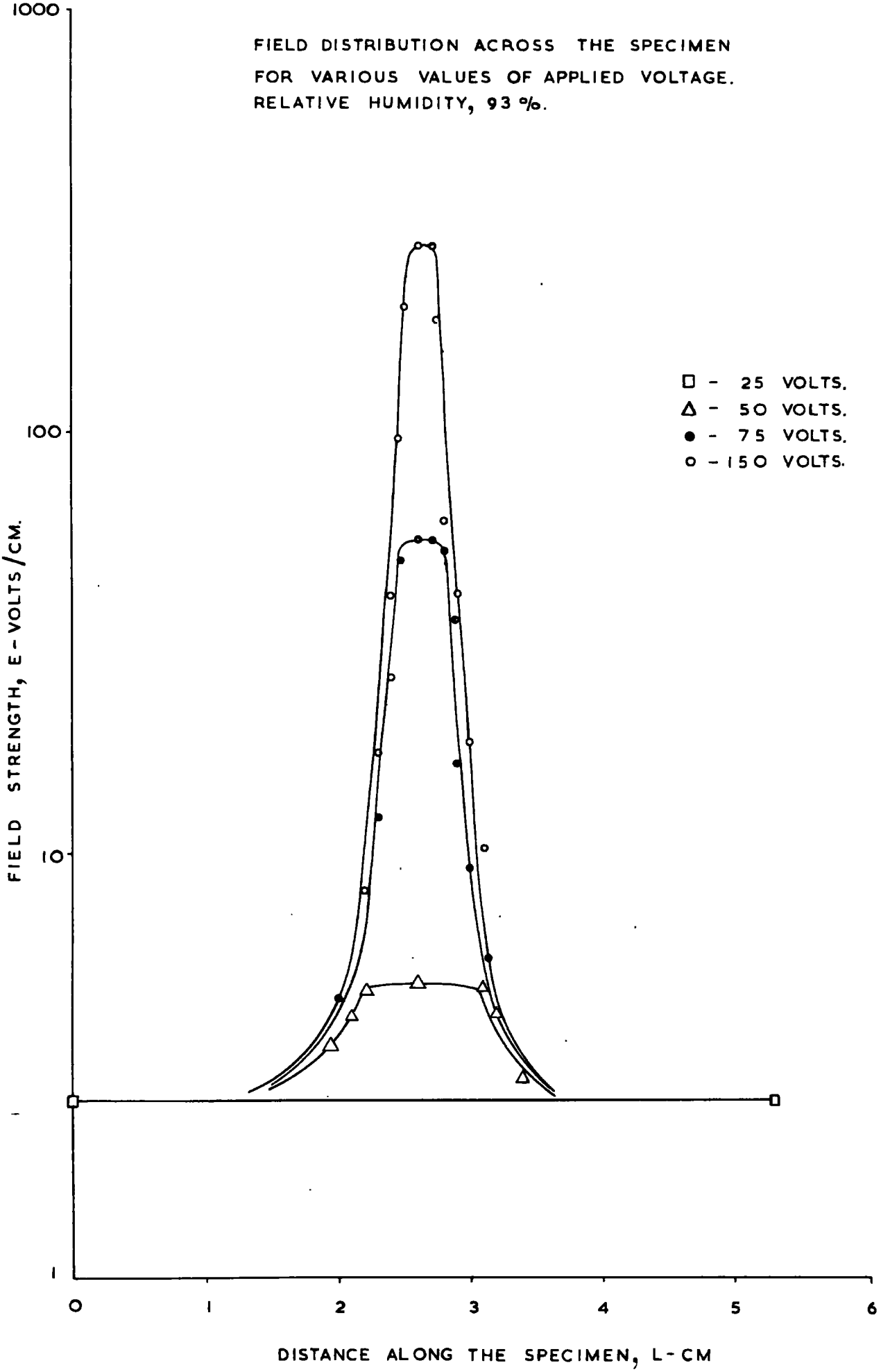
FIELD DISTRIBUTION ACROSS THE SPECIMEN
FOR VARIOUS VALUES OF APPLIED VOLTAGE.
RELATIVE HUMIDITY, 93 %.
□ - 25 VOLTS.
△ - 50 VOLTS.
● - 75 VOLTS.
○ - 150 VOLTS.
1000
100
10
1
FIELD STRENGTH, E - VOLTS/CM.
0
1
2
3
4
5
6
DISTANCE ALONG THE SPECIMEN, L - CM

of the band. As the dry bands are power initiated, it was decided to measure the dry band width at the half power point. This avoided any regions affected by the rounding off on either side of the band, and gave a sharply defined measurement. A certain amount of rounding off at the peak of the curve was also noted as well as the fact that all the curves appeared to be flat on the top. The flatness on the top of the curves may be accounted for by the limited resolution of the probe as shown in the appendix, page 61 . The width of the measured dry band is obviously dependent on the resolution of the probe as well as the accuracy at which the measurements were carried out, particularly when dealing with very narrow dry bands obtained at high voltages. In spite of this there were clear indications that the band continued to decrease with increasing voltages until breakdown occurred.

The results also show quite clearly that for higher humidity not only does the dry band form at a lower voltage, but it is more sharply defined; that is, the transition between the dry band and the remaining part of the specimen is more definite even at low voltages, and the dry band width is decreasing with increasing humidity.

In addition, the field distribution curves are useful because they give a clear picture of the electric stress in the dry band due to the applied voltage. They also show the build up of the electric field in the specimen as the voltage is increased and the dry band is formed.

The resistivity curves, Figs. 4.12 - 4.16, show quite

clearly the relatively high resistivity of the dry band compared with the rest of the surface. As expected the resistivity distribution across the specimen is initially constant and remains so until the non-uniform evaporation is initiated whereby a region of higher resistivity occurs, known as the dry band. Having previously obtained the relationship between surface resistivity and surface temperature, shown in Fig. 4.17, by measurements made on a sample cut from the same sheet of melinex as the actual test specimen and both treated in exactly the same way, it was now possible to determine the surface temperature in the dry band. Curves showing the temperature distribution for various applied voltages of a range of humidities are shown in Figs. 4.18 - 4.22. The transition between the dry band and the remaining part of the surface is apparent and as mentioned before, this is due to heat conduction as well as the fact that some heat, although comparatively little, is generated in this region. It was noted that the temperature distribution was fairly linear until non-uniform evaporation was initiated.

An infra-red thermometer using an indium antimonide cell cooled with liquid nitrogen was built to obtain accurate measurements of the temperature distribution across the specimen. Unfortunately, the device constructed for scanning was not working to complete satisfaction and consequently the results obtained did not give a continuous picture of the distribution. However, temperature readings were obtained from the centre of a dry band and these

FIG. 4.12

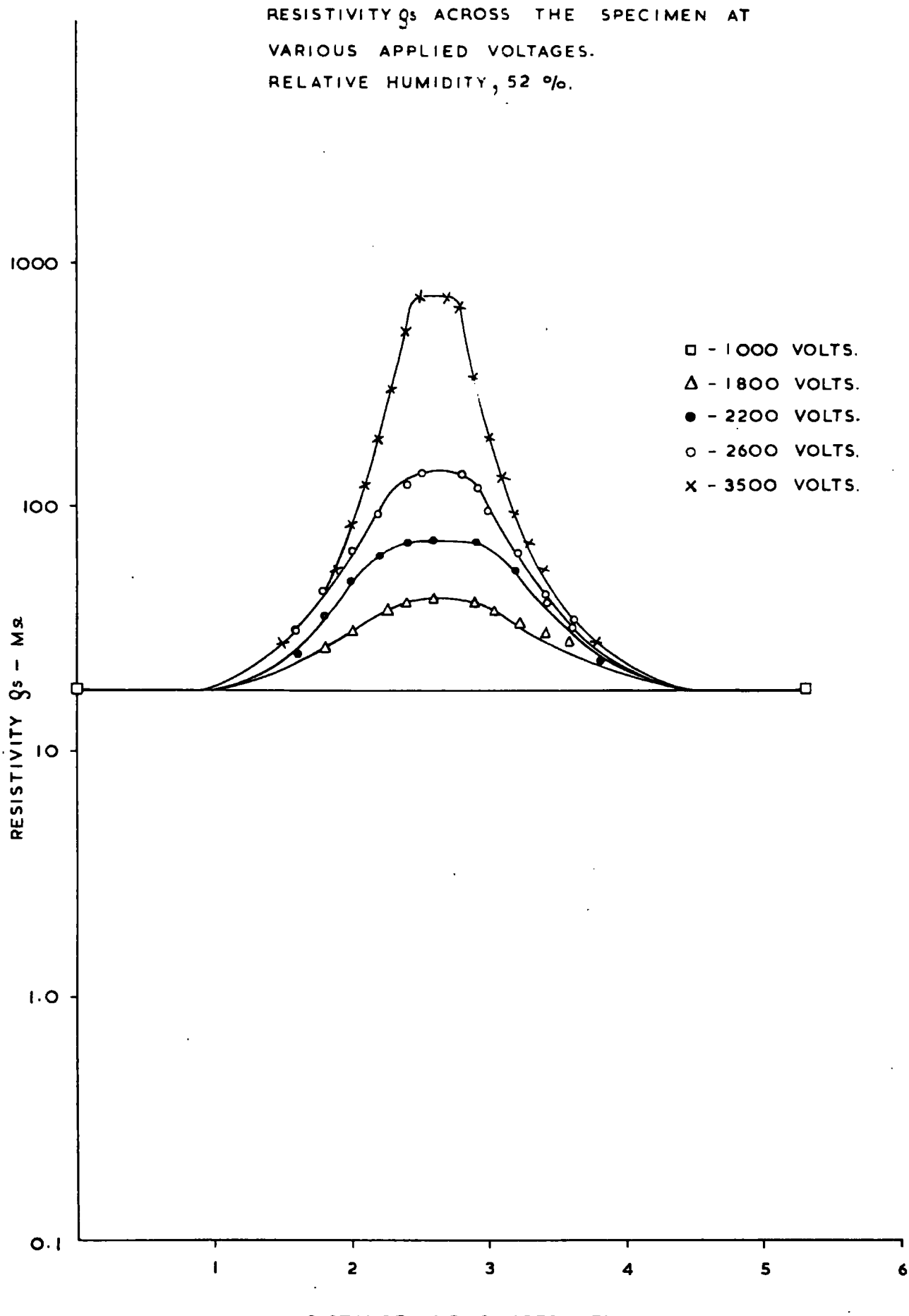
RESISTIVITY ρs ACROSS THE SPECIMEN AT
VARIOUS APPLIED VOLTAGES.
RELATIVE HUMIDITY, 52 %.
□ - 1000 VOLTS.
Δ - 1800 VOLTS.
● - 2200 VOLTS.
○ - 2600 VOLTS.
× - 3500 VOLTS.
1000
100
10
1.0
0.1
RESISTIVITY ρs - MΩ
1
2
3
4
5
6
DISTANCE ALONG SPECIMEN, L - CM.

FIG. 4.13

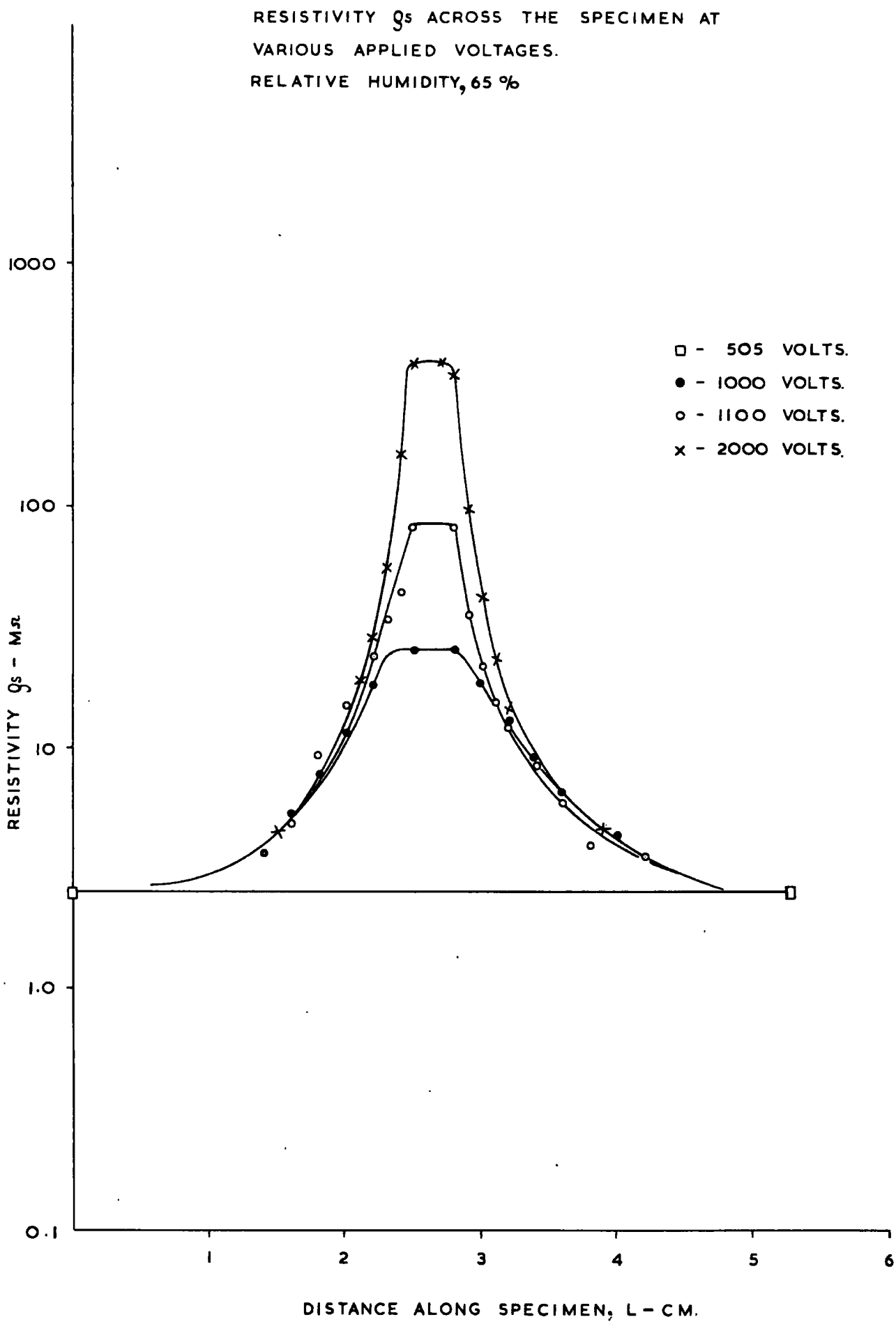
RESISTIVITY ρs ACROSS THE SPECIMEN AT
VARIOUS APPLIED VOLTAGES.
RELATIVE HUMIDITY, 65 %
□ - 505 VOLTS.
● - 1000 VOLTS.
○ - 1100 VOLTS.
× - 2000 VOLTS.
1000
100
10
1.0
0.1
RESISTIVITY ρs - MΩ
1
2
3
4
5
6
DISTANCE ALONG SPECIMEN, L - CM.

FIG. 4.14

RESISTIVITY ρ_s ACROSS THE SPECIMEN
AT VARIOUS APPLIED VOLTAGES.
RELATIVE HUMIDITY, 75·67 %.

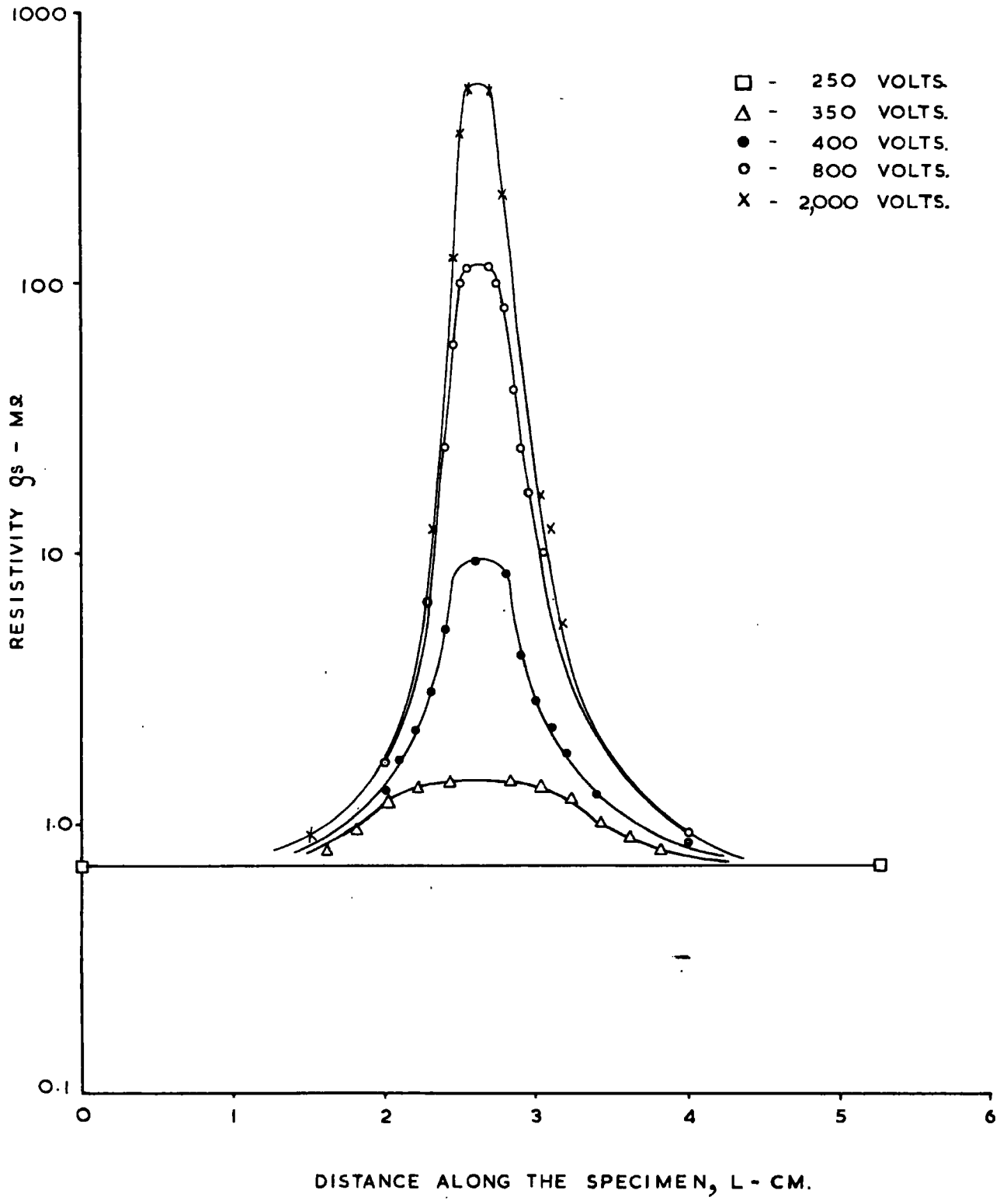

FIG. 4 . 15

RESISTIVITY ρ_s ACROSS THE SPECIMEN
AT VARIOUS APPLIED VOLTAGES.
RELATIVE HUMIDITY, 86.5 %

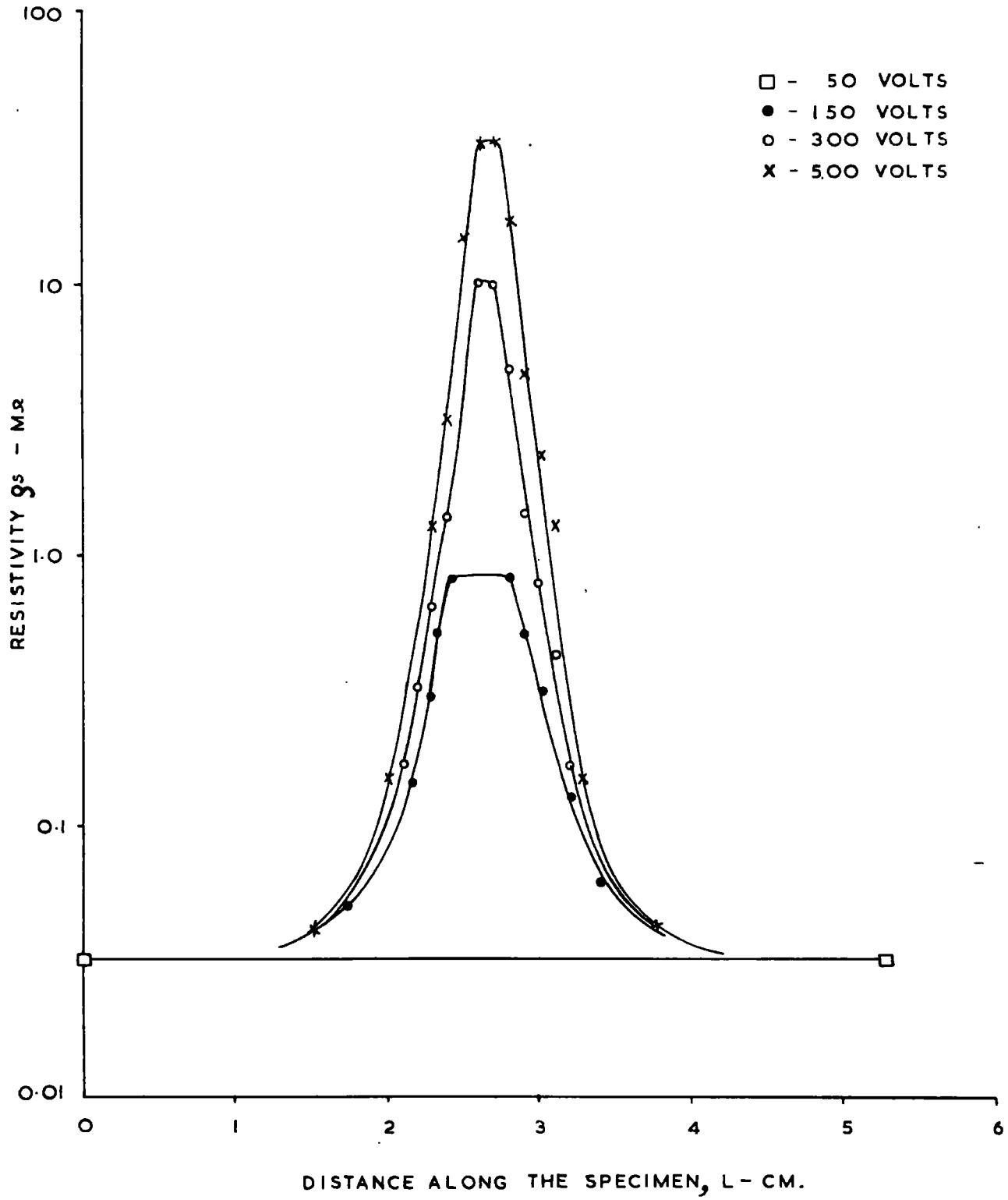

FIG. 4.16

RESISTIVITY ρ_s ACROSS THE SPECIMEN AT VARIOUS APPLIED VOLTAGES.
RELATIVE HUMIDITY 90%.

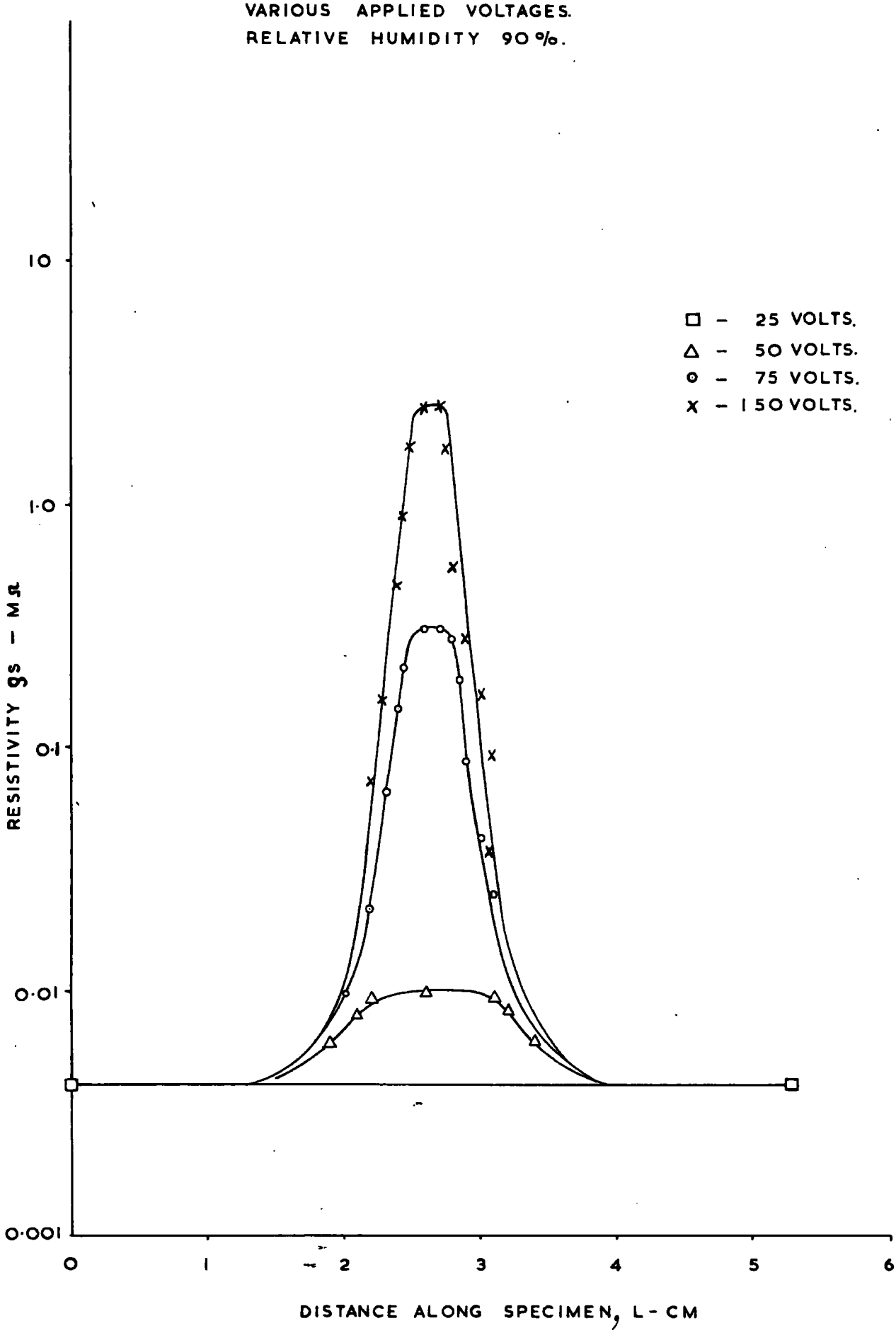

FIG. 4.17

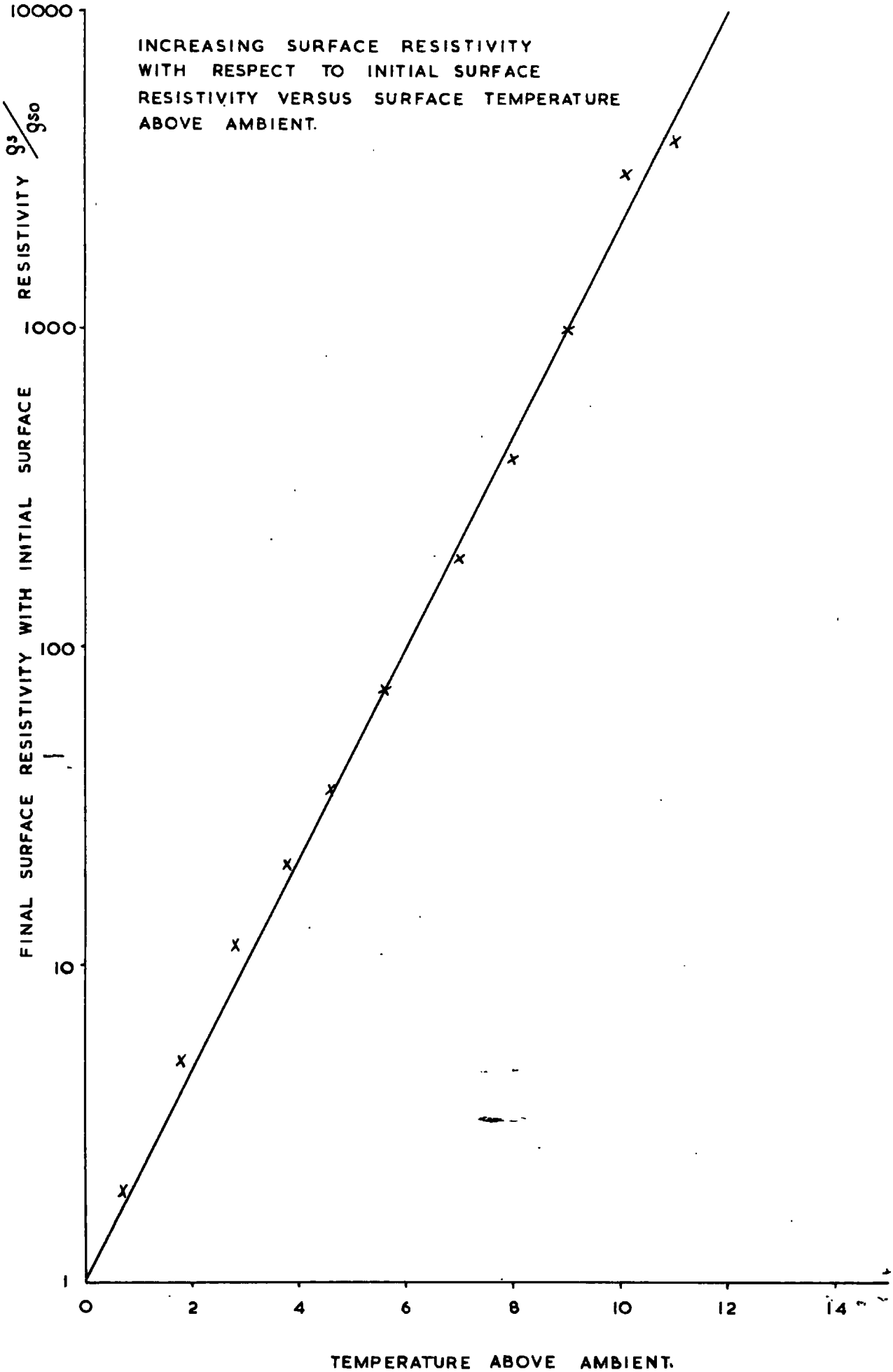
INCREASING SURFACE RESISTIVITY WITH RESPECT TO INITIAL SURFACE RESISTIVITY VERSUS SURFACE TEMPERATURE ABOVE AMBIENT.
FINAL SURFACE RESISTIVITY WITH INITIAL SURFACE RESISTIVITY g^s/g_{so}
10000
1000
100
10
1
0
2
4
6
8
10
12
14
TEMPERATURE ABOVE AMBIENT.

FIG. 4.18

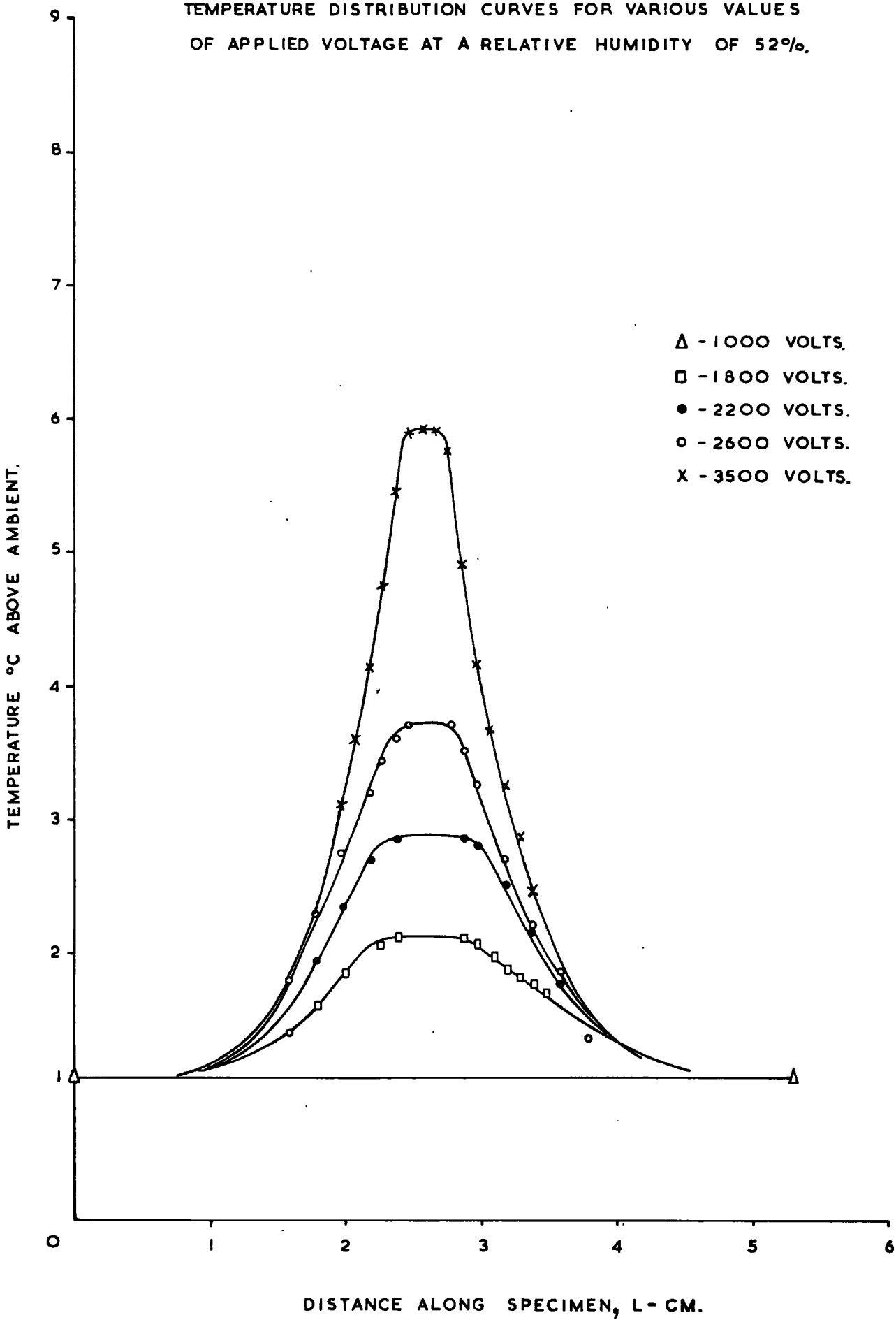
TEMPERATURE DISTRIBUTION CURVES FOR VARIOUS VALUES OF APPLIED VOLTAGE AT A RELATIVE HUMIDITY OF 52%.
Δ - 1000 VOLTS.
□ - 1800 VOLTS.
● - 2200 VOLTS.
o - 2600 VOLTS.
X - 3500 VOLTS.
TEMPERATURE °C ABOVE AMBIENT.
DISTANCE ALONG SPECIMEN, L - CM.
0
1
2
3
4
5
6
7
8
9

FIG. 4.19

TEMPERATURE DISTRIBUTION CURVES FOR VARIOUS VALUES OF APPLIED VOLTAGE. RELATIVE HUMIDITY. 65 %.

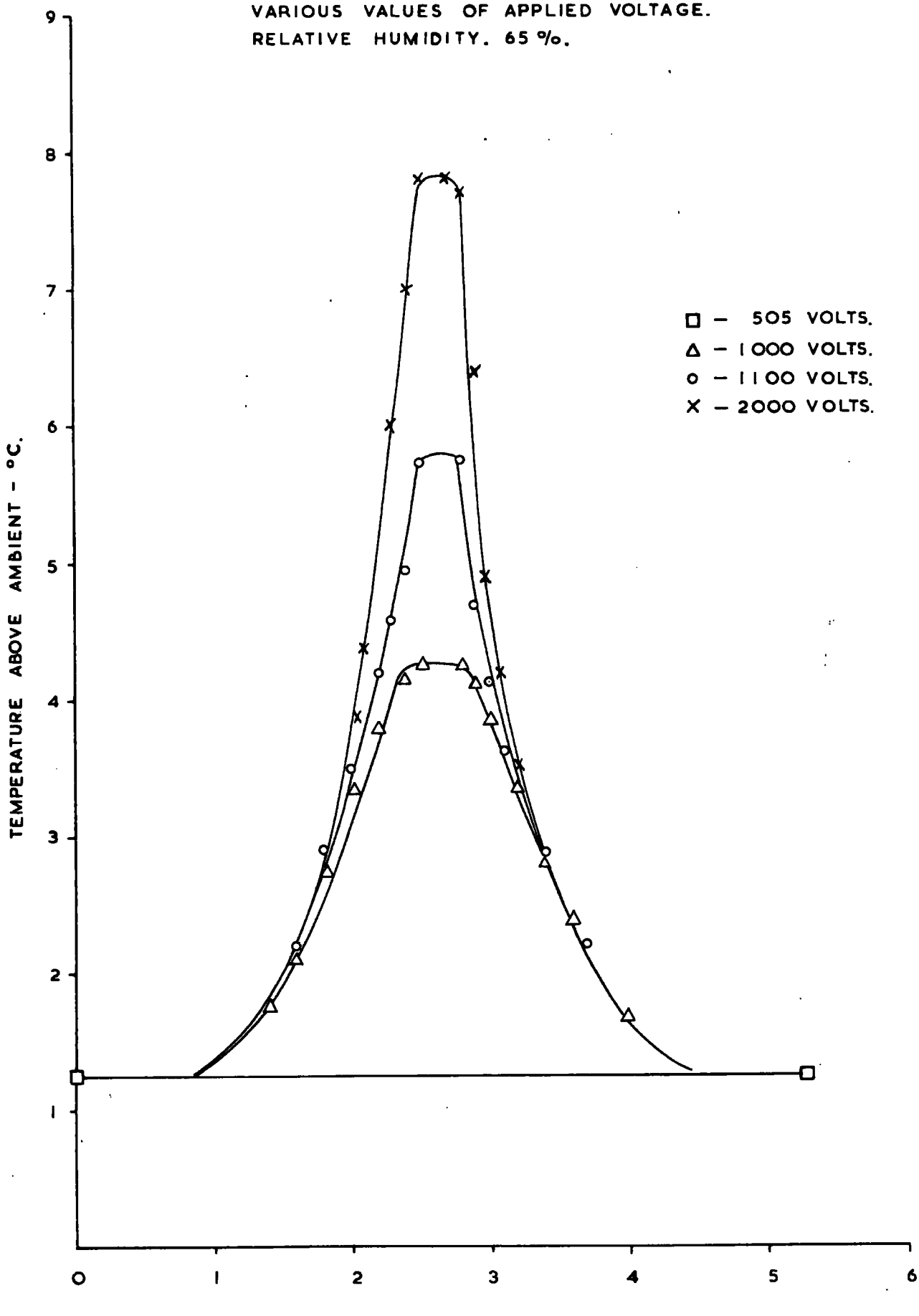

FIG. 4.20

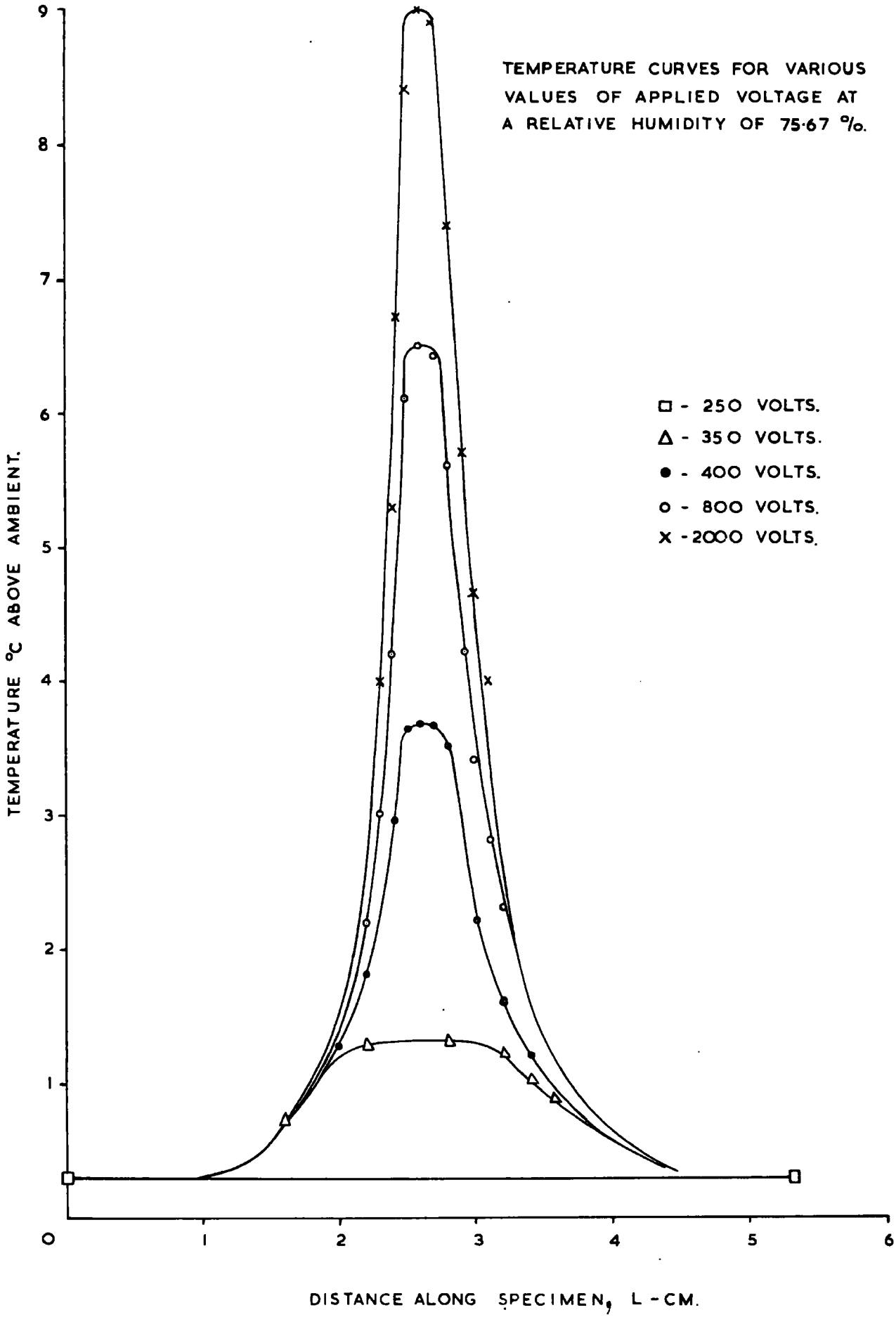
TEMPERATURE CURVES FOR VARIOUS VALUES OF APPLIED VOLTAGE AT A RELATIVE HUMIDITY OF 75·67 %.
□ - 250 VOLTS.
Δ - 350 VOLTS.
● - 400 VOLTS.
o - 800 VOLTS.
X - 2000 VOLTS.
TEMPERATURE °C ABOVE AMBIENT.
DISTANCE ALONG SPECIMEN, L - CM.
0
1
2
3
4
5
6
7
8
9

FIG. 4.21

TEMPERATURE DISTRIBUTION CURVES FOR VARIOUS VALUES OF APPLIED VOLTAGE AT A RELATIVE HUMIDITY OF 86·5 %.

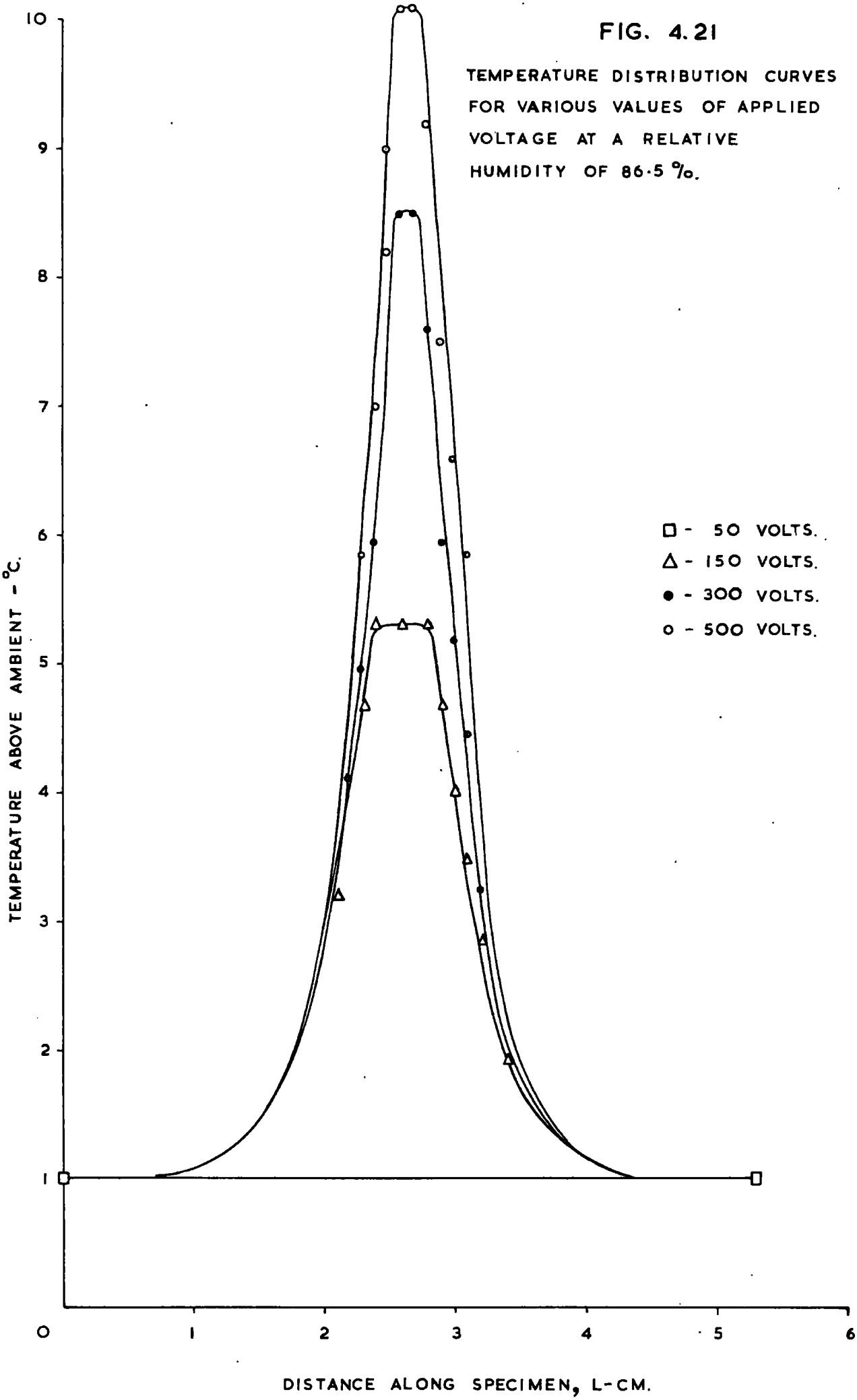

FIG. 4·22

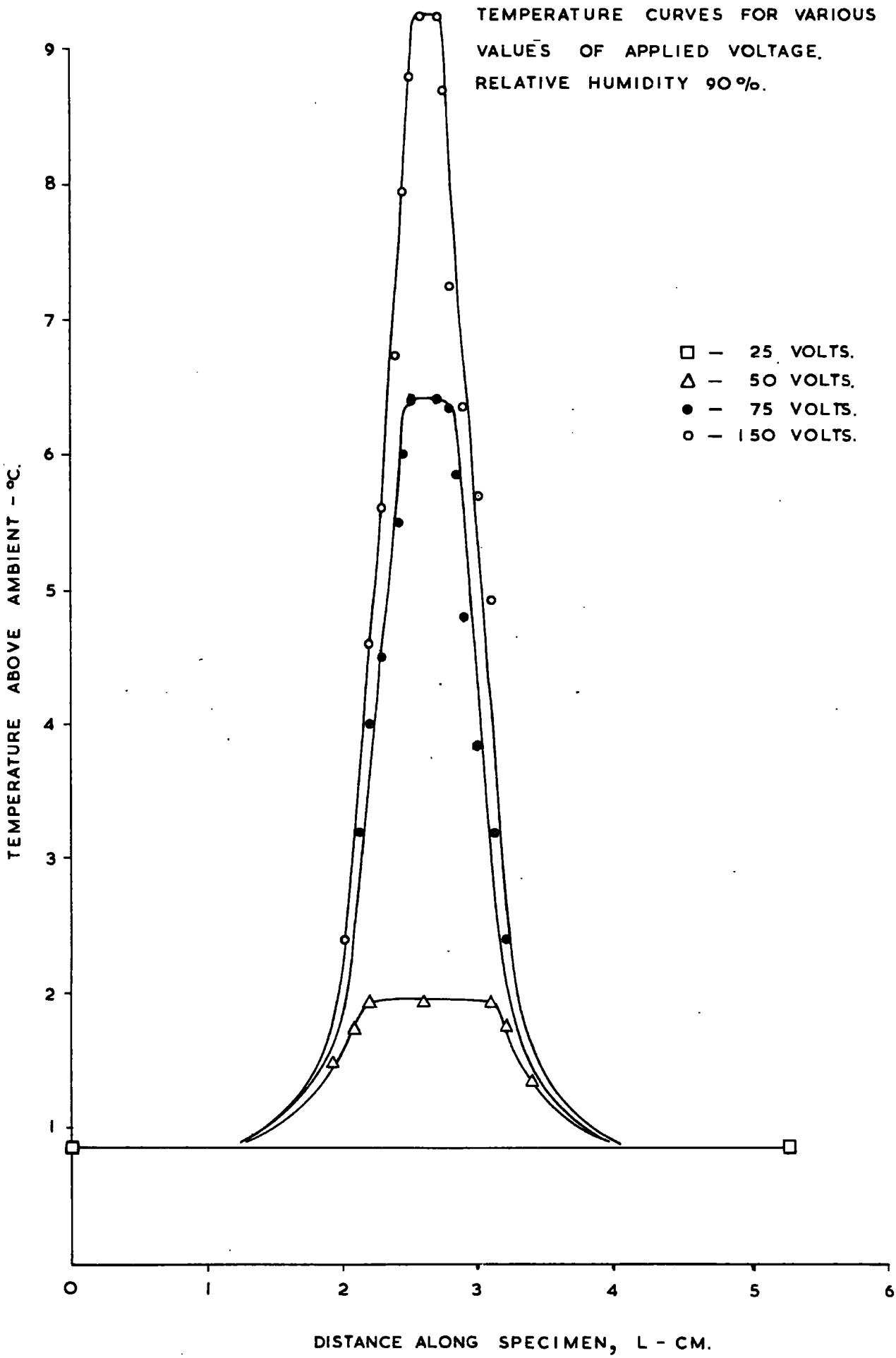
TEMPERATURE CURVES FOR VARIOUS VALUES OF APPLIED VOLTAGE.
RELATIVE HUMIDITY 90%.
□ — 25 VOLTS.
△ — 50 VOLTS.
● — 75 VOLTS.
○ — 150 VOLTS.
TEMPERATURE ABOVE AMBIENT - °C.
DISTANCE ALONG SPECIMEN, L - CM.
0
1
2
3
4
5
6
1
2
3
4
5
6
7
8
9

confirmed fairly well the temperature of the dry band as obtained from the resistivity versus temperature calibration. This comparison is shown in Fig. 4.23. The discrepancies between the two curves may be due to the fact that the infrared thermometer was working to the limit of its sensitivity and therefore the readings were not as accurate as one would wish. The calculated temperatures are less than the measured, at higher temperatures, and this may be due to the flatness of the peak of the curves affected by the resolution of the voltage probe as discussed in the Appendix, page 61.

FIG. 4.23

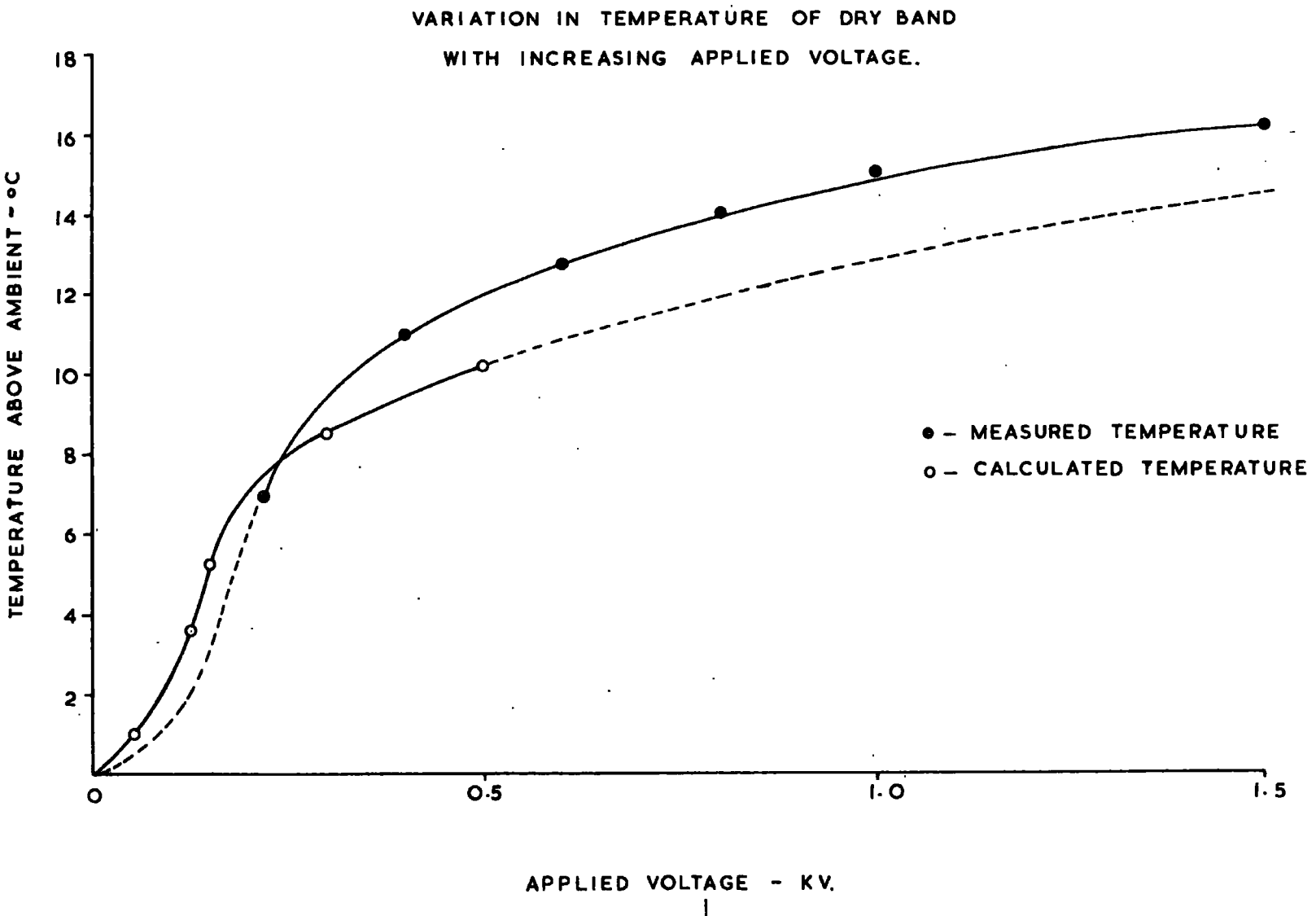
VARIATION IN TEMPERATURE OF DRY BAND
WITH INCREASING APPLIED VOLTAGE.
TEMPERATURE ABOVE AMBIENT - °C
18
16
14
12
10
8
6
4
2
0
0.5
1.0
1.5
● – MEASURED TEMPERATURE
o – CALCULATED TEMPERATURE
APPLIED VOLTAGE - KV.

4.3. FAN SPEED RESULTS

To study the effect of different convection rates on the formation of dry bands, measurements of current and dry band width versus applied voltage were made over a wide range of fan speeds. The greater the fan speed, the greater the convection losses and therefore the power dissipated at which a dry band could be initiated. Current voltage characteristics had previously been obtained by Salthouse[6]. The aim of this work was to find how the dry band width varied with applied voltage at different fan speeds. In particular, it was of interest to find whether or not the dry band width, once well formed, depended significally on convection losses.

On increasing the fan speed it was found that the voltage at which dry bands formed had increased; this is shown in Fig. 4.27. where the dry band width is plotted against applied voltage for a range of fan speeds. The same figure also shows quite clearly that once a dry band is well established, its width is not dependent on fan speed. It was also noted that the collapse of the dry band was faster at higher fan speeds, i.e. once the non-uniform evaporation had been initiated, the increase in voltage required to reduce the dry band to a narrow band was less. This suggests that the power dissipation at the critical voltage increases with increasing convection rates.

Fig. 4.28. illustrates the relationship between surface leakage current and applied voltage for increasing

FIG. 4.27

VARIATION IN DRY BAND WIDTH WITH APPLIED VOLTAGE FOR INCREASING FAN SPEEDS.

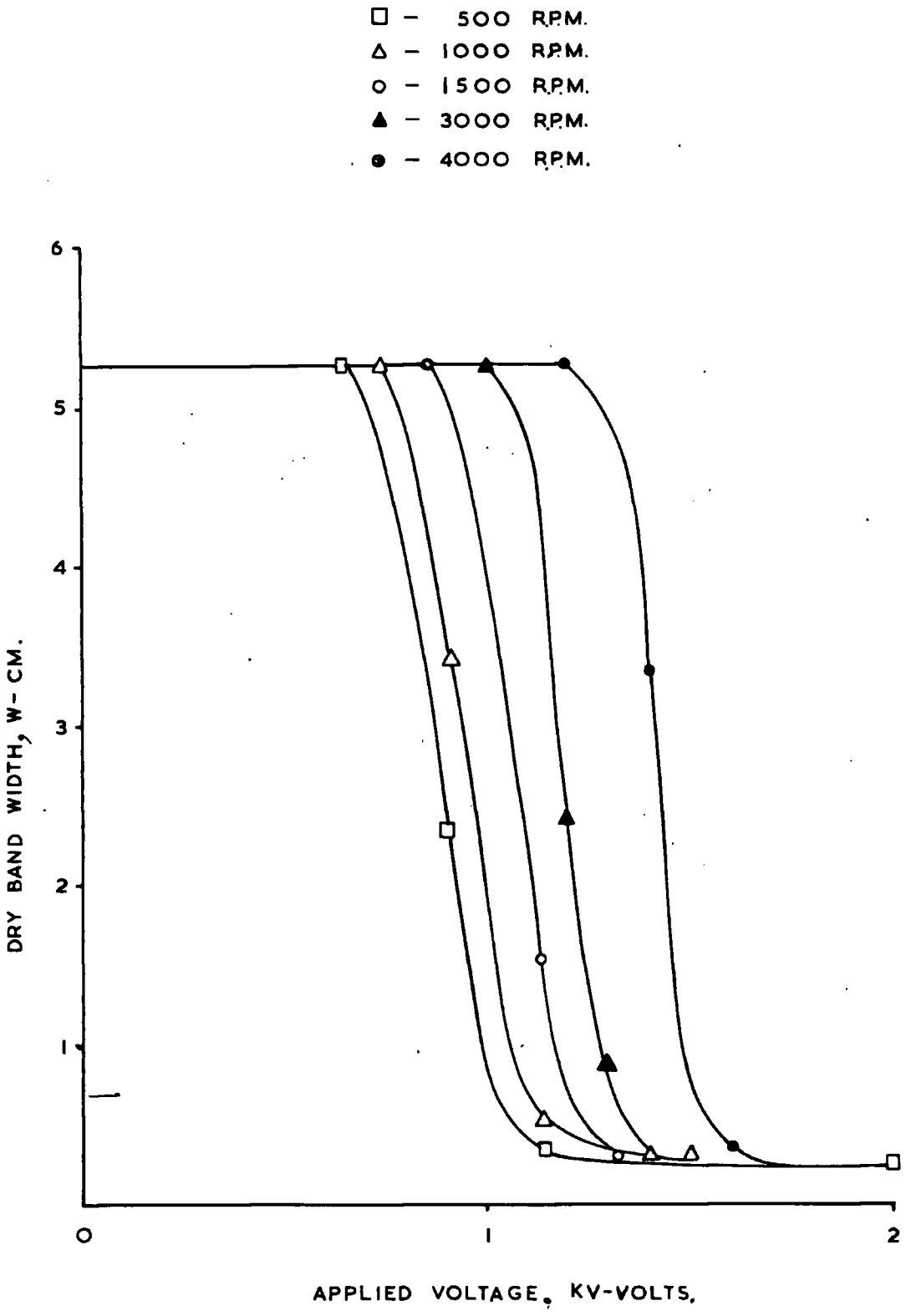

FIG. 4.26

VARIATION IN SURFACE LEAKAGE CURRENT WITH APPLIED VOLTAGE FOR INCREASING FAN SPEEDS.

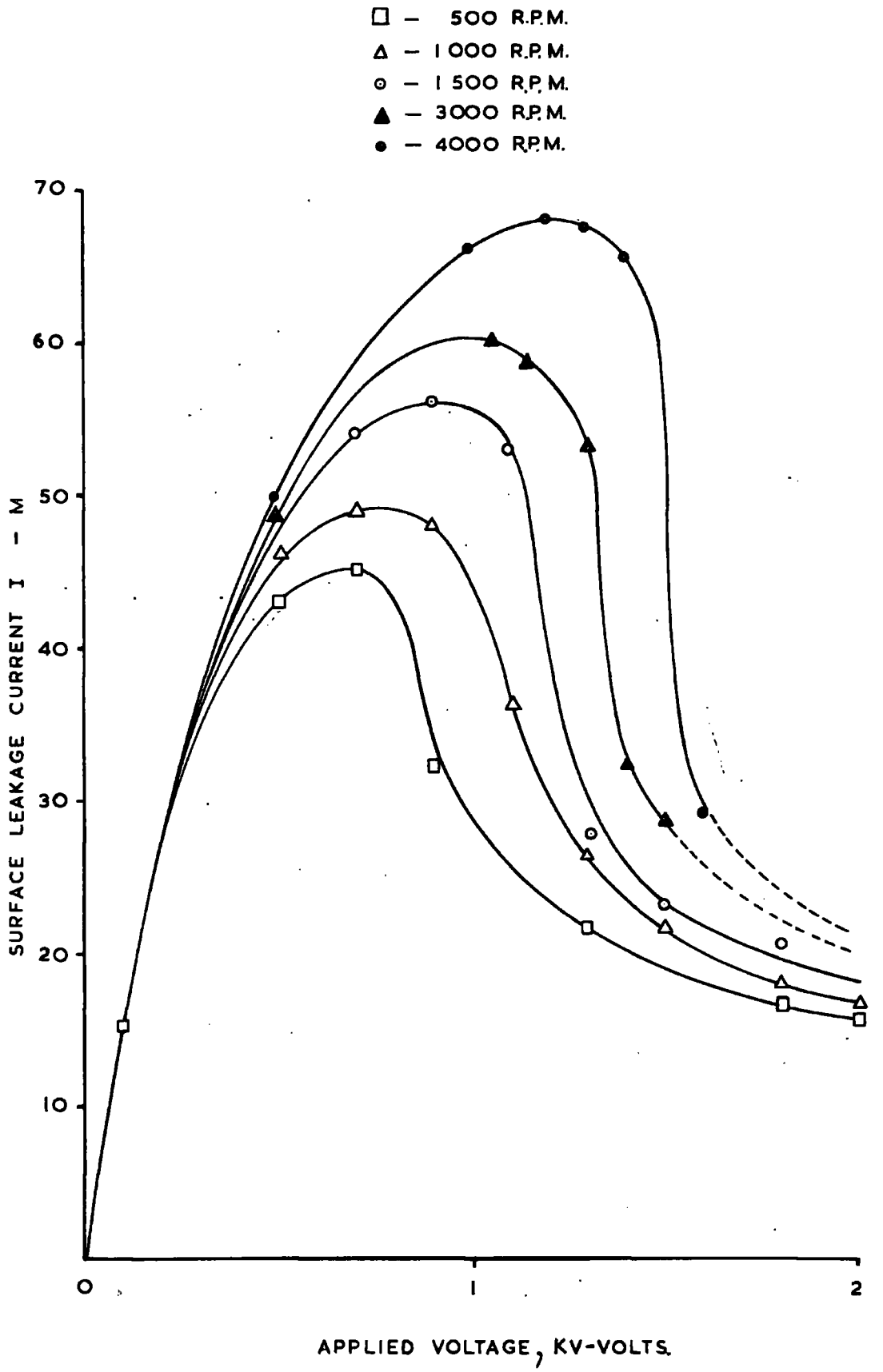

fan speeds, and this shows that not only does the critical voltage increase, but also the peak current associated with it. Consequently, more heat is generated in the surface, and once the non-uniform evaporation is initiated there is more heat available per unit area to accelerate the drying up of the surface, and thus the voltage collapses faster. This is confirmed in Fig. 4.29. where the dry band width is plotted against power dissipation per unit area for increasing fan speeds.

By increasing the fan speed, the power dissipated by convection increases, and since this is a case of forced convection at a relatively low temperature excess, Newton's law of cooling will apply. Therefore as a minimum temperature is required to initiate non-uniform evaporation, the power dissipated at this temperature must be proportional to the fan speed. This is confirmed in Fig. 4.28. where the power generated at the critical voltage is plotted against fan speed and shows a linear relationship.

FIG. 4.29

DRY BAND WIDTH VERSUS POWER DISSIPATION PER UNIT AREA IN THE DRY BAND.

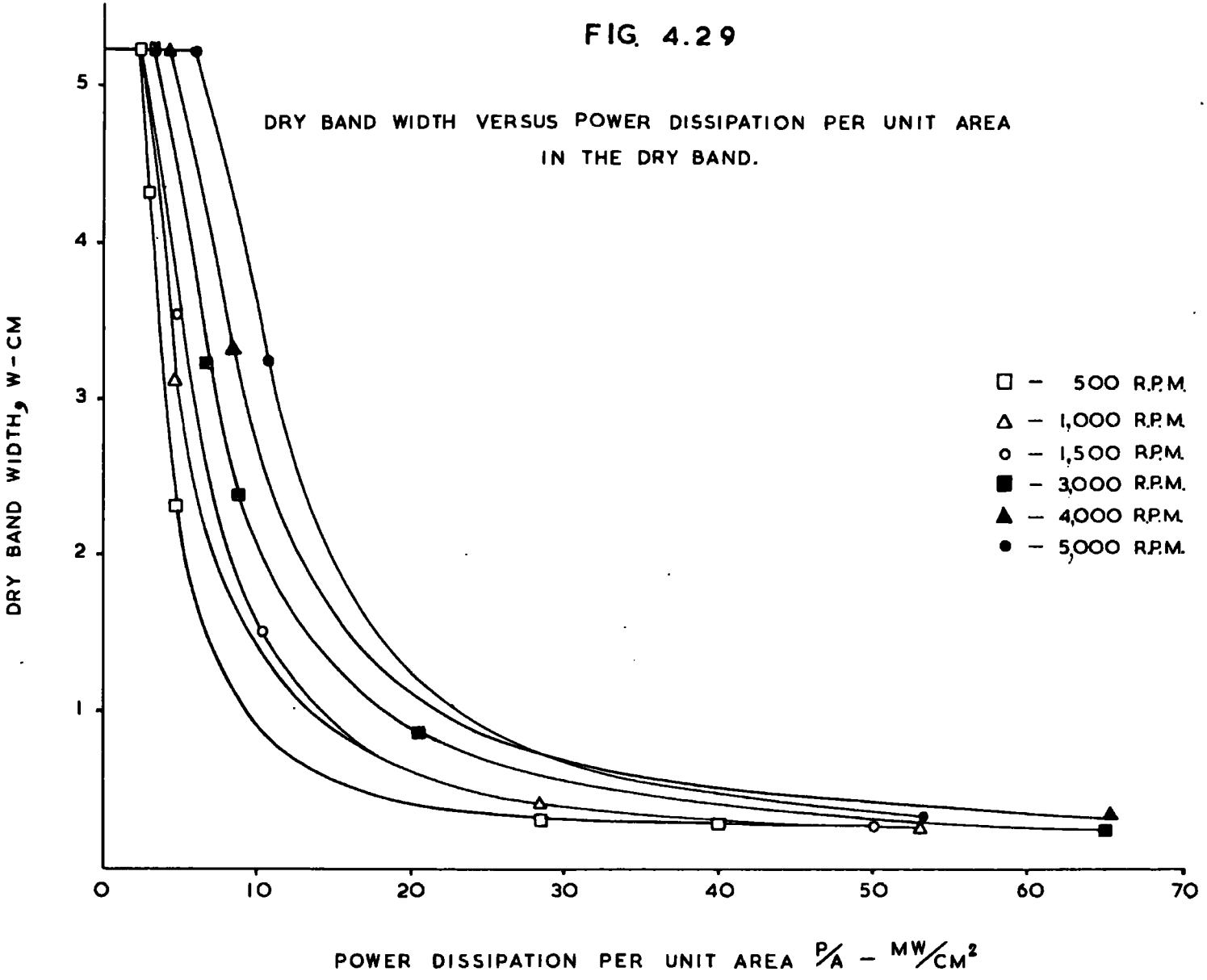

FIG. 4.28.

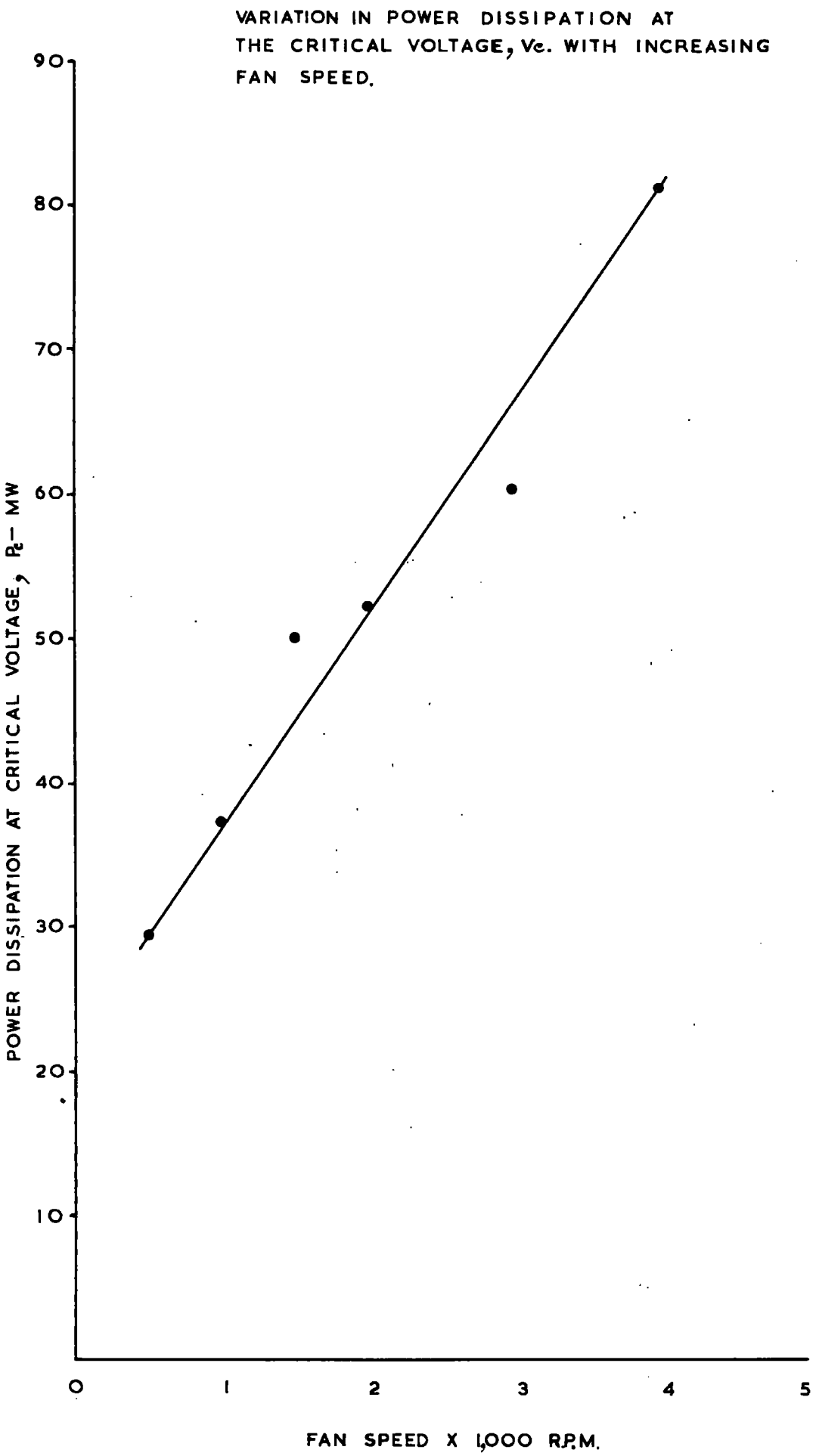
VARIATION IN POWER DISSIPATION AT THE CRITICAL VOLTAGE, Vc. WITH INCREASING FAN SPEED.
POWER DISSIPATION AT CRITICAL VOLTAGE, Pc — MW
90
80
70
60
50
40
30
20
10
0
1
2
3
4
5
FAN SPEED X 1,000 R.P.M.

5.0. CONCLUSIONS

The purpose of all electrical insulation is to prevent flow of leakage current where this is undesirable. Therefore it is very important that the insulation material chosen for a particular job should be as good as possible. However no insulation material yet known is completely perfect in preventing minute electric currents from flowing. The flow of current takes place mainly at the surface rather than in the bulk of the insulator due to a lower resistivity in the surface. With normal insulation this current flows in the surface contamination and the moisture inevitably adsorbed on the surface.

As the resistance of the surface is proportional to its length, it is easy to make an insulator sufficiently long to reduce the leakage current below an acceptable figure. However, in practice, the problem with insulation is not quite as simple as this, particularly when dealing with high voltages. All insulation in high voltage installations is subject to atmospheric pollution which forms a thin layer on the surface of the insulator and, when subjected to a high degree of humidity, forms an electrolytic film of much less resistivity than that of the actual surface. This completely alters the characteristic of any good insulator and very often results in tracking and flashover in high voltage installations. To be able to prevent breakdown of insulation it is essential to know what happens on the surface of insulation after

it has been subjected to pollution.

The work of this thesis is an attempt to give a clear picture of some of the characteristics of the surface of a non-conducting material, having previously been coated with a known substance and artificially polluted by dipping the specimen in a solution of Cobalt Chloride dissolved in Methanol. The electrical behaviour of the surface was measured while the sample was subjected to a number of artificial conditions. These were closely controlled and kept constant for sufficiently long periods of time to enable the surface to settle down according to the atmospheric conditions surrounding it.

No attempt was made to measure the surface behaviour of the sample while pollution was building up. This would require more elaborate equipment, as well as adding complications to the technique used in the measurements, such as, for instance, contamination of the probe.

Several tests were made to find a suitable degree of contamination so that a whole set of readings could be obtained without having the limitations of the equipment interfering with the validity of the results, particularly with regard to the supply voltage, which was limited to 5 kV. In order to use a less contaminated specimen it would have been necessary to have a much higher supply voltage. This would in turn, mean redesigning the probe to prevent flashover between the probe and the sample, and this would mean a poorer resolution of the probe; see appendix.

Measurements were made of the surface leakage current and the voltage distribution for increasing applied voltage. These results were obtained over a range of humidities from 43.0% to 93.0% on the same specimen. Similarly results were obtained over a range of fan speeds, and therefore different convection rates, at a single humidity. An attempt was made to develop an infrared technique to measure the surface temperature remotely.

5.1. CURRENT VOLTAGE CHARACTERISTICS

The results confirmed the work done by Salthouse[6]:-

$$V_c = \text{constant} \times \sqrt{R_{so}}$$

where V_c = the critical voltage

The initial surface resistance is a function of the relative humidity of the ambient in such a manner that for increasing humidities the initial resistance is decreasing. Thus the voltage required to raise the surface temperature sufficiently to cause significant evaporation is lower at higher humidities.

Initially the surface leakage current increases linearly with applied voltage; thus for low voltages there is no nett loss of moisture from the surface, as illustrated in Fig. 4.3. However, when the voltage is increased beyond the linear region, evaporation is initiated. The evaporation of moisture from the surface is uniform until the critical voltage is reached which corresponds to the maximum surface leakage current. At this point non-uniform evaporation is initiated and remains non-uniform for increasing voltages. The point where the system changes from uniform to non-uniform evaporation is less sharply defined at lower humidities. In fact, the results indicate that there is a critical humidity below which non-uniform evaporation does not occur.

5.2. DRY BAND WIDTH

The results confirm the collapse of the voltage distribution to a narrow band of high resistivity in a stable equilibrium. The collapse of the dry band occurs simultaneously with the collapse of the leakage current as illustrated in Fig. 4.3. The width of this band was taken as the distance between the half power points, as it was power initiated. This was confirmed by results illustrated in Fig. 4.25.

The width of the dry band was found to decrease with increasing voltage. This was particularly noticeable at low humidities where the transition from uniform to non-uniform evaporation was relatively slow compared with high humidities. This may be more easily understood by considering the power dissipation per unit area. At low humidities the surface resistivity is relatively large. Therefore an increase in voltage supply gives a relatively small change in power dissipation and consequently a small rise in surface temperature; whereas at high humidities the resistivity is low and the same increase in voltage will give rise to a larger power dissipation and the temperature increase would be correspondingly higher. Consequently a more drastic change in dry band width would occur.

The results indicate that the width of the dry band with respect to power dissipated per unit area in the band is closely related for all humidities down to 52% relative humidity, as illustrated in Fig. 4.25. The fact that no dry band was formed at lower humidities was due to the

voltage supply being limited to 5 kV. However, as the forming of dry bands is essentially dependent on moisture being present in the surface, it is reasonable to believe that a critical relative humidity exists below which evaporation is uniform for all voltages.

5.3. SURFACE RESISTIVITY AND TEMPERATURE DISTRIBUTION

The voltage distribution across the surface was linear for increasing voltages up to the critical voltage. This confirms uniform evaporation up to this point. When the applied voltage is increased beyond the critical point, the voltage distribution is no longer linear. A large portion of the applied voltage appears across a section of the surface. By measuring the gradient of the voltage distribution curve at a number of points a clear picture of field distribution is obtained. This confirms that once the critical voltage is reached, a section of the surface is subjected to a higher field strength compared with the remaining part of the surface. Since the impedance of the surface is purely resistive. The resistivity of this section is higher than the rest of the surface. This is illustrated by plotting the resistivity distribution across the surface, knowing the surface leakage current and the field distribution. The maximum field strength increases with increasing voltage in the dry band whereas it remains fairly constant for the rest of the surface. This shows that the resistivity of the dry band increases with increasing voltage. Therefore once a dry band is established, the remaining part of the surface remains in a stable condition, and increasing power dissipation due to increasing applied voltage is concentrated in the dry band.

The temperature across the surface was deducted from the resistivity distribution through a previously established

relationship between surface resistivity and temperature, shown in Fig. 4.17. This gives a clear picture of the build up of the temperature in the dry band as the voltage increases. One would, however, expect the temperature to be maximum in the centre of the dry band and not constant across a narrow section as shown in the temperature distribution curves. The flatness on top of the curves is due to the resolution of the capacitance probe as this would detect the average voltage over a given area rather than the peak voltage. Therefore the curves should have been slightly more peaked than shown. An infrared thermometer was developed to confirm the temperature distribution across the surface under non-uniform evaporation. Unfortunately the mechanical scanning device did not work satisfactorily; thus only readings from the centre of the dry band were obtained. It was found that the temperature calculated from the resistivity of the dry band was only 10% less than measured by the infrared thermometer. The temperatures compared favourably, particularly as the thermometer was working at the limit of its sensitivity and also as errors were introduced by the resolution of the capacitance probe.

5.4. FAN SPEED AND CONVECTION LOSSES.

By varying the speed of the fan circulating the air in the humidity chamber, it was possible to change the convection losses from the surface. Under these circumstances the power dissipation per unit area necessary to initiate a dry band increased with the fan speed. However once the dry band was well established, its width was independent of fan speed.

By increasing the fan speed, the convection losses increase, and the minimum power dissipation required to raise the temperature sufficiently to initiate non-uniform evaporation increases.

Once the dry band is established, most of the heat lost is concentrated in the dry band and therefore the temperature of the dry band will be affected by the rate of loss of heat rather than its width.

The collapse of the dry band is affected by the fan speed and is faster at higher convection losses. This is due to more heat being generated in the surface at the point where non-uniform evaporation is initiated; thus more heat energy is concentrated per unit area in the unstable region and this has an accelerating effect on the collapse of the voltage distribution.

By increasing the fan speed, the convection rate increases equally and a better cooling of the polluted surface is achieved. This has a preventive effect on the initiation of dry bands.

5.5. GENERAL COMMENTS

No attempt was made to apply the results in design of insulation; nevertheless some points regarding choice of material and design should be kept in mind. One important aspect of insulation is that it should have a uniform and high surface resistivity and be able to maintain this characteristic even when subjected to pollution. Therefore one would look for materials which have a low surface adhesion coupled with good mechanical stress properties. Materials with low surface adhesion do not readily adsorb matter present in industrial pollution, and are easily washed.

Non-uniform evaporation is initiated when the surface temperature reaches $3^{\circ}C$. above ambient; therefore to prevent dry bands forming, it is necessary to ensure that the surface temperature is kept well below its critical point. Thus it would be of great importance to use a material which is a good heat conductor. The bulk of the insulator would then absorb the heat generated in the surface and thus tend to maintain a uniform surface temperature.

This work has been carried out with voltages up to 5 kV, on a plain artificially polluted surface, but could be extended to real insulators. When working with higher voltages care should be taken to avoid flashover between measuring probe and insulator. Accurate measurements of real insulators can be achieved by using an infrared thermometer, scanning the surface at a safe distance.

The surface temperature distribution could thus be obtained, and by establishing the exact relationship between temperature and surface resistivity for the insulator, the behaviour of the insulation surface could be studied closely.

6.0. REFERENCES

1. James, A.G.
"A review of the problem of polluted insulation."
S.Q.J. IEE., Vol.35, No. 140, June 1965,
pp. 182-190.

2. Hampton, B.F.
"Flashover mechanism of polluted insulation."
Proc. IEE., Vol.111, No.5, May 1964, pp.985-990.

3. Alston,L.L. and Zoledziowski, S.
"Growth of discharges on polluted insulation."
Proc. IEE., Vol.110, No.7, July 1963,
pp.1260-1266.

4. Forrest, J.S.
"The characteristic and performance in service of high voltage porcelain insulators."
Journal IEE., Vol.89, Part II, 1942, pp.60.

5. McIlhagger,D.S., McCausland,I. and Girvan,S.B.
"The effects of applied voltage gradient on the surface resistivity of insulators in humid atmospheres."
SRC Conference on power systems, Glasgow, 1967.

6. Salthouse, E.C.
"Initiation of dry bands on polluted insulation."
Proc. IEE., Vol.115, No.11, November, 1968,
pp. 1707-1712.

7. British Standard 137.
"Specification for porcelain and toughened glass insulators for overhead power lines."
B.S. 137 : 1960, pp.65.

8. Lambeth,P.J., Looms,J.S.T., Stalewski, A. and Todd, W.G.
"Surface coatings for h.v. insulators in polluted areas."
Proc. IEE., Vol.113, No.5, May 1966, pp. 861-869.

9. Last, F.H., Pegg,T.H., Sellers,N., Stalewski, A. and Whittaker, E.B.
"Live washing of h.v. insulators in polluted areas."
ibid., pp. 847-860.

10. Parkman, N.
"Electrical breakdown by tracking."
Proc. IEE., Vol.109, Part B, Supplement No. 22, pp. 448-453.

11. Johnson, F.W.
"Adsorbed films on the surface of glazed porcelain."
Phil. Mag., 1934, No.28, pp. 637-680.

12. Johnson, F.W.
"Surface resistivity of adsorbed moisture on glazed porcelain."
ibid., 1937, No.24, pp.797-807.

13. McIlhagger, D.S.
"A criterion for the onset of 'dry band' formation on high voltage insulator surfaces in humid atmospheres."
SRC Conference on power systems, Glasgow, 1967.

14. Smail, G.G., Brooksbank,R.J. and Thornton, W.M.
"The electrical resistance of moisture films on glazed porcelain."
J. IEE., 1931, No.69, pp. 427-436.

15. Löberg,J.O. and Salthouse, E.C.
"Voltage divisions between non-linear resistances with positive temperature coefficients."
Electronics Letters, Vol.4, No.25, December 1968. pp. 552.

16. Przoylowicz, E.P., Staudenmayer, W.J., Perry, E.S., Baitsholts, A.D. and Tischer, T.N.
"Precoated sheets for thin layer chromatography."
Conference on analytical chemistry and applied spectroscopy, Pittsburg, 1965.

17. Jacob, M.
"Heat transfer."
Vol.1, John Wiley, 1949.

18. Imperial Chemical Industries Limited.
"Melinex polyester film for the electrical industry."
Information service note No. 878.

7.0. APPENDIXES

7.1. TEST SAMPLE

The test samples were cut from Eastman Chromagram sheets, as shown in Fig. 4.1, used in thin layer chromatography. These sheets are made from a thin coating of a porous absorbant on a flexible polyester support. The coating is of specially prepared silica gel bonded by a small quantity of polyvinyl alcohol to provide flexibility and abrasion resistance for normal handling.[16]. The silica gel layer was found to be uniform and constant on all the samples, and had a high electrical resistivity when dry. Because of high resistivity it was necessary to introduce an artificial pollution on the surface. This was done by immersing the whole sheet in a solution of Cobalt Chloride dissolved in Methanol; the sheet was then dried between filter papers to remove excess pollution and placed in an air drying oven at a temperature of approximately $50^{o}C$. Cobalt Chloride was used because of the colour change, dependent on the amount of moisture adsorbed by the surface. At high humidities, the colour was pale pink whereas at low humidities the colour was blue. Thus when a dry band appeared it could be identified.

The base of the Eastman Chromagram sheets is made from polyethylene terephtalate, a dimensionally stable material over a wide range of humidities[18]. It was, however, noticed that when the sample was subjected to an

atmosphere with high relative humidity, a slight buckling occurred. To prevent this from happening during the tests, the sample was left in a highly humid atmosphere for 24 hours. The specimen was then mounted between two brass electrodes and tightly stretched.

7.2. CALIBRATION OF THE PROBE

In order to fully understand the results it was necessary to determine the resolution of the probe.

The probe casing was machined from a brass rod to the dimensions shown in Fig. 7.1. The actual probe was situated inside the probe casing and insulated from this by a p.t.f.e. holder which fitted the casing tightly. It was, however, possible to move the probe while inside its casing and thus accurately set the distance d from the probe tip to the end of the casing. The lead carrying the signal from the probe was earthed with the probe casing.

The probe was mounted on an arm and its position was measured with a travelling microscope. Two parallel copper strips on a veroboard were used as a test sample, and a constant voltage was applied between them. The distance between the copper strips was accurately measured by the travelling microscope. The distance between the end of the probe casing and the surface of the veroboard was set by feeler gauges,

The signal from the probe was fed to a sensitive valve voltmeter, and sets of readings were taken scanning the probe across the copper strips at various values of s and d. It was found that the distance d made very little difference to the resolution of the probe. However, d made a considerable difference to the probe signal as shown in Fig. 7.2. The signal to noise ratio appeared to be good even at maximum probe signal which corresponded to a value of d equal to $^1/16$". With d set to $^1/16$",

FIG. 7.1

SKETCH SHOWING CROSS SECTIONAL VIEW OF PROBE AND CALIBRATION SPECIMEN

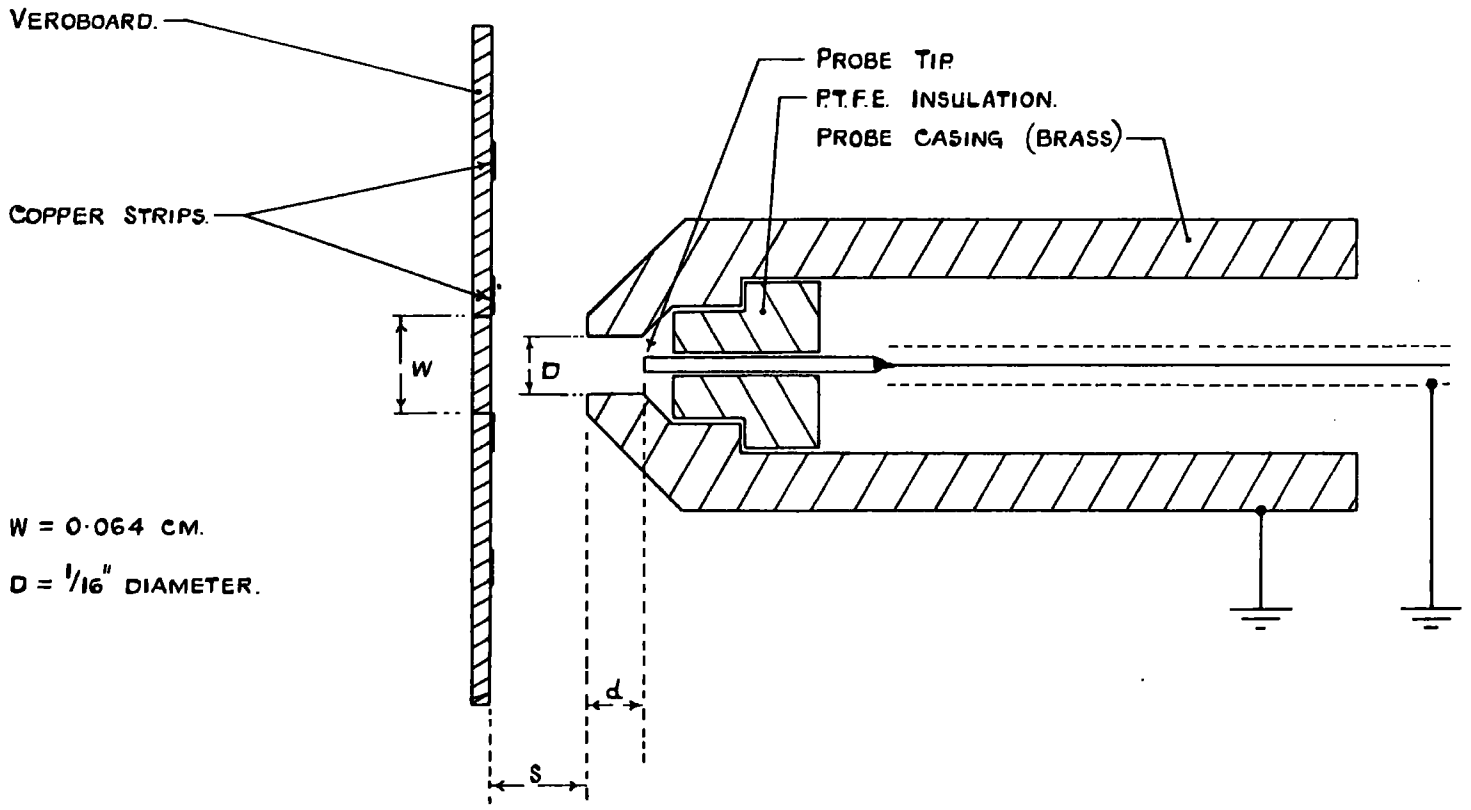

FIG. 7·2.

METER DEFLECTION VERSUS PROBE DISPLACEMENT, WITH S = 1/6"

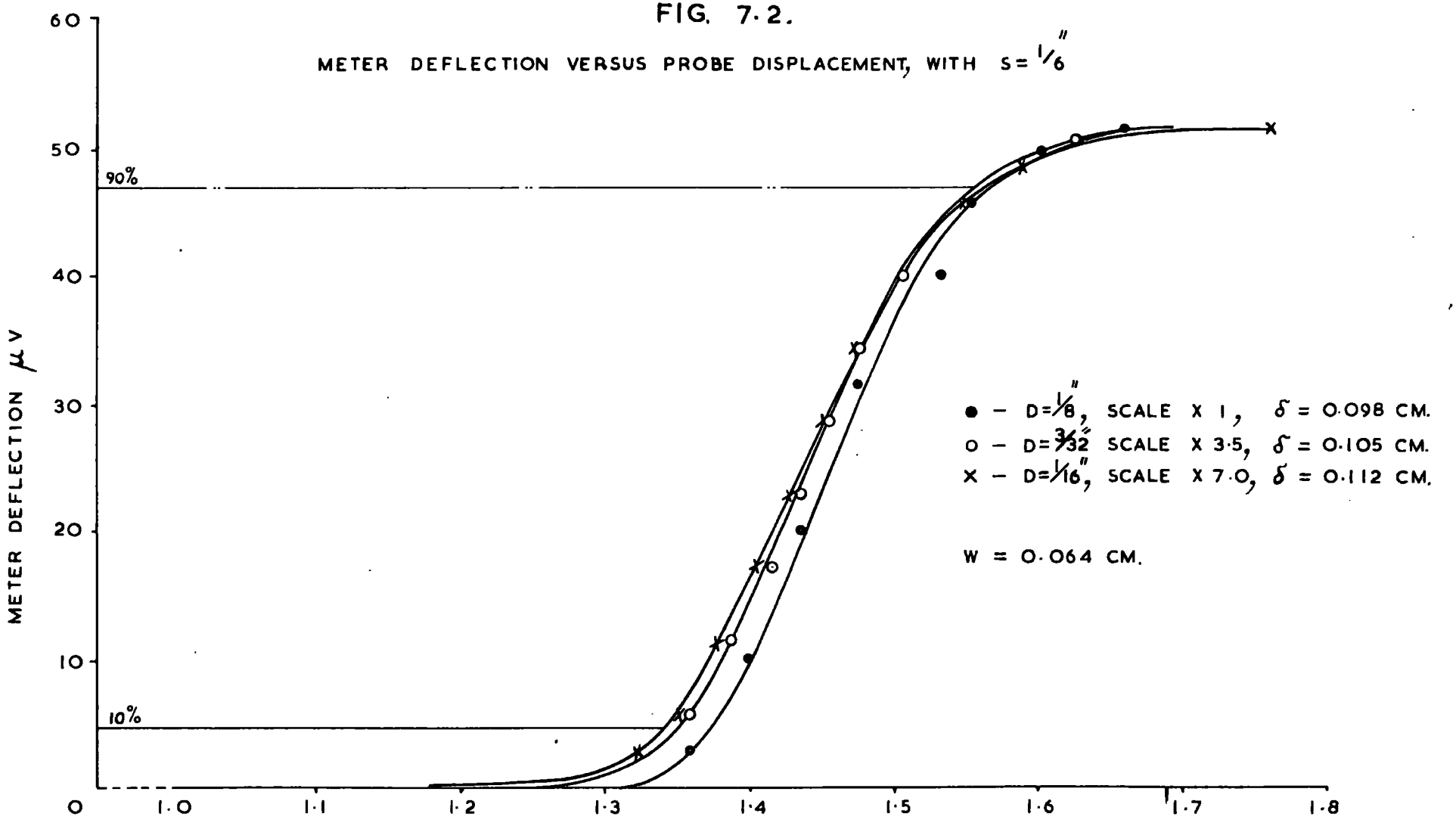

sets of results were recorded for various values of s as shown in Table 7.1. The curves plotted from these results are shown in Fig. 7.3.

The probe displacement from 10% to 90% of applied voltage was taken as 2δ where δ is the resolution of the probe.

Fig. 7.4. shows the relationship between the distance s and the resolution of the probe, compared with the distance between the copper strips. The resolution of the probe improves with decreasing s; thus it is important to keep s to a minimum. It was found that flashover between the probe casing and the surface of the specimen did not occur for voltages less than 5kV; thus it was decided to set the probe at a distance of $^{1}/16$" from the surface throughout the tests; therefore the resolution of the probe was approximately two millimetres in all the experiments.

FIG. 7·3.

METER DEFLECTION ~ PROBE DISPLACEMENT, WITH D= 1/16"

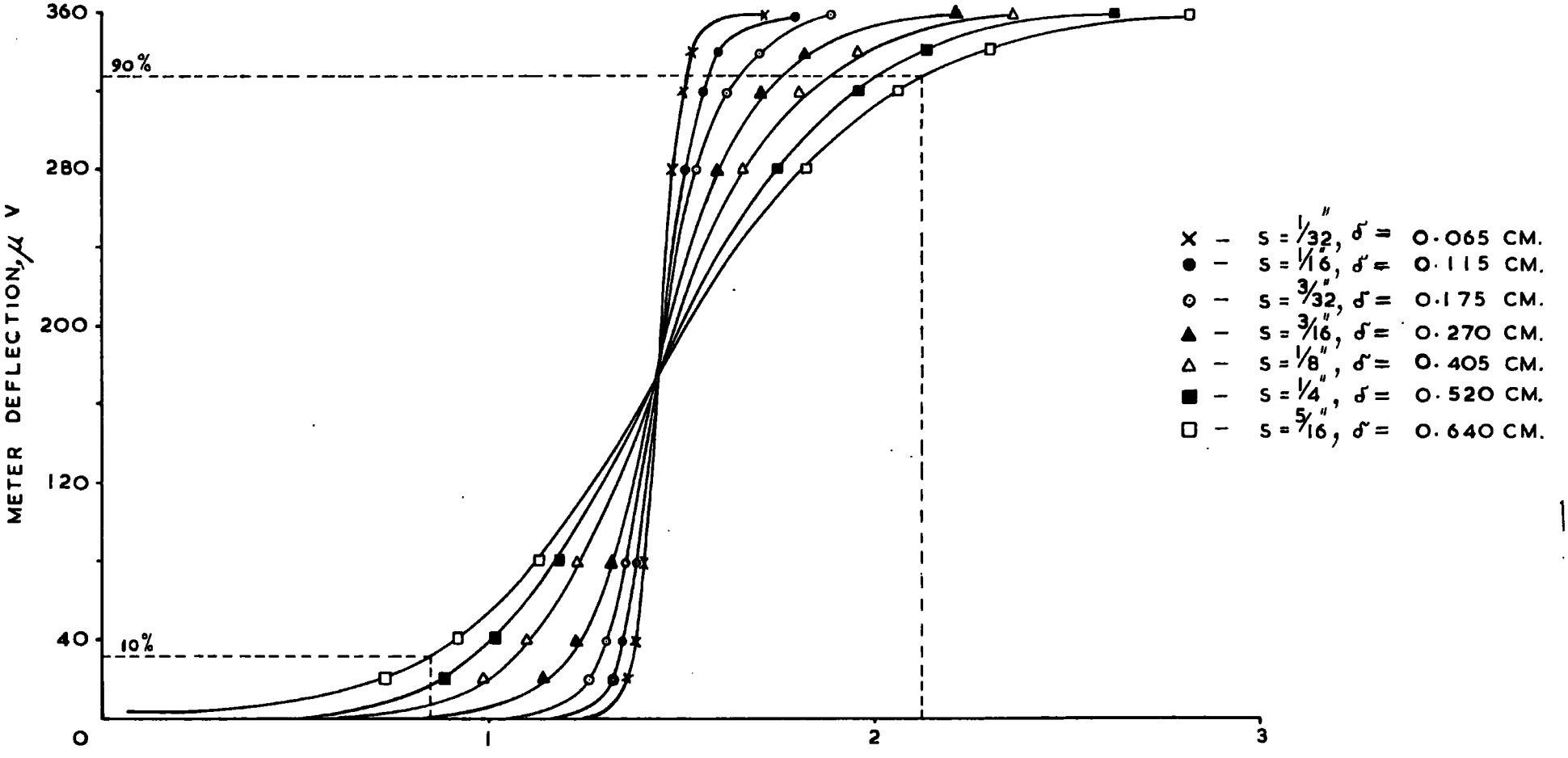

FIG 7.4

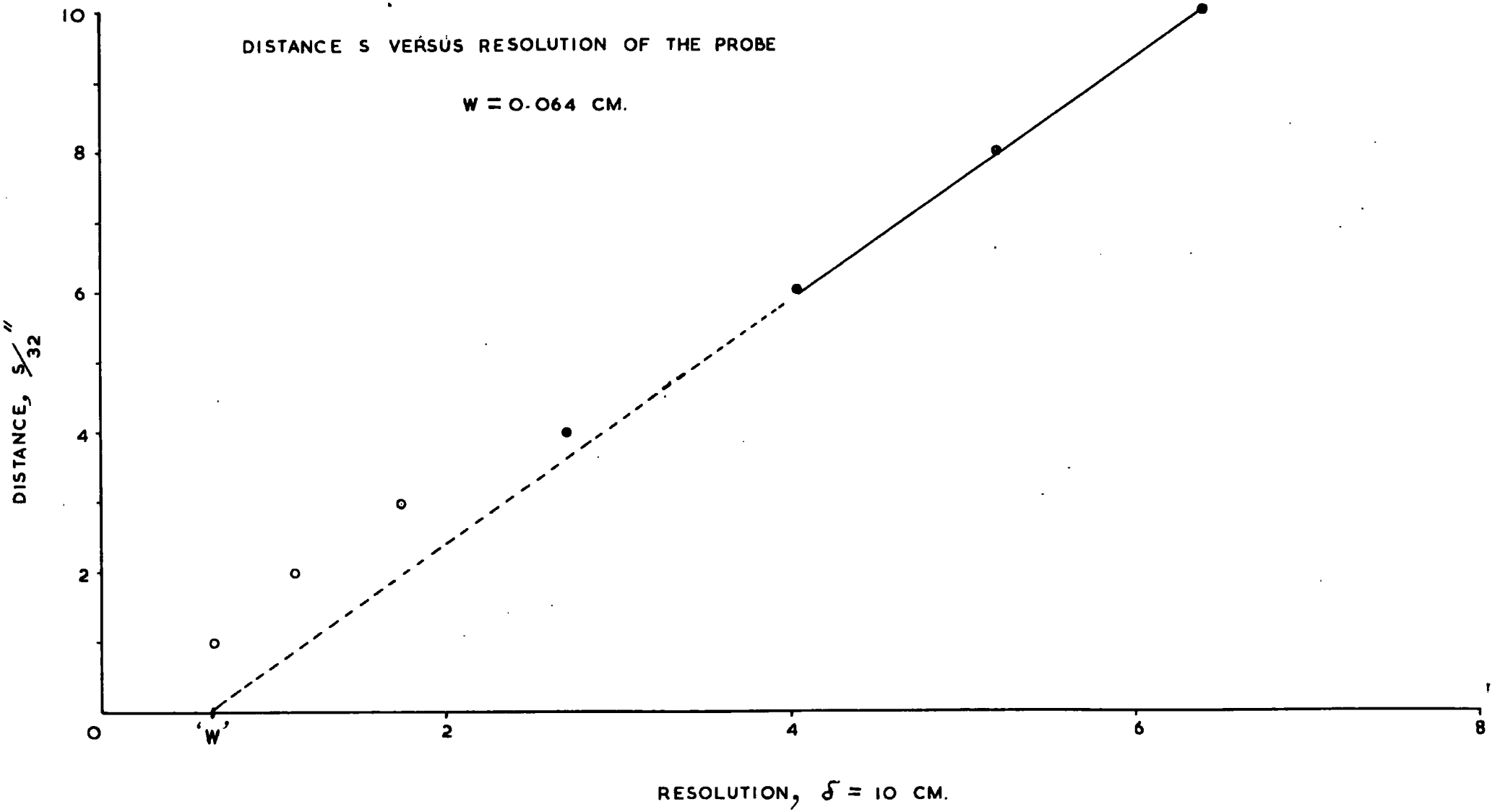
DISTANCE S VERSUS RESOLUTION OF THE PROBE
W = 0.064 CM.
DISTANCE, S/32"
RESOLUTION, δ = 10 CM.
'W'
0
2
4
6
8
10

7.3. MEASUREMENT TECHNIQUE

The surface leakage current was measured by a Hewlett Packard Voltmeter connected across a 'resistance box' in series with the specimen under test as shown in Fig. 7.5. The 'resistance box' contained a range of high tolerance resistors; thus, depending on the voltage applied to the specimen, a suitable resister could be chosen so as to give a satisfactory deflection on the meter. The values of these resistors were very small compared with the surface resistance, even when the specimen was subjected to high humidities. Therefore the voltage drop across the resistors could be neglected in comparison with the applied voltage.

The voltage supply to the specimen was obtained by an auto-transformer connected to the mains via a "Variac" and thus giving a continuously variable supply. The system was protected by an adjustable overload trip. The applied voltage was measured by an "Avometer."

The voltage distribution was measured by scanning a capacitance probe over the surface of the specimen. The probe was mounted on an arm which was geared to a shaft mounted externally on the lid of the test chamber. The output of the probe was fed through a screened cable to a pre-amplifier, the output of which was connected to a tuned amplifier with a narrow band width. The purpose of using a tuned amplifier was to filter out any noise signals picked up by the probe. The signal was then fed through an a.c./d.c. converter to the Y-amplifier of a chart recorder as shown in Fig. 7.6.

FIG. 7.5

CURRENT MONITORING CIRCUIT.

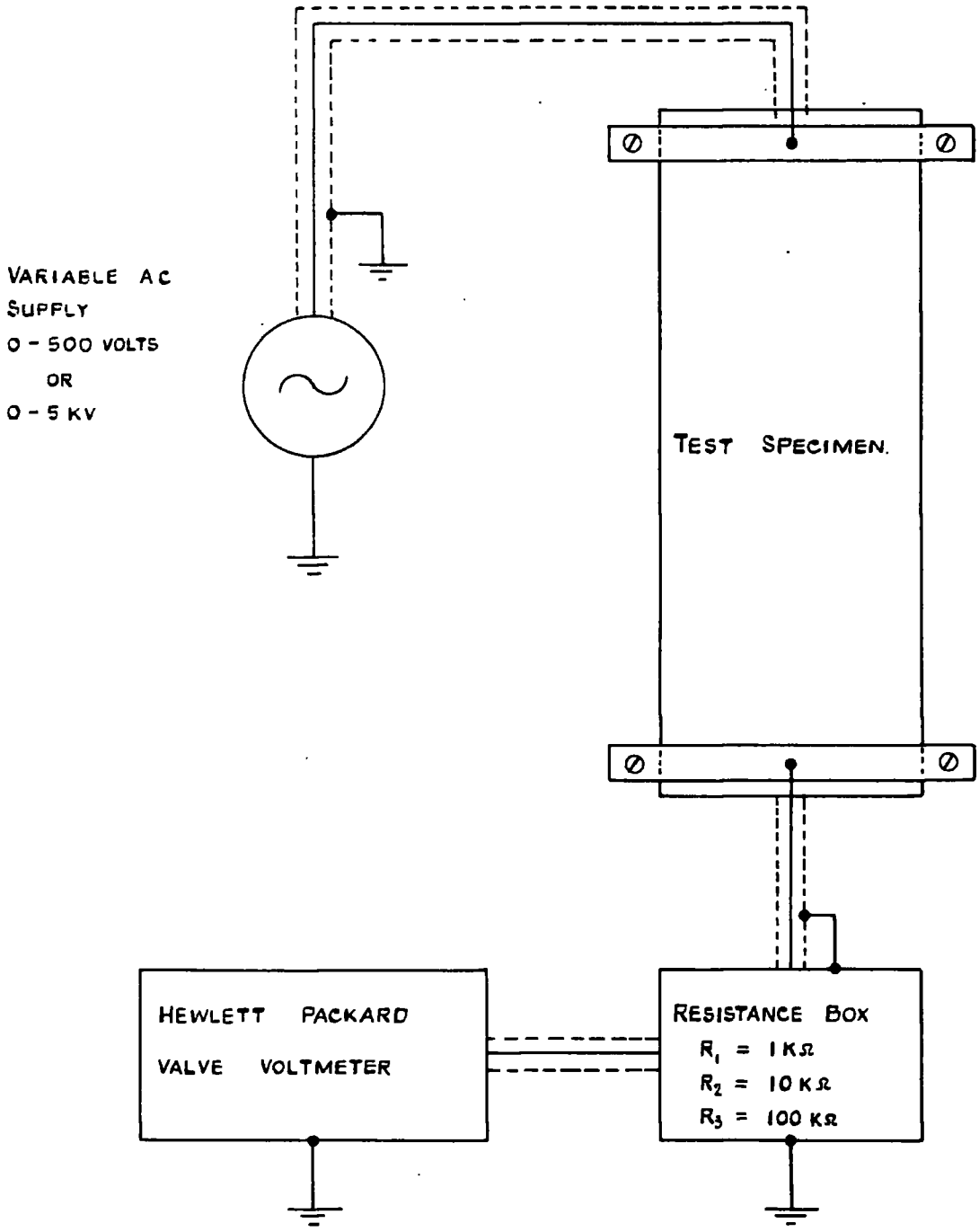

FIG. 7.6

CIRCUIT FOR VOLTAGE DISTRIBUTION MEASUREMENT

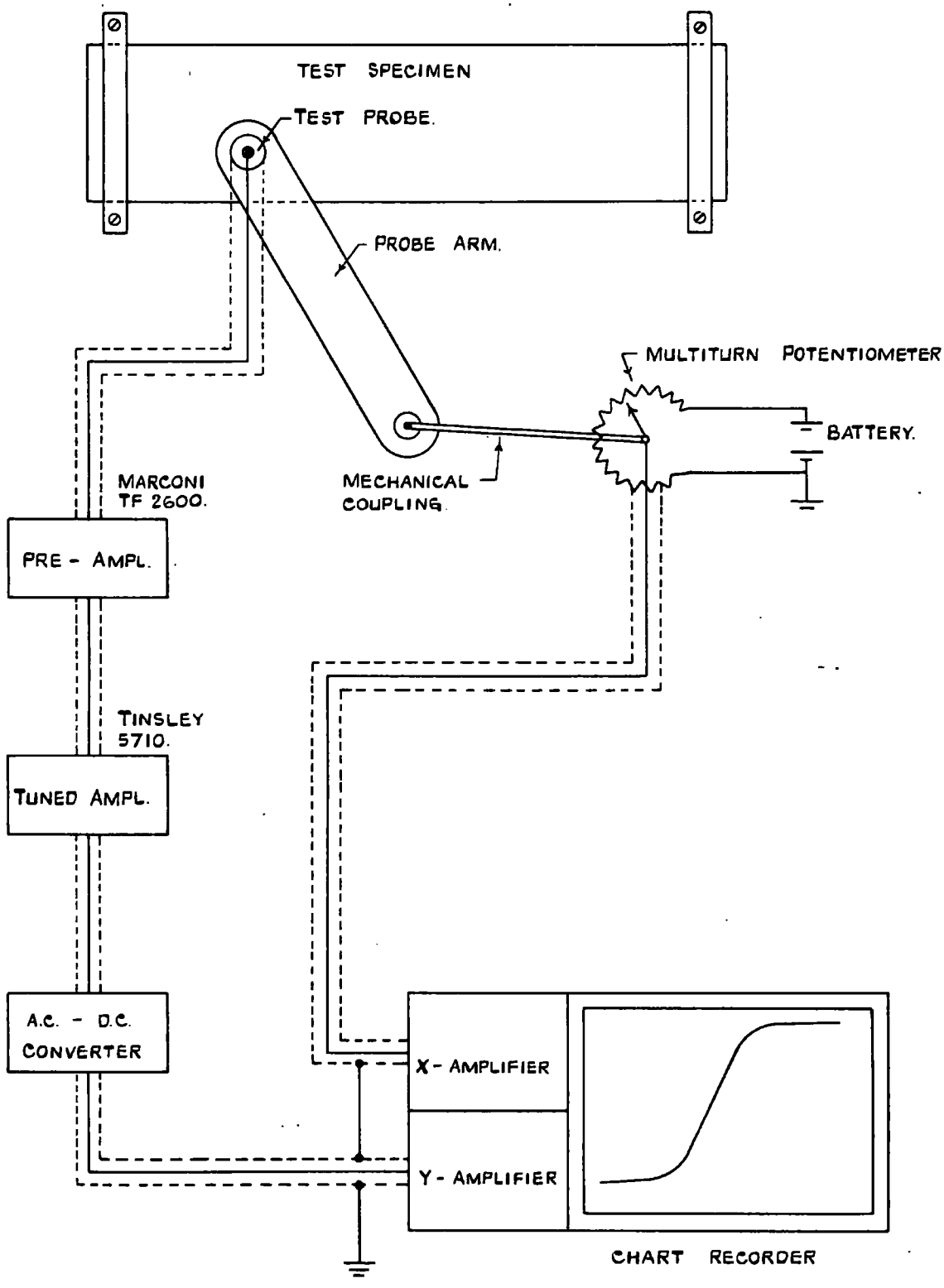

The pre-amplifier used was a Marconi Valve Voltmeter the output of which was proportional to the meter deflection. A direct calibration of the chart recordings was obtained from this meter.

The X deflection on the chart recorder was obtained from the wiper of a multiturn potentiometer coupled to the probe shaft. A d.c. supply was connected across the potentiometer, thus the potential on the wiper was proportional to the position of the probe.

The probe was not allowed to scan the entire surface as this would cause the earthed probe casing to come into contact with the electrodes and thus short circuiting the supply. Therefore it was necessary to calibrate the probe signal to the actual voltage it was measuring. This was done by disconnecting the 'resistance box' and thus interrupting the current flowing through the surface, but maintaining the supply voltage. Then by varying the supply voltage a set of results of probe output readings were taken as shown in Table 7.2. and plotted in Fig. 7.7.

In the fan speed tests, the fan speed was altered by varying the d.c. voltage driving the fan motor. The fan speed was recorded by a stroboflash.

FIG. 7·7

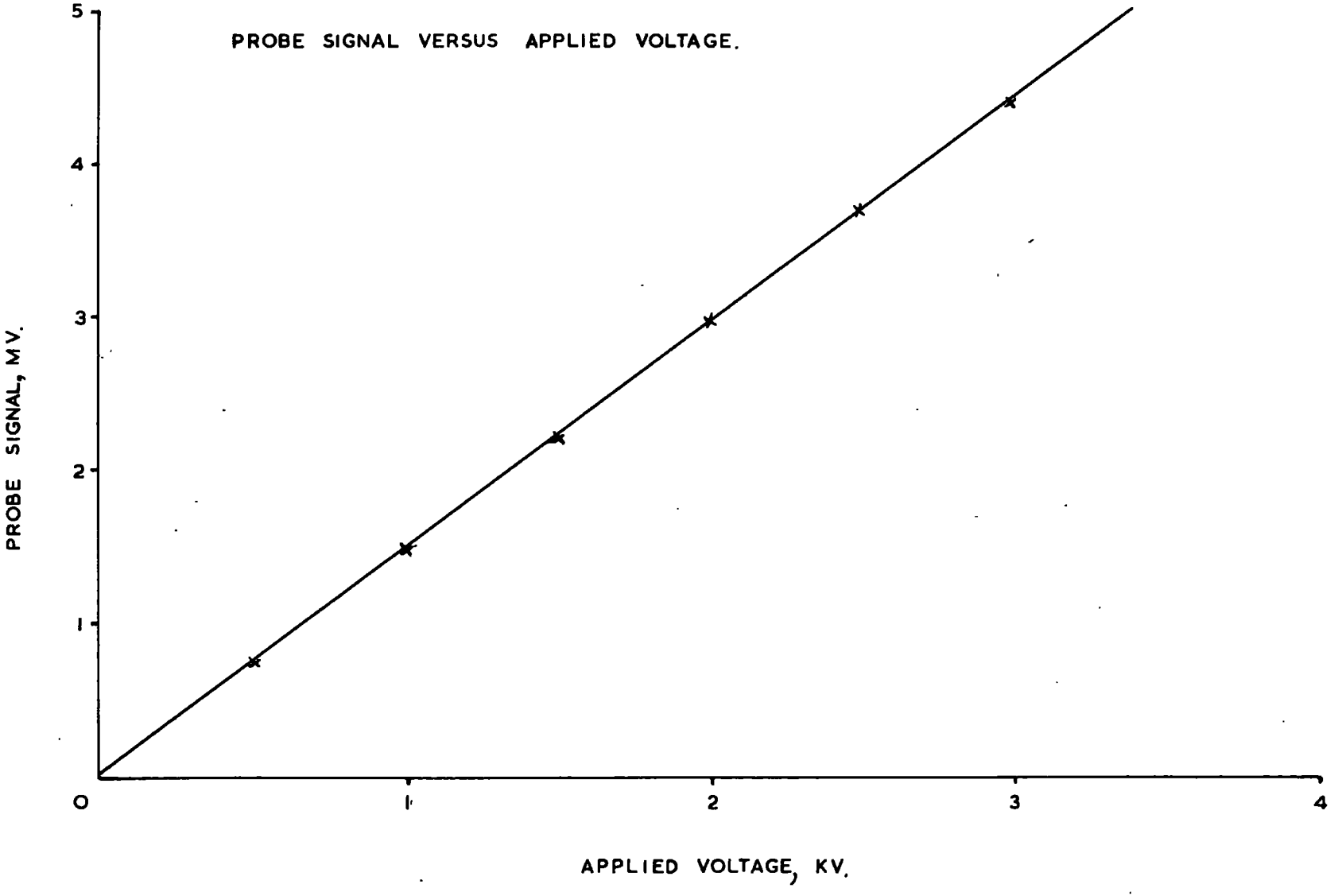
PROBE SIGNAL VERSUS APPLIED VOLTAGE.
PROBE SIGNAL, M.V.
APPLIED VOLTAGE, KV.
0
1
2
3
4
5

7.4. HUMIDITY AND TEMPERATURE CONTROL

The relative humidity was controlled by using a saturated salt solution in the bottom of the glass trough as shown in Fig. 7.8. Analar grade chemicals dissolved in de-ionised water were used in all the tests, and particulars of these are shown in Table 7.3. No trouble was experienced with salt creeping. It was found that salt only crept up the side of the container when there was an appreciable air leak. The saturated salt solutions were extremely easy to make, and gave a good stability of relative humidity throughout.

To attain the high degree of stability it was, of course, necessary to keep the ambient temperature constant. The test chamber, made up of a glass trough with an aluminium lid sealed on to it, was therefore placed in a waterbath. The temperature of the waterbath was controlled by a thermostat to an accuracy of $\pm$ 0.5 ^{o}C. and set to 25^{o}C. The water in the bath was circulated continuously to ensure an even temperature distribution. It was also necessary to keep the temperature constant throughout all the experiments in order to be able to compare all the results with each other. If the ambient temperature had been allowed to change, the rate of heat dissipated from the surface would change as this is a function of the ambient temperature. Furthermore, the container was painted black to avoid any change in the surface characteristic due to any strong light shining on the surface. The lid of the container was, however, supplied with a glass

FIG. 7.8.

DIAGRAM OF TEST CHAMBER.

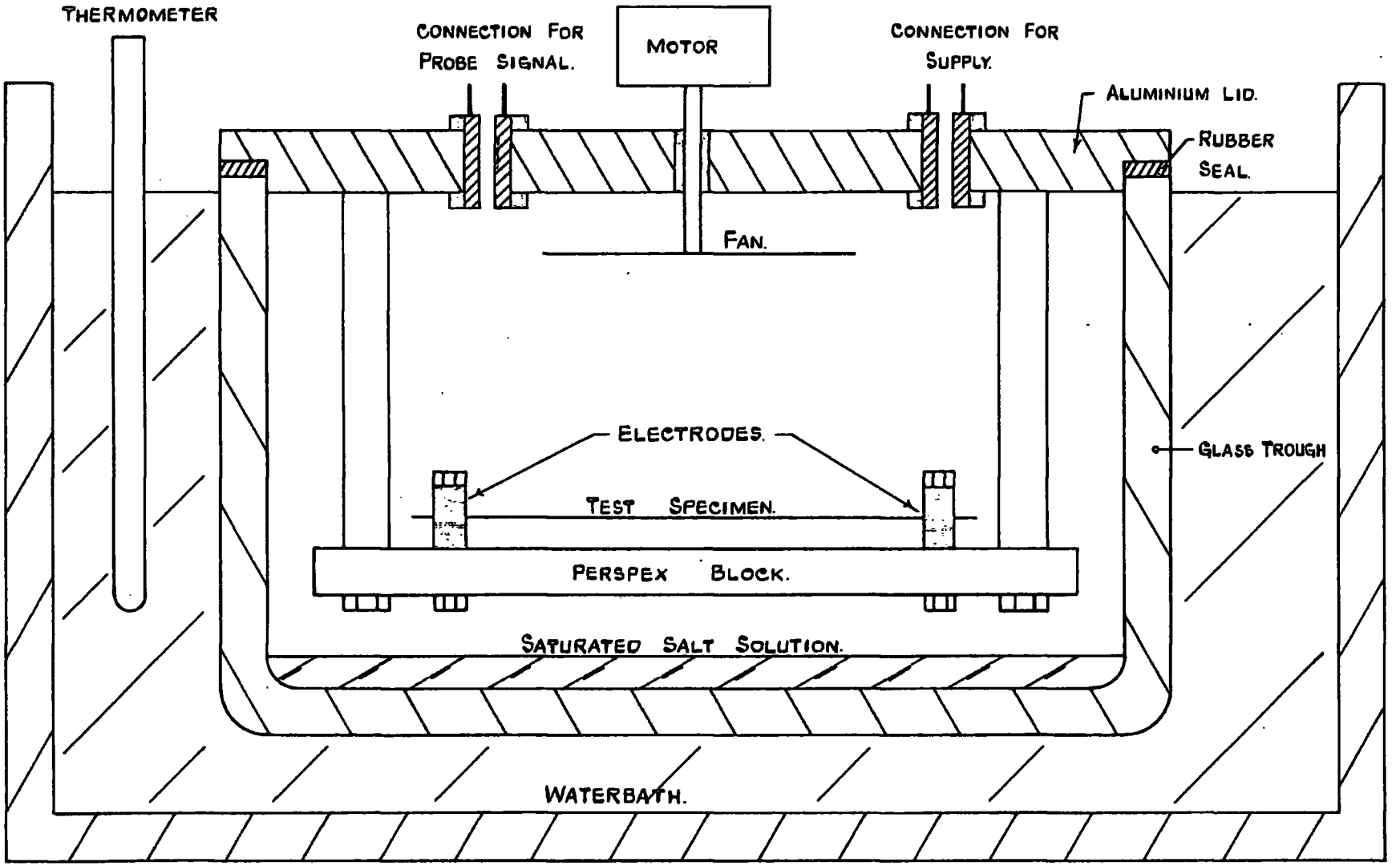

window through which the specimen could be seen. To ensure an even temperature distribution of ambient of the specimen, a small circulating fan was mounted inside the container. The motor driving the fan was mounted outside the container to avoid interference from heat generated in the motor.

7.5. INFRARED THERMOMETER

The aim of developing an infrared thermometer was to be able to measure the temperature distribution across the surface, accurately, while dry bands were forming.

A suitable container was built to accommodate the test specimen and the thermometer. The container was built of ¼" thick aluminium sheets and sealed properly to avoid air leaks. The container had no window for inspecting the specimen as light would have interfered with the infrared thermometer reading. It was also painted with a matt black spray to simulate black box radiation.

The principle of operation of the thermometer is shown in Fig. 7.9. The wavelength of infrared light is of the order of 5 μm; thus an ordinary glass lens for focussing is useless. Therefore a reflecting objective was used, the focal length of which is shown in Fig. 7.10. The thermometer cell was an indium antimonide cell, RPY51, made by Mullard Limited, and mounted in the bottom of a glass dewar. The cell window was only 0.5 millimetres square, therefore accurate focussing and alignment was required to obtain a correct temperature reading. Liquid Nitrogen was used to cool the cell to the required reference temperature of 77^{o}K. As the dewar was very small it could only hold a small quantity of Nitrogen lasting for a short while; thus it was required to top it up once every two to three minutes. The main difficulty in working with such low temperature was that of condensation forming on the cell window. As soon as condensation formed, the infrared

FIG. 7.9

SCHEMATIC DIAGRAM OF INFRARED THERMOMETER.

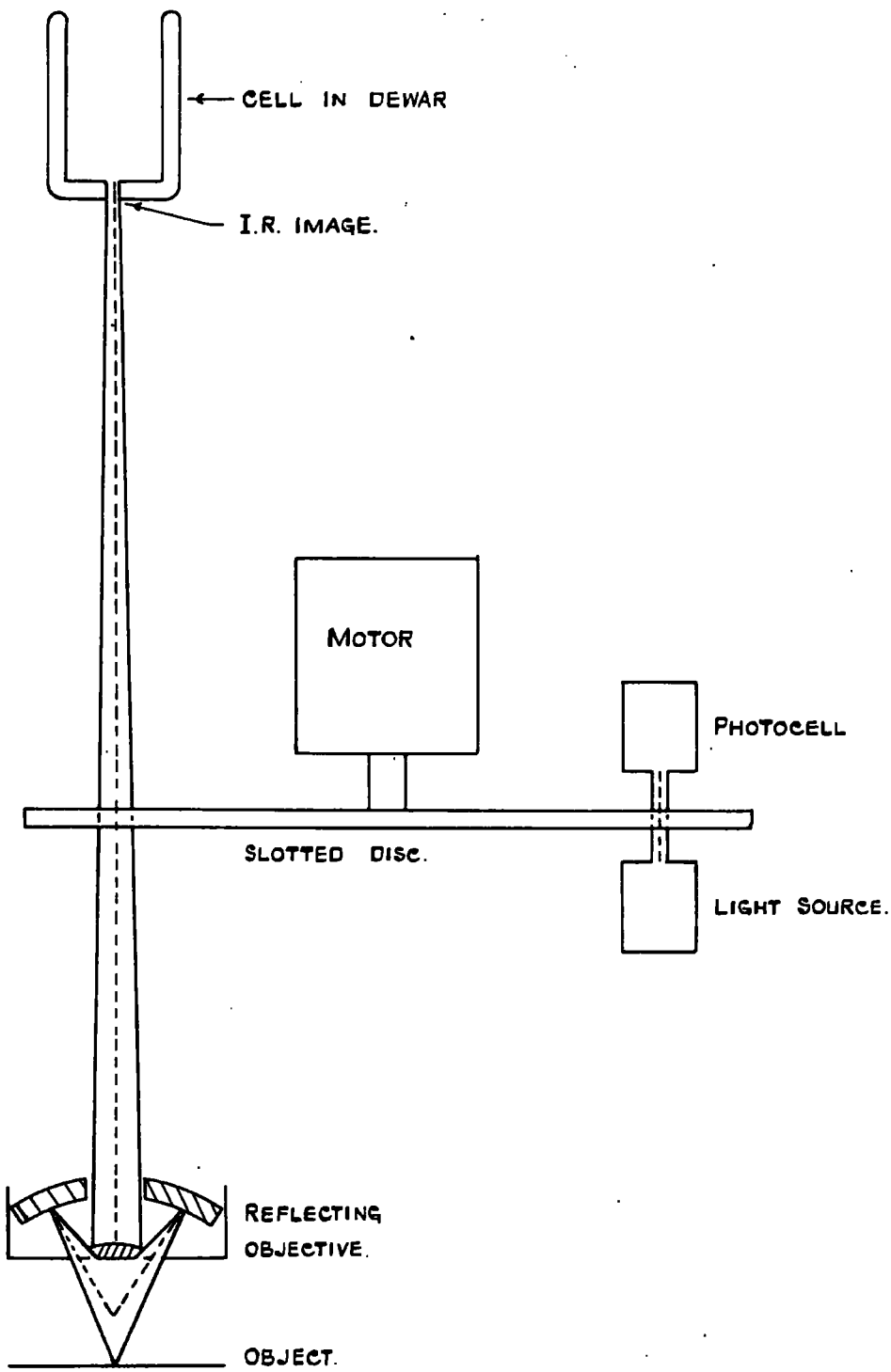

FIG. 7.10

FOCAL LENGTH OF REFLECTING OBJECTIVE

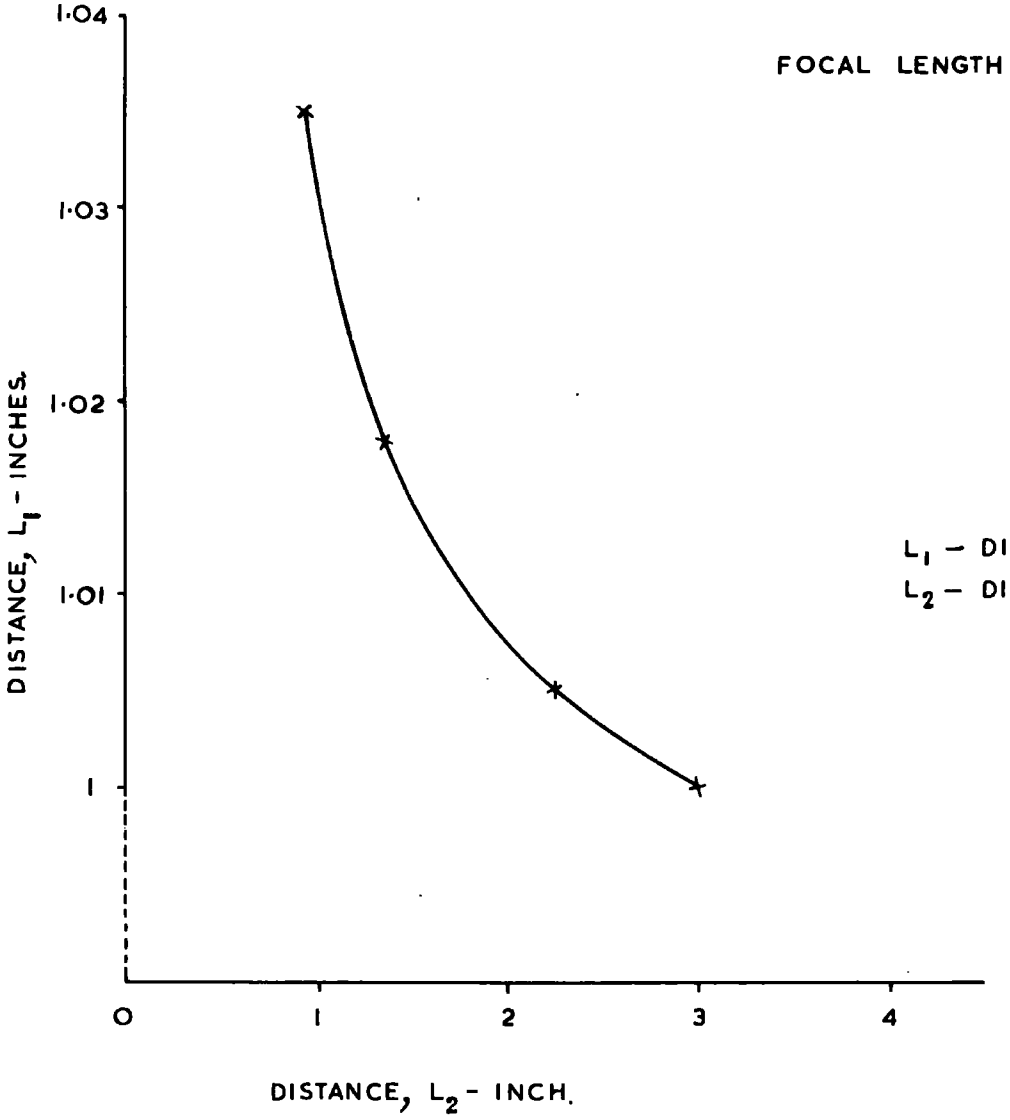

L_1 – DISTANCE BETWEEN LENS AND OBJECT.
L_2 – DISTANCE BETWEEN LENS AND CELL.

radiation measured by the cell was attenuated.

A chopper disc was positioned between the reflecting lens and the cell, thus the output from the cell could be fed directly to an a.c. amplifier with high gain. The chopper disc had sixteen radial slots which produced a one to one mark to space ratio. The speed of the d.c. motor was controlled by a variable d.c. supply with a negative feedback system to give a constant speed. The speed of the disc was set so that the frequency of the cell output was 800 $^{c}/_{s}$ throughout.

A reference signal was derived from a small lamp, the light from which was chopped by the disc and picked up by a photocell as shown in Fig. 7.9. The reference signal was used to switch the phase sensitive rectifiers, consisting of transistors rather than diodes, as a low forward voltage drop was necessary to enable operation in the millivolt range. By using a reference signal exactly in phase with the cell signal, this type of rectifier reduces the bandwidth to almost any desired degree, and eliminates any change in the d.c. output level due to changes in chopper frequency.

The block diagram in Fig. 7.11 shows the electronic layout including a set zero control. The meter used was a 200 μA meter having a coil resistance of 1.5 kΩ.

The thermometer was calibrated by using a tungsten wire as heat source. The temperature of this wire was measured by a thermocouple as shown in Fig. 7.12. A set of current readings versus temperature was taken for the tungsten wire. These readings are shown in Table 7.4. and

FIG. 7·11

DIAGRAM SHOWING THE PRINCIPLE OF OPERATION OF THE INFRARED THERMOMETER.

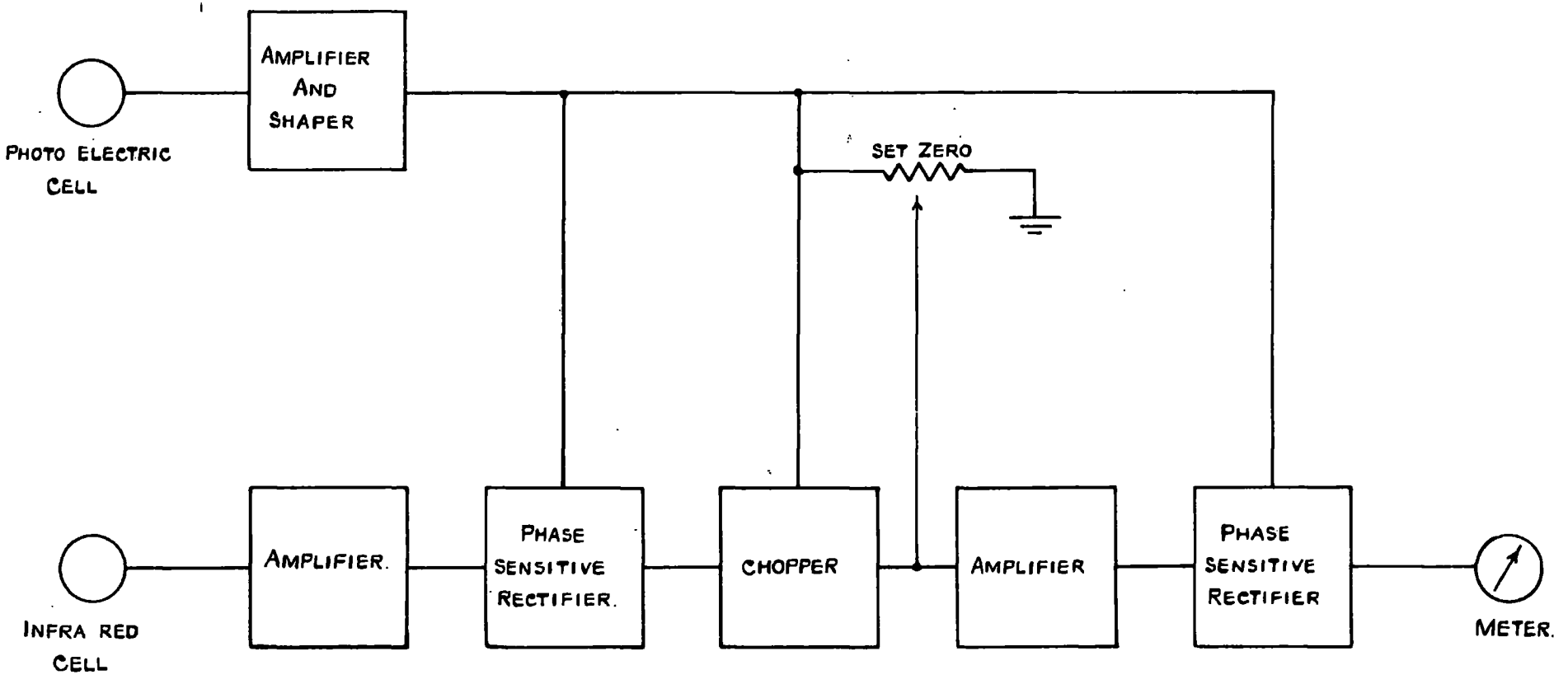

FIG. 7·12.

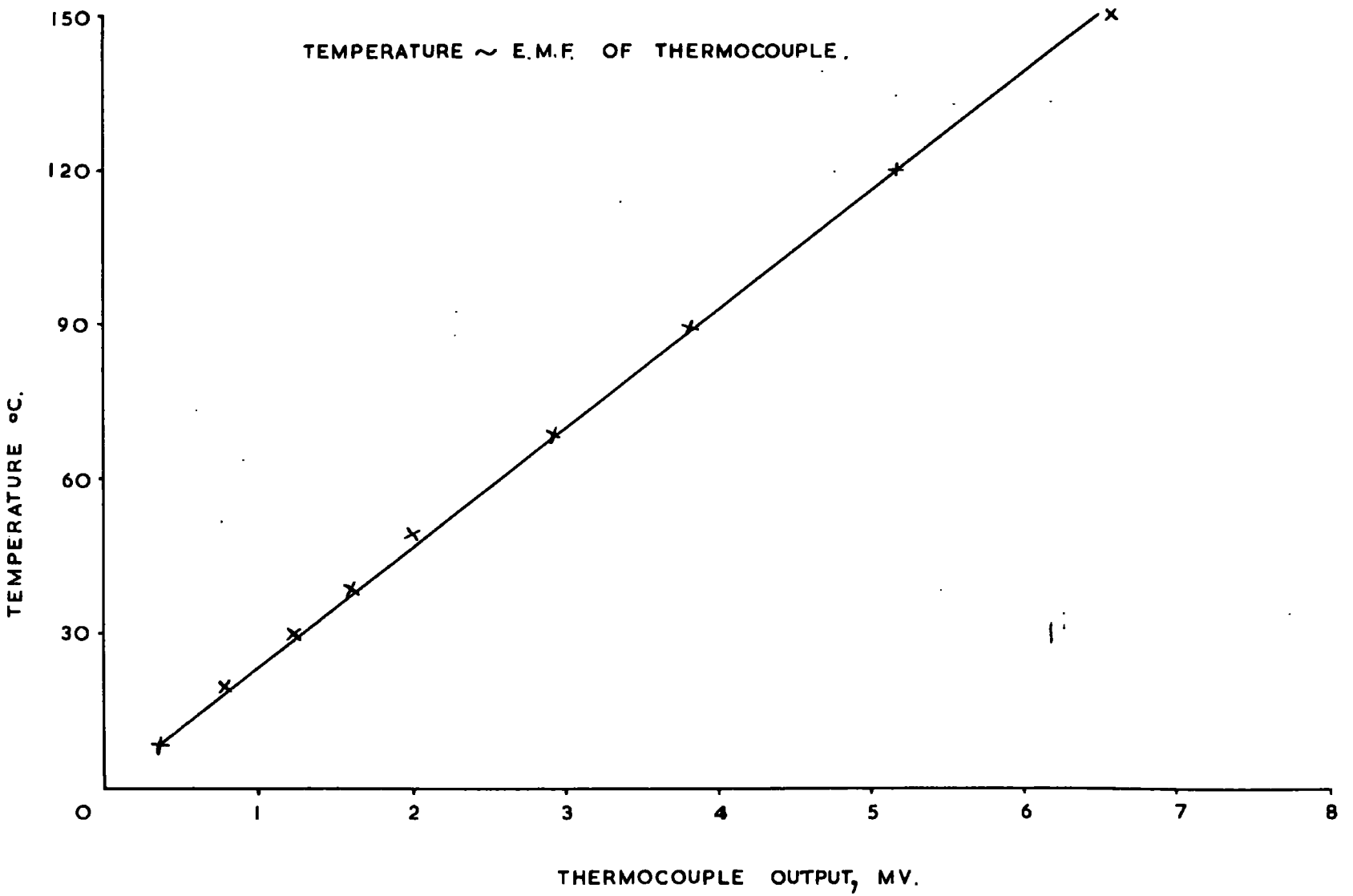
TEMPERATURE ~ E.M.F. OF THERMOCOUPLE.
150
120
90
60
30
0
TEMPERATURE °C.
1
2
3
4
5
6
7
8
THERMOCOUPLE OUTPUT, MV.

plotted in Fig. 7.13. A set of thermometer readings was taken for increasing heating current and a calibration chart for temperature versus meter deflection was derived for the various meter ranges as shown in Fig. 7.14.

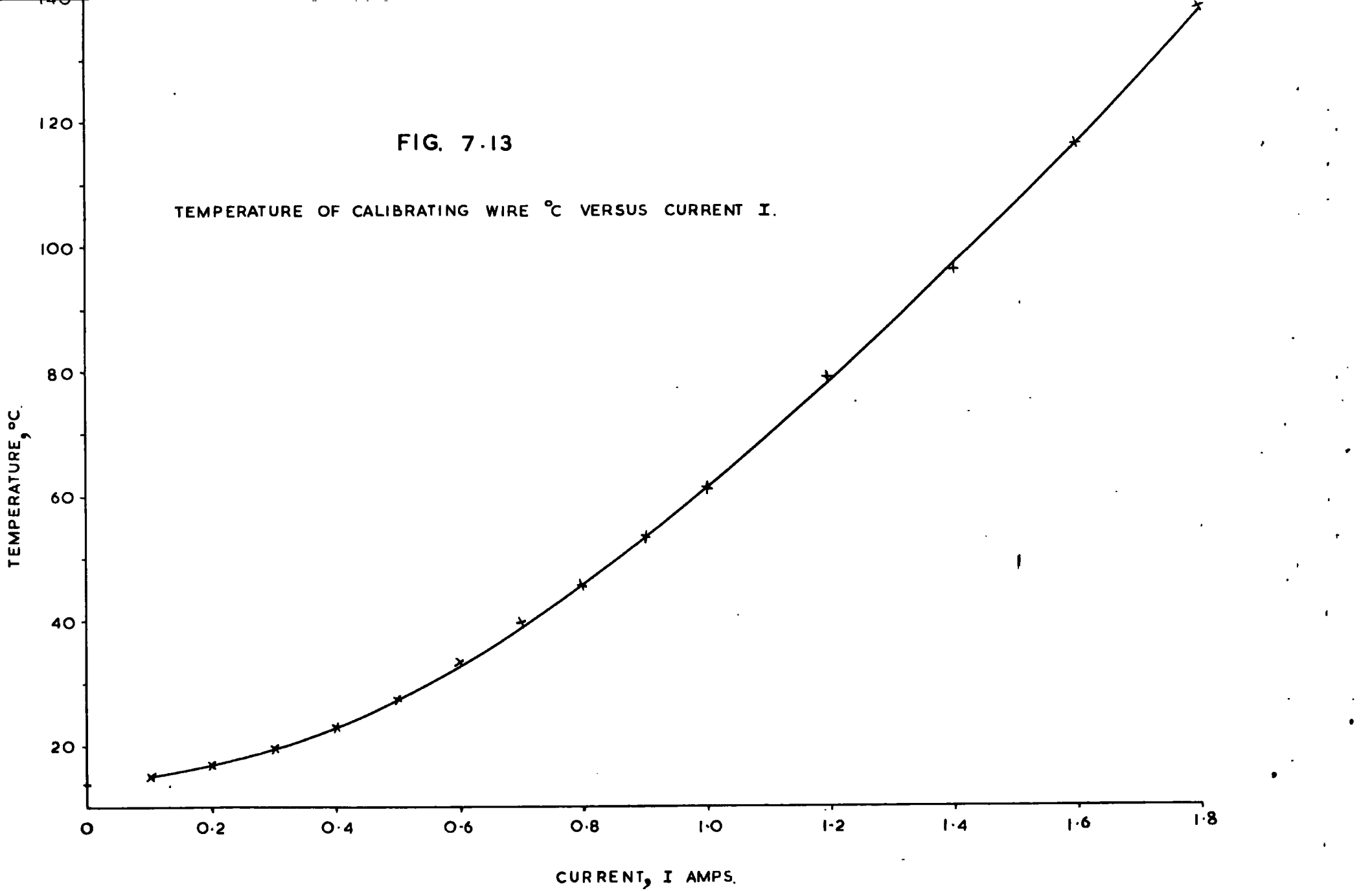

FIG. 7·13

TEMPERATURE OF CALIBRATING WIRE °C VERSUS CURRENT I.

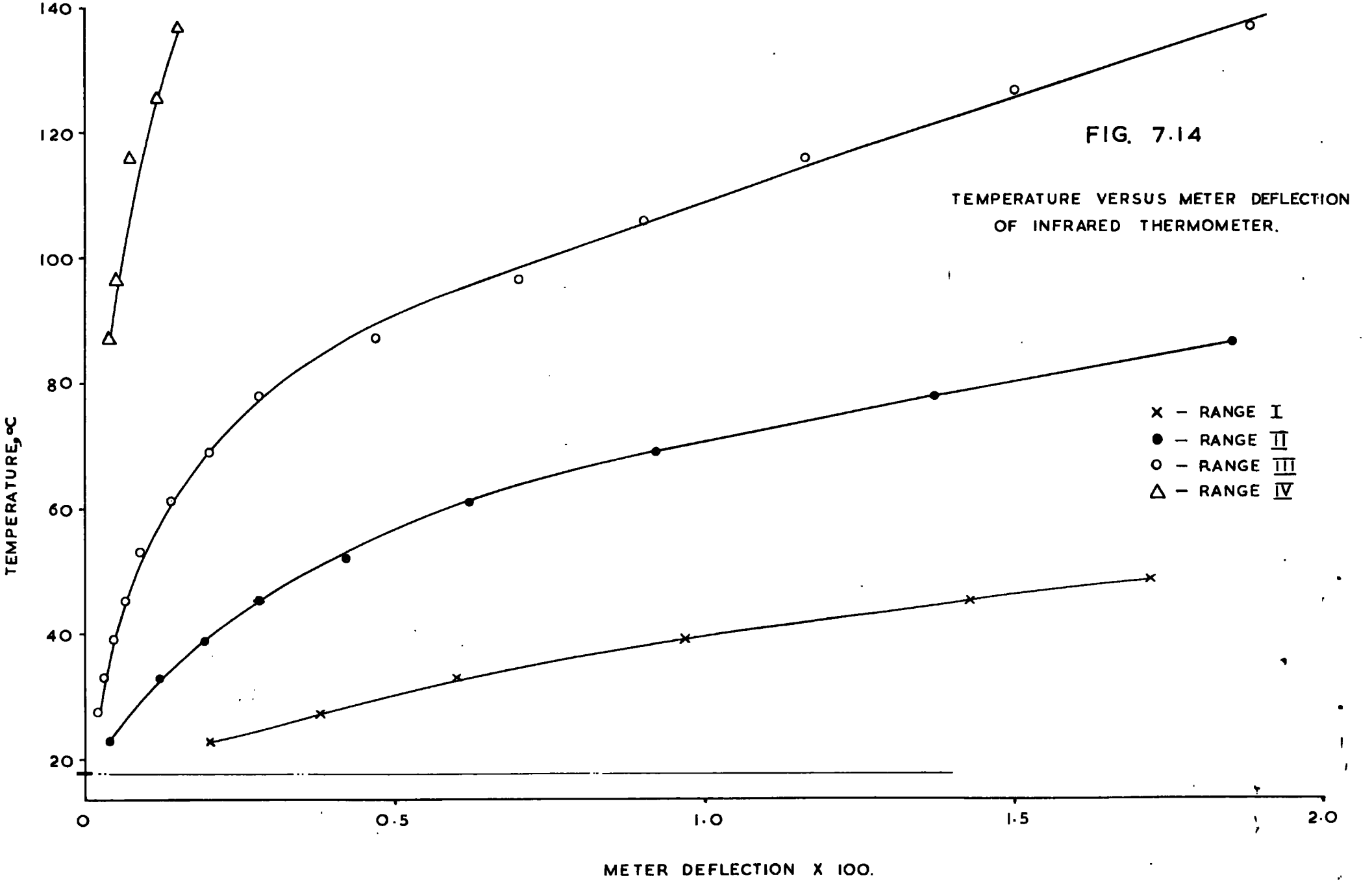

FIG. 7.14

TEMPERATURE VERSUS METER DEFLECTION OF INFRARED THERMOMETER.

7.6. RESISTIVITY VERSUS TEMPERATURE CALIBRATION

This was achieved by varying the temperature of the specimen and measuring the surface resistance, in an atmosphere of constant relative humidity. The ambient temperature was kept constant by a thermostatically controlled waterbath as described earlier.

The test sample was clamped firmly to a block of perspex. A cavity had been machined in the perspex and a thin sheet of perspex glued to the side to seal the cavity. Water was pumped through the cavity from an auxiliary waterbath.

The temperature of the auxiliary waterbath was thermostatically controlled by a small immersion heater. The waterbath could also be cooled to temperatures well below the ambient. This was achieved by allowing a stream of cold water to run through a coiled copper tube submerged in the waterbath.

The initial surface resistivity was taken as the resistivity at ambient temperature, and the surface resistivity was measured at a range of temperatures as shown in Table 7.5. A ratio of surface resistivity to initial surface resistivity was obtained and plotted against temperature ^{o}C. above ambient, as shown in Fig. 4.17.

T A B L E 4.1

Relative humidity: 43.0%

Initial surface resistance: 890 MΩ

Applied voltage kV	Current I_s - μA	Dry Band Width W - cm
1.0	1.09	5.28
1.5	1.58	5.28
2.0	2.02	5.28
3.0	2.70	5.28
3.5	3.04	5.28

T A B L E 4.2

Relative humidity: 52.0%

Initial surface resistance: 76.8 MΩ

Applied voltage kV	Current I_s - μA	Dry Band Width W - cm
1.0	10.1	5.28
1.4	11.5	5.28
1.8	12.7	5.28
2.2	13.3	1.720
2.6	12.7	1.130
3.0	11.0	0.512
3.5	9.3	0.512

TABLE 4.3

Relative humidity: 65.0%

Initial surface resistance: 9.6 MΩ

Applied voltage kV	Current I_s - μA	Dry Band Width W - cm
0.5	35.5	5.28
1.0	33.0	1.30
1.1	27.5	0.70
1.2	24.0	0.59
1.5	20.0	0.45
2.0	15.8	0.45
2.5	13.6	0.45

TABLE 4.4

Relative humidity: 75.67%

Initial surface resistance: 1.037 MΩ

Applied voltage kV	Current I_s - μA	Dry Band Width W - cm
0.10	77.0	5.280
0.25	110.0	5.280
0.35	104.0	2.370
0.40	75.0	0.520
0.80	38.0	0.378
1.5	23.6	0.338
2.0	19.4	0.294

T A B L E 4.5

Relative humidity: 86.5%

Initial surface resistance: 0.142 MΩ

Applied voltage volts	Current I_s - μA	Dry Band Width W - cm
50	275	5.280
75	320	5.280
100	270	5.280
125	235	2.150
150	190	0.680
300	96	0.335
500	66	0.300
1500	29	0.300

TABLE 4.6

Relative humidity: 93.0%

Initial surface resistance: 21.2 kΩ

Applied voltage	Current	Dry Band Width
volts	I_s - μA	W - cm
25	1060	5.28
35	1280	5.28
50	810	2.15
75	305	0.46
100	243	0.32
150	177	0.29
250	120	0.29

TABLE 4.7

Relative humidity: 86.5%

Initial surface resistance: 6.3 MΩ

Fan speed: 500 r.p.m.

Applied voltage volts	Current I_s - μA	Dry Band Width W - cm
100	15.4	5.28
500	43.0	5.28
700	45.0	5.28
900	32.0	2.33
1100	27.0	0.30
1500	20.0	0.29
2000	15.5	0.29

TABLE 4.8

Relative humidity: 86·5%

Initial surface resistance: 6.53 MΩ

Fan speed: 1000 r.p.m.

Applied voltage	Current	Dry Band Width
volts	I_s - μA	W - cm
100	15.0	5.28
500	46.0	5.28
700	49.0	5.28
900	48.0	3.14
1100	36.0	0.42
1500	21.5	0.28
2000	17.0	0.25

T A B L E 4.9

Relative humidity: 86.5%

Initial surface resistance: 6.53 M Ω

Fan speed: 1500 r.p.m.

Applied voltage volts	Current I_s - μA	Dry Band Width W - cm
100	14.8	5.28
500	50.0	5.28
700	54.0	5.28
900	56.0	5.28
1100	53.0	1.50
1500	23.0	0.23

TABLE 4.10

Relative humidity: 86.5%

Initial surface resistance: 5.13 MΩ

Fan speed: 2000 r.p.m.

Applied voltage	Current	Dry Band Width
volts	I_s - μA	W - cm
100	18.3	5.28
500	57.0	5.28
900	64.5	5.28
1100	34.0	1.95
1300	28.0	0.28
1500	24.5	0.22

TABLE 4.11

Relative humidity: 86.5%

Initial surface resistance: 7.22 MΩ

Fan speed: 3000 r.p.m.

Applied voltage	Current	Dry Band Width
volts	I_s - μA	W - cm
100	13.2	5.28
900	56.5	5.28
1050	60.0	3.25
1200	56.0	2.40
1300	53.0	0.89
1500	28.5	0.24

T A B L E 4.12

Relative humidity: 86.5%

Initial surface resistance: 7.65 MΩ

Fan speed: 4000 r.p.m.

Applied voltage volts	Current I_s - μA	Dry Band Width W - cm
100	12.5	5.28
500	50.0	5.28
1000	66.0	5.28
1200	68.0	5.28
1400	65.5	3.33
1600	29.0	0.24

TABLE 4.13

Relative humidity: 86.5%

Initial surface resistance: 9.00 MΩ

Fan speed: 5000 r.p.m.

Applied voltage	Current	Dry Band Width
volts	I_s - μA	W - cm
100	10	5.28
1000	62	5.28
1600	68	3.25
1800	28	0.32
1900	27	0.24

T A B L E 4.14

Relative humidity: 86.5%

Initial surface resistance: 11.2 MΩ

Fan speed: 6000 r.p.m.

Applied voltage	Current	Dry Band Width
volts	I_s - μA	W - cm
100	9.8	5.28
1500	64.5	5.28
2000	67.0	5.28
2300	67.0	5.28
2500	21.0	0.39

TABLE 7.1

This table gives the values of probe displacement versus probe voltage for some values of s with d = 1/16".

Probe voltage	Probe displacements. cm		
μV - volts	s = 1/16"	s = 3/16"	s = 1/4"
20	1.32	1.16	0.86
40	1.35	1.24	1.00
80	1.38	1.31	1.17
120	1.41	1.37	1.30
240	1.48	1.52	1.60
280	1.51	1.59	1.74
320	1.55	1.71	1.94
340	1.59	1.82	2.12

TABLE 7.2

$d = {}^{1}/_{16}"$

$s = {}^{1}/_{16}"$

Applied voltage kV	Probe signal mV
0.5	0.75
1.0	1.50
1.5	2.20
2.0	2.95
2.5	3.70
3.0	4.40

T A B L E 7.3

The values of relative humidity from saturated salt solutions at a temperature of 25°C were obtained from:

Fionnuala, E.M. and O'Brien, M.A.
"Control of humidity by saturated salt solutions."
J. Sci. Instrum., 25, p.73, 1948.

Type of salt	Relative humidity
Potassium Sulphate	93.00 %
Potassium Chloride	86,50 %
Sodium Chloride	75.67 %
Sodium Nitrate	65.00 %
Magnesium Nitrate	52.00 %
Potassium Carbonate	43.00 %

The value for Sodium Nitrate was taken from the N.P.L. tables.

T A B L E 7.4

Temperature of the tungsten wire versus current.

Current I - Amps	Temperature $^{o}C.$
0.1	15.0
0.2	16.7
0.3	19.3
0.4	22.8
0.5	27.5
0.6	33.0
0.7	39.8
0.8	45.4
0.9	53.0
1.0	61.0
1.2	78.5
1.4	96.0
1.6	116.0
1.8	138.0

T A B L E 7.5

Surface resistivity with respect to initial surface resistivity versus temperature above ambient.

$\frac{\rho_s}{\rho_{so}}$	Temperature °C.
1.9	0.75
5.0	1.80
11.5	2.80
21.0	3.80
35.0	4.60
72.0	5.60
190.0	7.00
390.0	8.00
980.0	9.00
3000.0	10.10
3900.0	11.00